NORSAR Scientific Report No. 2-2008

Semiannual Technical Summary

1 January - 30 June 2008

Frode Ringdal (ed.)

Kjeller, August 2008

REPORT DOCUMENTATION PAGE

Form Approved
OMB No. 0704-0188

1. REPORT DATE *(DD-MM-YYYY)*	2. REPORT TYPE	3. DATES COVERED *(From - To)*
15-08-2008	Semiannual Technical Summary	1 January - 30 June 2008

4. TITLE AND SUBTITLE
Semiannual Technical Summary, 1 January - 30 June 2008

5a. CONTRACT NUMBER
FA2521-06-C-8003

5b. GRANT NUMBER

5c. PROGRAM ELEMENT NUMBER
NDC Support / R&D

6. AUTHOR(S)
Frode Ringdal (Ed.)

5d. PROJECT NUMBER
T/6110

5e. TASK NUMBER
SOW Task 4.2 & 4.3

5f. WORK UNIT NUMBER
CDRL sequence nos. A001-A004

7. PERFORMING ORGANIZATION NAME(S) AND ADDRESS(ES)
Stiftelsen NORSAR
Post Box 53
NO-2027 Kjeller
Norway

8. PERFORMING ORGANIZATION REPORT NUMBER
Scientific Report No. 2-2008

9. SPONSORING/MONITORING AGENCY NAME(S) AND ADDRESS(ES)
AFTAC/TTS, 1030 South Highway A1A MS 1000, Patrick AFB, FL 32925-3002

Army Space and Missile Defense Command , 1515 Wilson Blvd., Suite 720
Arlington, VA 22209

10. SPONSOR/MONITOR'S ACRONYM(S)
AFTAC/TTS & USASMDC

11. SPONSOR/MONITOR'S REPORT NUMBER(S)

12. DISTRIBUTION/AVAILABILITY STATEMENT
Approved for public release; distribution unlimited

13. SUPPLEMENTARY NOTES

14. ABSTRACT

This report describes the activities carried out at NORSAR under Contract No. FA2521-06-C-8003 (T/6110) for the period 1 January - 30 June 2008. In addition, it provides summary information on operation and maintenance (O&M) activities at the Norwegian National Data Center (NDC) during the same period. The O&M activities, including operation of transmission links within Norway and to Vienna, Austria, are being funded jointly by the CTBTO/PTS and the Norwegian Government, with the understanding that the funding of O&M activities for primary stations in the International Monitoring System (IMS) will gradually be transferred to the CTBTO/PTS. The O&M statistics presented in this report are included for the purpose of completeness, and in order to maintain consistency with earlier reporting practice. Some of the research activities described in this report are funded (cont.)

15. SUBJECT TERMS
NORSAR, Norwegian Seismic Array

16. SECURITY CLASSIFICATION OF:			17. LIMITATION OF ABSTRACT	18. NUMBER OF PAGES	19a. NAME OF RESPONSIBLE PERSON
a. REPORT	b. ABSTRACT	c. THIS PAGE			Capt. Edward Talley, AFTAC/TTX
U	U	U	SAR	93	19b. TELEPHONE NUMBER *(Include area code)* (321) 494-9471

Reset

Standard Form 298 (Rev. 8/98)
Prescribed by ANSI Std. Z39.18

Abstract (cont.)

by the United States Government, and the United States also covers the cost of transmission of selected data from the Norwegian NDC to the United States NDC.

The seismic arrays operated by NOR-NDC comprise the Norwegian Seismic Array (NOA), the Arctic Regional Seismic Array (ARCES) and the Spitsbergen Regional Array (SPITS). This report presents statistics for these three arrays as well as for additional seismic stations which through cooperative agreements with institutions in the host countries provide continuous data to NOR-NDC. These additional stations include the Finnish Regional Seismic Array (FINES) and the Hagfors array in Sweden (HFS).

The NOA Detection Processing system has been operated throughout the period with an uptime of 100%. A total of 2,465 seismic events have been reported in the NOA monthly seismic bulletin during the reporting period. On-line detection processing and data recording at the NDC of data from ARCES, FINES, SPITS and HFS data have been conducted throughout the period. Processing statistics for the arrays for the reporting period are given.

A summary of the activities at the NOR-NDC and relating to field installations during the reporting period is provided in Section 4. Norway is now contributing primary station data from two seismic arrays: NOA (PS27) and ARCES (PS28), one auxiliary seismic array SPITS (AS72), and one auxiliary three-component station on the island of Jan Mayen(AS73). These data are being provided to the IDC via the global communications infrastructure (GCI). Continuous data from the three arrays are in addition being transmitted to the US NDC. The performance of the data transmission to the US NDC has been satisfactory during the reporting period.

So far among the Norwegian stations, the NOA and the ARCES array (PS27 and PS28 respectively), the radionuclide station at Spitsbergen (RN49) and the auxiliary seismic stations on Spitsbergen (AS72) and Jan Mayen (AS73) have been certified. Provided that adequate funding continues to be made available (from the PTS and the Norwegian Ministry of Foreign Affairs), we envisage continuing the provision of data from these and other Norwegian IMS-designated stations in accordance with current procedures. The IMS infrasound station at Karasjok (IS37) has not yet been built, and discussions are continuing with the local authorities in order to obtain the permissions required for the establishment of the station.

Summaries of four scientific and technical contributions are presented in Chapter 6 of this report.

Section 6.1 is an initial study of high-frequency signals recorded at ARCES. We have carried out an initial study of seismic events at regional distances recorded by the ARCES high-frequency seismic system, which was installed on 23 March 2008. The main conclusion is that these new observations consistently show remarkably efficient propagation at frequencies up to 30 Hz and above. This result is similar to what has been previously observed at the Spitsbergen array for paths from Novaya Zemlya crossing the Barents Sea. The Spitsbergen studies showed that energy exceeding 20 Hz can be recorded with good signal-to-noise ratio even for small events at epicentral distances as large as 1000 km and we see the same result in this study.

Among the filter bands studied in this contribution, the best filter band for regional event detection across intraplate paths generally appears to be either 4-8 Hz or 8-16 Hz. However, the most remarkable feature in this study is the strong SNR even at the highest frequencies (15-30 and

30-45 Hz). While such frequency bands would not be used for detection purposes, the high frequency data could be very important for signal characterization.

We note that the available high-frequency data so far does not include events to the east and north-east of the ARCES array, and the high-frequency propagation from the Novaya Zemlya region to ARCES is therefore still unknown. As more data is accumulated, we may be in a position to carry out a more detailed study of the propagation characteristics for additional paths in the region, and make a more systematic study of the benefits from combining the high-frequency observations from Spitsbergen and ARCES. The usefulness of the horizontal components for high-frequency S-phase detection, already demonstrated for the Spitsbergen array, is also an area that needs further study for ARCES.

Section 6.2 describes the setup of an experimental infrasound deployment in Karasjok, northern Norway. In mid-March 2008 NORSAR carried out an experimental installation of three micro-barometers at the stations ARA1, ARA2 and ARB2 of the ARCES seismic array. The purpose of this experiment was to compare the relative performance of microbarographs and seismometers in detecting infrasonic signals. The full ARCES array has a diameter of about 3 km, whereas the distances between the three infrasound stations are about 200 -300 m.

The microbarometers used in the experimental infrasound array are Martec MB2500 instruments with a bandwidth from 0.01 – 27 Hz and a sensitivity of 20 mV/Pa. Each barometer is about 35 cm high with a diameter of 15 cm and a weight of 7 kg. The lower part of the instrument is the measurement chamber containing a barometric aneroid bellow, which is deformed by small variations of atmospheric pressure. The deformation of the bellow in turn is measured by a displacement transducer.

In order to suppress wind noise the decision was made to use porous hoses. At each pit four 12 m long porous hoses were installed in a cross-type layout. The hoses are connected to a manifold outside of the pit, and therefore only one inlet penetrates the vault and connects to the barometer. For stations ARA1 and ARB2 we used only the porous hoses, for station ARA2 we additionally encased the hose by a plastic drainage pipe. At the time of the installation we still had a snow cover of up to 1.5 m depths. At all stations the hoses/pipes have been buried as deep into the snow as possible.

Section 6.3 is an initial study of data from the experimental installation of infrasound sensors at the ARCES array. We have begun an investigation aimed at comparing the quality of recording of infrasound signals when using seismometers versus recordings using microbarographs. Even taking into account the very efficient recording of such signals by the ARCES seismometers, our expectation would be that significant improvement would be obtained when using microbarographs. Nevertheless, the much larger number of seismic sensors would be a factor that should also be taken into account.

We have made direct comparisons of signals from the two types of sensors for a presumed explosion in NW Russia at a site reportedly used for destroying old ammunition. The infrasonic signal is very clear in both cases and looks quite similar on the two sensors. One interesting observation is the differences in signal-to-noise ratio (SNR) between the two types of recordings. While the SNR of the infrasonic signal is high in both cases, it is clearly superior for the microbarograph. This is by no means surprising; in fact, the most surprising feature is that the seismic trace is so close to the microbarograph trace in terms of both SNR and waveform characteristics. We also note that “noise” on the seismic trace comprises both the usual

"background noise" and the actual seismic signals, which naturally are not visible on the microbarograph trace.

We demonstrate that an infrasound signal detector based on continuous slowness analysis is applicable both to the seismometer and microbarograph data at the ARCES array. To avoid spurious detections at the microbarographs, additional constraints must be applied to the SNR of the signals. Data quality checks were introduced to discard instances where sensors show anomalous amplitudes. A much larger number of detections are found on the microbarograph data compared to the seismic data, clearly illustrating the improved sensitivity to infrasound signals as compared to recordings at the seismic sensors.

In parallel with the present study, we have processed the same data set using cross-correlation techniques combined with a detection statistic. These results are comparable to those presented in the present study, but a detailed comparison will require further work concerning setting of window and filter parameters, threshold setting and data quality control.

For the time interval April - June 2008 we have also processed the infrasound data from Apatity, as well as from the stations of the Swedish Infrasound Network using the method described in this contribution. A natural next step is to combine the signal detections from this dense network of six infrasound stations in Northern Europe to obtain information about the infrasound sources.

Section 6.4 is a continued overview of NORSAR system responses, specifically addressing the NORES and ARCES arrays. This series of contributions is aiming to recalculate and organize all of the system instrument responses of the seismic facilities operated by NORSAR, from the time of the first installation to the present. All sources of information are being catalogued and archived. Furthermore, detailed documentation is being compiled, describing the methodology followed to obtain the necessary information, the calculation of the responses, as well as more practical issues, such as organizing and storing the results for future usage. Therefore, no information such as individual instrument poles and zeroes, serial numbers, sensitivity values, etc. are provided here; instead, the reader is referred to the relevant NORSAR internal documentation.

Frode Ringdal

AFTAC Project Authorization	:	T/6110
Purchase Request No.	:	F3KTK85290A1
Name of Contractor	:	Stiftelsen NORSAR
Effective Date of Contract	:	1 March 2006
Contract Expiration Date	:	30 September 2011
Amount of Contract	:	$ 1,003,494.00
Project Manager	:	Frode Ringdal +47 63 80 59 00
Title of Work	:	The Norwegian Seismic Array (NORSAR) Phase 3
Period Covered by Report	:	1 January - 30 June 2008

The views and conclusions contained in this document are those of the authors and should not be interpreted as necessarily representing the official policies, either expressed or implied, of the U.S. Government.

Part of the research presented in this report was supported by the Army Space and Missile Defense Command, under contract no. W9113M-05-C-0224. Other activities were supported and monitored by AFTAC, Patrick AFB, FL32925, under contract no. FA2521-06-C-8003. Other sponsors are acknowledged where appropriate.

The operational activities of the seismic field systems and the Norwegian National Data Center (NDC) are currently jointly funded by the Norwegian Government and the CTBTO/PTS, with the understanding that the funding of appropriate IMS-related activities will gradually be transferred to the CTBTO/PTS.

Table of Contents

Page

1 Summary

This report describes the activities carried out at NORSAR under Contract No. FA2521-06-C-8003 for the period 1 January - 30 June 2008. In addition, it provides summary information on operation and maintenance (O&M) activities at the Norwegian National Data Center (NOR-NDC) during the same period. The O&M activities, including operation of transmission links within Norway and to Vienna, Austria are being funded jointly by the CTBTO/PTS and the Norwegian Government, with the understanding that the funding of O&M activities for primary stations in the International Monitoring System (IMS) will gradually be transferred to the CTBTO/PTS. The O&M statistics presented in this report are included for the purpose of completeness, and in order to maintain consistency with earlier reporting practice. Some of the research activities described in this report are funded by the United States Government, and the United States also covers the cost of transmission of selected data from the Norwegian NDC to the United States NDC.

The seismic arrays operated by NOR-NDC comprise the Norwegian Seismic Array (NOA), the Arctic Regional Seismic Array (ARCES) and the Spitsbergen Regional Array (SPITS). This report presents statistics for these three arrays as well as for additional seismic stations which through cooperative agreements with institutions in the host countries provide continuous data to NOR-NDC. These additional stations include the Finnish Regional Seismic Array (FINES) and the Hagfors array in Sweden (HFS).

The NOA Detection Processing system has been operated throughout the period with an uptime of 100%. A total of 2,465 seismic events have been reported in the NOA monthly seismic bulletin during the reporting period. On-line detection processing and data recording at the NDC of data from ARCES, FINES, SPITS and HFS data have been conducted throughout the period. Processing statistics for the arrays for the reporting period are given.

A summary of the activities at the NOR-NDC and relating to field installations during the reporting period is provided in Section 4. Norway is now contributing primary station data from two seismic arrays: NOA (PS27) and ARCES (PS28), one auxiliary seismic array SPITS (AS72), and one auxiliary three-component station on the island of Jan Mayen(AS73). These data are being provided to the IDC via the global communications infrastructure (GCI). Continuous data from the three arrays are in addition being transmitted to the US NDC. The performance of the data transmission to the US NDC has been satisfactory during the reporting period.

So far among the Norwegian stations, the NOA and the ARCES array (PS27 and PS28 respectively), the radionuclide station at Spitsbergen (RN49) and the auxiliary seismic stations on Spitsbergen (AS72) and Jan Mayen (AS73) have been certified. Provided that adequate funding continues to be made available (from the PTS and the Norwegian Ministry of Foreign Affairs), we envisage continuing the provision of data from these and other Norwegian IMS-designated stations in accordance with current procedures. The IMS infrasound station at Karasjok (IS37) has not yet been built, and discussions are continuing with the local authorities in order to obtain the permissions required for the establishment of the station.

Summaries of four scientific and technical contributions are presented in Chapter 6 of this report.

Section 6.1 is an initial study of high-frequency signals recorded at ARCES. We have carried out an initial study of seismic events at regional distances recorded by the ARCES high-fre-

quency seismic system, which was installed on 23 March 2008. The main conclusion is that these new observations consistently show remarkably efficient propagation at frequencies up to 30 Hz and above. This result is similar to what has been previously observed at the Spitsbergen array for paths from Novaya Zemlya crossing the Barents Sea. The Spitsbergen studies showed that energy exceeding 20 Hz can be recorded with good signal-to-noise ratio even for small events at epicentral distances as large as 1000 km and we see the same result in this study.

Among the filter bands studied in this contribution, the best filter band for regional event detection across intraplate paths generally appears to be either 4-8 Hz or 8-16 Hz. However, the most remarkable feature in this study is the strong SNR even at the highest frequencies (15-30 and 30-45 Hz). While such frequency bands would not be used for detection purposes, the high frequency data could be very important for signal characterization.

We note that the available high-frequency data so far does not include events to the east and north-east of the ARCES array, and the high-frequency propagation from the Novaya Zemlya region to ARCES is therefore still unknown. As more data is accumulated, we may be in a position to carry out a more detailed study of the propagation characteristics for additional paths in the region, and make a more systematic study of the benefits from combining the high-frequency observations from Spitsbergen and ARCES. The usefulness of the horizontal components for high-frequency S-phase detection, already demonstrated for the Spitsbergen array, is also an area that needs further study for ARCES.

Section 6.2 describes the setup of an experimental infrasound deployment in Karasjok, northern Norway. In mid-March 2008 NORSAR carried out an experimental installation of three micro-barometers at the stations ARA1, ARA2 and ARB2 of the ARCES seismic array. The purpose of this experiment was to compare the relative performance of microbarographs and seismometers in detecting infrasonic signals. The full ARCES array has a diameter of about 3 km, whereas the distances between the three infrasound stations are about 200 -300 m.

The microbarometers used in the experimental infrasound array are Martec MB2500 instruments with a bandwidth from 0.01 – 27 Hz and a sensitivity of 20 mV/Pa. Each barometer is about 35 cm high with a diameter of 15 cm and a weight of 7 kg. The lower part of the instrument is the measurement chamber containing a barometric aneroid bellow, which is deformed by small variations of atmospheric pressure. The deformation of the bellow in turn is measured by a displacement transducer.

In order to suppress wind noise the decision was made to use porous hoses. At each pit four 12 m long porous hoses were installed in a cross-type layout. The hoses are connected to a manifold outside of the pit, and therefore only one inlet penetrates the vault and connects to the barometer. For stations ARA1 and ARB2 we used only the porous hoses, for station ARA2 we additionally encased the hose by a plastic drainage pipe. At the time of the installation we still had a snow cover of up to 1.5 m depths. At all stations the hoses/pipes have been buried as deep into the snow as possible.

Section 6.3 is an initial study of data from the experimental installation of infrasound sensors at the ARCES array. We have begun an investigation aimed at comparing the quality of recording of infrasound signals when using seismometers versus recordings using microbarographs. Even taking into account the very efficient recording of such signals by the ARCES seismometers, our expectation would be that significant improvement would be obtained when using

microbarographs. Nevertheless, the much larger number of seismic sensors would be a factor that should also be taken into account.

We have made direct comparisons of signals from the two types of sensors for a presumed explosion in NW Russia at a site reportedly used for destroying old ammunition. The infrasonic signal is very clear in both cases and looks quite similar on the two sensors. One interesting observation is the differences in signal-to-noise ratio (SNR) between the two types of recordings. While the SNR of the infrasonic signal is high in both cases, it is clearly superior for the microbarograph. This is by no means surprising; in fact, the most surprising feature is that the seismic trace is so close to the microbarograph trace in terms of both SNR and waveform characteristics. We also note that "noise" on the seismic trace comprises both the usual "background noise" and the actual seismic signals, which naturally are not visible on the microbarograph trace.

We demonstrate that an infrasound signal detector based on continuous slowness analysis is applicable both to the seismometer and microbarograph data at the ARCES array. To avoid spurious detections at the microbarographs, additional constraints must be applied to the SNR of the signals. Data quality checks were introduced to discard instances where sensors show anomalous amplitudes. A much larger number of detections are found on the microbarograph data compared to the seismic data, clearly illustrating the improved sensitivity to infrasound signals as compared to recordings at the seismic sensors.

In parallel with the present study, we have processed the same data set using cross-correlation techniques combined with a detection statistic. These results are comparable to those presented in the present study, but a detailed comparison will require further work concerning setting of window and filter parameters, threshold setting and data quality control.

For the time interval April - June 2008 we have also processed the infrasound data from Apatity, as well as from the stations of the Swedish Infrasound Network using the method described in this contribution. A natural next step is to combine the signal detections from this dense network of six infrasound stations in Northern Europe to obtain information about the infrasound sources.

Section 6.4 is a continued overview of NORSAR system responses, specifically addressing the NORES and ARCES arrays. This series of contributions is aiming to recalculate and organize all of the system instrument responses of the seismic facilities operated by NORSAR, from the time of the first installation to the present. All sources of information are being catalogued and archived. Furthermore, detailed documentation is being compiled, describing the methodology followed to obtain the necessary information, the calculation of the responses, as well as more practical issues, such as organizing and storing the results for future usage. Therefore, no information such as individual instrument poles and zeroes, serial numbers, sensitivity values, etc. are provided here; instead, the reader is referred to the relevant NORSAR internal documentation.

Frode Ringdal

2 Operation of International Monitoring System (IMS) Stations in Norway

2.1 PS27 — Primary Seismic Station NOA

The mission-capable data statistics were 100%, the same as for the previous reporting period. The net instrument availability was 96.165%.

There were no outages of all subarrays at the same time in the reporting period.

Monthly uptimes for the NORSAR on-line data recording task, taking into account all factors (field installations, transmissions line, data center operation) affecting this task were as follows:

2008		Mission Capable	Net instrument availability
January	:	100%	98.408%
February	:	100%	97.130%
March	:	100%	95.235%
April	:	100%	95.236%
May	:	100%	95.234%
June	:	100%	95.766%

B. Paulsen

NOA Event Detection Operation

In Table 2.1.1 some monthly statistics of the Detection and Event Processor operation are given. The table lists the total number of detections (DPX) triggered by the on-line detector, the total number of detections processed by the automatic event processor (EPX) and the total number of events accepted after analyst review (teleseismic phases, core phases and total).

	Total DPX	Total EPX	Accepted Events		Sum	Daily
			P-phases	Core Phases		
Jan	11,411	765	195	52	247	8.0
Feb	10,918	825	231	52	283	9.8
Mar	12,130	1,016	326	59	385	12.4
Apr	8,553	984	293	89	382	12.7
May	5,354	1,044	601	69	670	21.6
Jun	6,544	880	433	65	498	16.6
	54,910	5,514	2,079	386	2,465	13.5

Table 2.1.1. *Detection and Event Processor statistics, 1 January - 30 June 2008.*

NOA detections

The number of detections (phases) reported by the NORSAR detector during day 001, 2008, through day 182, 2008, was 54,910, giving an average of 301 detections per processed day (182 days processed).

B. Paulsen

U. Baadshaug

2.2 PS28 — Primary Seismic Station ARCES

The mission-capable data statistics were 99.904%, as compared to 99.994% for the previous reporting period. The net instrument availability was 97.639%.

The main outages in the period are presented in Table 2.2.1.

Day	Period
31 Jan	13.54-14.14
31 Jan	14.14-14.36
31 Jan	14.54-15.03
31 Jan	21.46-22.08
31 Jan	22.42-22.56
01 Feb	04.11-04.24
01 Feb	04.28-04.46
12 Mar	12.36-12.47
12 Mar	12.49-12.50
12 Mar	13.05-13.14
15 May	14.37-14.43
15 May	14.44-14.53
20 May	20.03-20.08
20 May	20.09-20.18
20 May	23.29-23.38
21 May	08.30-08.38
09 Jun	12.54-13.04
30 Jun	16.15-16.22
30 Jun	17.46-17.52
30 Jun	17.53-18.00
30 Jun	19.42-19.48
30 Jun	19.54-20.03

Table 2.2.1. *The main interruptions in recording of ARCES data at NDPC, 1 January - 30 June 2008.*

Monthly uptimes for the ARCES on-line data recording task, taking into account all factors (field installations, transmission lines, data center operation) affecting this task were as follows:

2008		Mission Capable	Net instrument availability
January	:	99.758%	99.639%
February	:	99.925%	99.913%
March	:	99.954%	99.449%
April	:	100%	98.588%
May	:	99.893%	93.276%
June	:	99.895%	95.062%

B. Paulsen

Event Detection Operation

ARCES detections

The number of detections (phases) reported during day 001, 2008, through day 182, 2008, was 168,466, giving an average of 926 detections per processed day (182 days processed).

Events automatically located by ARCES

During days 001, 2008, through 182, 2008, 10,378 local and regional events were located by ARCES, based on automatic association of P- and S-type arrivals. This gives an average of 57.0 events per processed day (182 days processed). 57% of these events are within 300 km, and 83 % of these events are within 1000 km.

U. Baadshaug

2.3 AS72 — Auxiliary Seismic Station Spitsbergen

The mission-capable data for the period were 95.609%, as compared to 89.160% for the previous reporting period. The net instrument availability was 79.659%.

The main outages in the period are presented in Table 2.3.1.

Day	Period
25 Mar	09.42-09.59
25 Mar	14.28-00.00
26 Mar	00.00-08.59
26 Mar	09.35-23.59
27 Mar	00.00-23.59
28 Mar	00.00-23.59
29 Mar	00.00-23.59
30 Mar	00.00-23.59
31 Mar	00.00-23.59
01 Apr	00.00-23.59
02 Apr	00.00-13.42
23 Apr	08.07-08.22
23 Apr	09.27-09.42
04 Jun	07.03-07.19

Table 2.31. *The main interruptions in recording of Spitsbergen data at NDPC, 1 January - 30 June 2008.*

Monthly uptimes for the Spitsbergen on-line data recording task, taking into account all factors (field installations, transmissions line, data center operation) affecting this task were as follows:

2008		Mission Capable	Net instrument availability
January	:	100%	85.633%
February	:	99.999%	85.711%
March	:	79.406%	68.021%
April	:	94.683%	80.610%
May	:	99.999%	85.655%
June	:	99.963%	72.515%

B. Paulsen

Event Detection Operation

Spitsbergen array detections

The number of detections (phases) reported from day 001, 2008, through day 182, 2008, was 392,136, giving an average of 2,228 detections per processed day (182 days processed).

Events automatically located by the Spitsbergen array

During days 001, 2008 through 182, 2008, 30,527 local and regional events were located by the Spitsbergen array, based on automatic association of P- and S-type arrivals. This gives an average of 173.4 events per processed day (182 days processed). 77% of these events are within 300 km, and 92% of these events are within 1000 km.

U. Baadshaug

2.4 AS73 — Auxiliary Seismic Station at Jan Mayen

The IMS auxiliary seismic network includes a three-component station on the Norwegian island of Jan Mayen. The station location given in the protocol to the Comprehensive Nuclear-Test-Ban Treaty is 70.9˚N, 8.7˚W.

The University of Bergen has operated a seismic station at this location since 1970. A so-called Parent Network Station Assessment for AS73 was completed in April 2002. A vault at a new location (71.0^{o}N, 8.5^{o}W) was prepared in early 2003, after its location had been approved by the PrepCom. New equipment was installed in this vault in October 2003, as a cooperative effort between NORSAR and the CTBTO/PTS. Continuous data from this station are being transmitted to the NDC at Kjeller via a satellite link installed in April 2000. Data are also made available to the University of Bergen.

The station was certified by the CTBTO/PTS on 12 June 2006.

J. Fyen

2.5 IS37 — Infrasound Station at Karasjok

The IMS infrasound network will include a station at Karasjok in northern Norway. The coordinates given for this station are 69.5˚N, 25.5˚E. These coordinates coincide with those of the primary seismic station PS28.

A site survey for this station was carried out during June/July 1998 as a cooperative effort between the CTBTO/PTS and NORSAR. The site survey led to a recommendation on the exact location of the infrasound station. There was, however, a strong local opposition against establishing the station at the recommended location, and two alternative sites were identified. The appropriate applications were sent to the local authorities to obtain the permissions needed to establish the station at one of these alternative locations. Both applications were turned down by the local governing council in June 2007. Discussions are currently underway with local stakeholders, in an attempt to identify a location for the station that will be acceptable to all parties.

A site preparation contract has been signed with the PTS. Due to scarce vegetation, possible high winds and difficult arctic operating conditions, the PTS has accepted our proposal to build a station comprising 9 elements.

J. Fyen

2.6 RN49 — Radionuclide Station on Spitsbergen

The IMS radionuclide network includes a station on the island of Spitsbergen. This station has been selected to be among those IMS radionuclide stations that will monitor for the presence of relevant noble gases upon entry into force of the CTBT.

A site survey for this station was carried out in August of 1999 by NORSAR, in cooperation with the Norwegian Radiation Protection Authority. The site survey report to the PTS contained a recommendation to establish this station at Platåberget, near Longyearbyen. The infrastructure for housing the station equipment was established in early 2001, and a noble gas detection system, based on the Swedish “SAUNA” design, was installed at this site in May 2001, as part of PrepCom’s noble gas experiment. A particulate station (“ARAME” design)

was installed at the same location in September 2001. A certification visit to the particulate station took place in October 2002, and the particulate station was certified on 10 June 2003. Both systems underwent substantial upgrading in May/June 2006. The equipment at RN49 is being maintained and operated under a contract with the CTBTO/PTS.

S. Mykkeltveit

3 Contributing Regional Seismic Arrays

3.1 NORES

NORES has been out of operation since lightning destroyed the station electronics on 11 June 2002.

B. Paulsen

3.2 Hagfors (IMS Station AS101)

Data from the Hagfors array are made available continuously to NORSAR through a cooperative agreement with Swedish authorities.

The mission-capable data statistics were 99.970%, as compared to 99.980% for the previous reporting period. The net instrument availability was 99.880%.

The main outages in the period are presented in Table 3.2.1.

Day	Period
22 Jan	09.03-09.06
31 Jan	17.43-17.46
04 Feb	23.03-23.06
02 Mar	00.03-00.07
02 Mar	06.03-06.07
12 Mar	05.03-05.07
21 Mar	05.04-05.07
24 Mar	17.44-17.47
13 Apr	10.24-10.27
18 Apr	03.44-03.47
25 Apr	08.04-08.08
25 Apr	19.24-19.28
03 May	22.44-22.48
04 May	14.04-14.08
17 May	02.25-02.28
17 May	19.05-19.08
18 May	12.25-12.28
27 May	09.05-09.08
29 May	11.05-11.08
15 Jun	14.25-14.29
19 Jun	04.25-04.28

Day	Period
24 Jun	06.45-06.48
27 Jun	02.45-02.49

Table 3.2.1. *The main interruptions in recording of Hagfors data at NDPC, 1 January - 30 June 2008.*

Monthly uptimes for the Hagfors on-line data recording task, taking into account all factors (field installations, transmissions line, data center operation) affecting this task were as follows:

2008		Mission Capable	Net instrument availability
January	:	99.987%	99.986%
February	:	99.992%	99.429%
March	:	99.962%	99.961%
April	:	99.968%	99.967%
May	:	99.943%	99.942%
June	:	99.970%	99.969%

B. Paulsen

Hagfors Event Detection Operation

Hagfors array detections

The number of detections (phases) reported from day 001, 2008, through day 182, 2008, was 137,784, giving an average of 757 detections per processed day (182 days processed).

Events automatically located by the Hagfors array

During days 001, 2008, through 182, 2008, 3,563 local and regional events were located by the Hagfors array, based on automatic association of P- and S-type arrivals. This gives an average of 19.6 events per processed day (182 days processed). 79% of these events are within 300 km, and 95% of these events are within 1000 km.

U. Baadshaug

3.3 FINES (IMS station PS17)

Data from the FINES array are made available continuously to NORSAR through a cooperative agreement with Finnish authorities.

The mission-capable data statistics were 99.986%, as compared to 96.691% for the previous reporting period. The net instrument availability was 98.800%.

The main outages in the period are presented in Table 3.3.1.

Day	Period
05 Jan	23.24-00.00
20 Feb	13.57-13.58
21 Feb	10.04-10.05

Table 3.2.1. *The main interruptions in recording of FINES data at NDPC, 1 January - 30 June 2008.*

Monthly uptimes for the FINES on-line data recording task, taking into account all factors (field installations, transmissions line, data center operation) affecting this task were as follows:

2008		Mission Capable	Net instrument availability
January	:	99.920%	99.661%
February	:	99.994%	99.421%
March	:	100%	99.796%
April	:	100%	97.209%
May	:	100%	100%
June	:	100%	96.630%

B. Paulsen

FINES Event Detection Operation

FINES detections

The number of detections (phases) reported during day 001, 2008, through day 182, 2008, was 53,021, giving an average of 291 detections per processed day (182 days processed).

Events automatically located by FINES

During days 001, 2008, through 182, 2008, 2,062 local and regional events were located by FINES, based on automatic association of P- and S-type arrivals. This gives an average of 11.3 events per processed day (182 days processed). 89% of these events are within 300 km, and 95% of these events are within 1000 km.

U. Baadshaug

3.4 Regional Monitoring System Operation and Analysis

The Regional Monitoring System (RMS) was installed at NORSAR in December 1989 and has been operated at NORSAR from 1 January 1990 for automatic processing of data from ARCES and NORES. A second version of RMS that accepts data from an arbitrary number of arrays and single 3-component stations was installed at NORSAR in October 1991, and regular operation of the system comprising analysis of data from the 4 arrays ARCES, NORES, FINES and GERES started on 15 October 1991. As opposed to the first version of RMS, the one in current operation also has the capability of locating events at teleseismic distances.

Data from the Apatity array was included on 14 December 1992, and from the Spitsbergen array on 12 January 1994. Detections from the Hagfors array were available to the analysts and could be added manually during analysis from 6 December 1994. After 2 February 1995, Hagfors detections were also used in the automatic phase association.

Since 24 April 1999, RMS has processed data from all the seven regional arrays ARCES, NORES, FINES, GERES (until January 2000), Apatity, Spitsbergen, and Hagfors. Starting 19 September 1999, waveforms and detections from the NORSAR array have also been available to the analyst.

Phase and event statistics

Table 3.5.1 gives a summary of phase detections and events declared by RMS. From top to bottom the table gives the total number of detections by the RMS, the number of detections that are associated with events automatically declared by the RMS, the number of detections that are not associated with any events, the number of events automatically declared by the RMS, and finally the total number of events worked on interactively (in accordance with criteria that vary over time; see below) and defined by the analyst.

New criteria for interactive event analysis were introduced from 1 January 1994. Since that date, only regional events in areas of special interest (e.g, Spitsbergen, since it is necessary to acquire new knowledge in this region) or other significant events (e.g, felt earthquakes and large industrial explosions) were thoroughly analyzed. Teleseismic events of special interest are also analyzed.

To further reduce the workload on the analysts, a new processing scheme was introduced on 2 February 1995. The GBF (Generalized Beamforming) program is used as a pre-processor to RMS, and only phases associated with selected events in northern Europe are considered in the automatic RMS phase association. All detections, however, are still available to the analysts and can be added manually during analysis.

	Jan 08	Feb 08	Mar 08	Apr 08	May 08	Jun 08	Total
Phase detections	154.415	145.482	161,045	141.179	156,807	141,294	900,222
- Associated phases	4,564	9,622	7,540	6,329	6,086	5,103	39,244
- Unassociated phases	149,851	135,860	153,505	134,850	150,721	136,191	860,978
Events automatically declared by RMS	941	1,719	1,456	1,158	1,155	1,000	7,429
No. of events defined by the analyst	51	182	81	94	94	75	577

Table 3.5.1. RMS phase detections and event summary 1 January - 30 June 2008.

U. Baadshaug

B. Paulsen

4 NDC and Field Activities

4.1 NDC Activitities

NORSAR functions as the Norwegian National Data Center (NDC) for CTBT verification. Six monitoring stations, comprising altogether 132 field sensors plus radionuclide monitoring equipment, will be located on Norwegian territory as part of the future IMS as described elsewhere in this report. The four seismic IMS stations are all in operation today, and all of them are currently providing data to the CTBTO on a regular basis. PS27, PS28, AS73 and RN49 are all certified. The infrasound station in northern Norway is planned to be established within next year. Data recorded by the Norwegian stations is being transmitted in real time to the Norwegian NDC, and provided to the IDC through the Global Communications Infrastructure (GCI). Norway is connected to the GCI with a frame relay link to Vienna.

Operating the Norwegian IMS stations continues to require significant efforts by personnel both at the NDC and in the field. Strictly defined procedures as well as increased emphasis on regularity of data recording and timely data transmission to the IDC in Vienna have led to increased reporting activities and implementation of new procedures for the NDC. The NDC carries out all the technical tasks required in support of Norway's treaty obligations. NORSAR will also carry out assessments of events of special interest, and advise the Norwegian authorities in technical matters relating to treaty compliance. A challenge for the NDC is to carry 40 years' experience over to the next generation of personnel.

Verification functions; information received from the IDC

After the CTBT enters into force, the IDC will provide data for a large number of events each day, but will not assess whether any of them are likely to be nuclear explosions. Such assessments will be the task of the States Parties, and it is important to develop the necessary national expertise in the participating countries. An important task for the Norwegian NDC will thus be to make independent assessments of events of particular interest to Norway, and to communicate the results of these analyses to the Norwegian Ministry of Foreign Affairs.

Monitoring the Arctic region

Norway will have monitoring stations of key importance for covering the Arctic, including Novaya Zemlya, and Norwegian experts have a unique competence in assessing events in this region. On several occasions in the past, seismic events near Novaya Zemlya have caused political concern, and NORSAR specialists have contributed to clarifying these issues.

International cooperation

After entry into force of the treaty, a number of countries are expected to establish national expertise to contribute to the treaty verification on a global basis. Norwegian experts have been in contact with experts from several countries with the aim of establishing bilateral or multilateral cooperation in this field. One interesting possibility for the future is to establish NORSAR as a regional center for European cooperation in the CTBT verification activities.

NORSAR event processing

The automatic routine processing of NORSAR events as described in NORSAR Sci. Rep. No. 2-93/94, has been running satisfactorily. The analyst tools for reviewing and updating the solutions have been continually modified to simplify operations and improve results. NORSAR is currently applying teleseismic detection and event processing using the large-aperture NOA array as well as regional monitoring using the network of small-aperture arrays in Fennoscandia and adjacent areas.

Communication topology

Norway has implemented an independent subnetwork, which connects the IMS stations AS72, AS73, PS28, and RN49 operated by NORSAR to the GCI at NOR_NDC. A contract has been concluded and VSAT antennas have been installed at each station in the network. Under the same contract, VSAT antennas for 6 of the PS27 subarrays have been installed for intra-array communication. The seventh subarray is connected to the central recording facility via a leased land line. The central recording facility for PS27 is connected directly to the GCI (Basic Topology). All the VSAT communication is functioning satisfactorily. As of 10 June 2005, AS72 and RN49 are connected to NOR_NDC through a VPN link.

Jan Fyen

4.2 Status Report: Provision of data from Norwegian seismic IMS stations to the IDC

Introduction

This contribution is a report for the period January - June 2008 on activities associated with provision of data from Norwegian seismic IMS stations to the International Data Centre (IDC) in Vienna. This report represents an update of contributions that can be found in previous editions of NORSAR's Semiannual Technical Summary. All four Norwegian seismic stations providing data to the IDC have now been formally certified.

Norwegian IMS stations and communications arrangements

During the reporting interval, Norway has provided data to the IDC from the four seismic stations shown in Fig. 4.2.1. PS27 —NOA is a 60 km aperture teleseismic array, comprised of 7 subarrays, each containing six vertical short period sensors and a three-component broadband instrument. PS28 — ARCES is a 25-element regional array with an aperture of 3 km, whereas AS72 — Spitsbergen array (station code SPITS) has 9 elements within a 1-km aperture. AS73 — JMIC has a single three-component broadband instrument.

The intra-array communication for NOA utilizes a land line for subarray NC6 and VSAT links based on TDMA technology for the other 6 subarrays. The central recording facility for NOA is located at the Norwegian National Data Center (NOR_NDC).

Continuous ARCES data are transmitted from the ARCES site to NOR_NDC using a 64 kbits/s VSAT satellite link, based on BOD technology.

Continuous SPITS data were transmitted to NOR_NDC via a VSAT terminal located at Platåberget in Longyearbyen (which is the site of the IMS radionuclide monitoring station

RN49 installed during 2001) up to 10 June 2005. The central recording facility (CRF) for the SPITS array has been moved to the University of Spitsbergen (UNIS). A 512 bps SHDSL link has been established between UNIS and NOR_NDC. Data from the array elements to the CRF are transmitted via a 2.4 Ghz radio link (Wilan VIP-110). Both AS72 and RN49 data are now transmitted to NOR_NDC over this link using VPN technology.

A minimum of seven-day station buffers have been established at the ARCES and SPITS sites and at all NOA subarray sites, as well as at the NOR_NDC for ARCES, SPITS and NOA. In addition, each individual site of the SPITS array has a 14-day buffer.

The NOA and ARCES arrays are primary stations in the IMS network, which implies that data from these stations is transmitted continuously to the receiving international data center. Since October 1999, this data has been transmitted (from NOR_NDC) via the Global Communications Infrastructure (GCI) to the IDC in Vienna. Data from the auxiliary array station SPITS — AS72 have been sent in continuous mode to the IDC during the reporting period. AS73 — JMIC is an auxiliary station in the IMS, and the JMIC data have been available to the IDC throughout the reporting period on a request basis via use of the AutoDRM protocol (Kradolfer, 1993; Kradolfer, 1996). In addition, continuous data from all three arrays is transmitted to the US_NDC.

Uptimes and data availability

Figs. 4.2.2 and 4.2.3 show the monthly uptimes for the Norwegian IMS primary stations ARCES and NOA, respectively, for the reporting period given as the hatched (taller) bars in these figures. These barplots reflect the percentage of the waveform data that is available in the NOR_NDC data archives for these two arrays. The downtimes inferred from these figures thus represent the cumulative effect of field equipment outages, station site to NOR_NDC communication outage, and NOR_NDC data acquisition outages.

Figs. 4.2.2 and 4.2.3 also give the data availability for these two stations as reported by the IDC in the IDC Station Status reports. The main reason for the discrepancies between the NOR_NDC and IDC data availabilities as observed from these figures is the difference in the ways the two data centers report data availability for arrays: Whereas NOR_NDC reports an array station to be up and available if at least one channel produces useful data, the IDC uses weights where the reported availability (capability) is based on the number of actually operating channels.

Use of the AutoDRM protocol

NOR_NDC's AutoDRM has been operational since November 1995 (Mykkeltveit & Baadshaug, 1996). The monthly number of requests by the IDC for JMIC data for the period January - June 2008 is shown in Fig. 4.2.4.

NDC automatic processing and data analysis

These tasks have proceeded in accordance with the descriptions given in Mykkeltveit and Baadshaug (1996). For the reporting period NOR_NDC derived information on 425 supplementary events in northern Europe and submitted this information to the Finnish NDC as the NOR_NDC contribution to the joint Nordic Supplementary (Gamma) Bulletin, which in turn is forwarded to the IDC. These events are plotted in Fig. 4.2.5.

Data access for the station NIL at Nilore, Pakistan

NOR_NDC continued to provide access to the seismic station NIL at Nilore, Pakistan, through a VSAT satellite link between NOR_NDC and Pakistan's NDC in Nilore. On 10 December 2006, the VSAT ground station in Nilore was damaged by lightning. It was brought back into operation on 14 December 2006 through use of spare units stored on-site.

Current developments and future plans

NOR_NDC is continuing the efforts towards improving and hardening all critical data acquisition and data forwarding hardware and software components, so as to meet the requirements related to operation of IMS stations.

The NOA array was formally certified by the PTS on 28 July 2000, and a contract with the PTS in Vienna currently provides partial funding for operation and maintenance of this station. The ARCES array was formally certified by the PTS on 8 November 2001, and a contract with the PTS is in place which also provides for partial funding of the operation and maintenance of this station. The operation of the two IMS auxiliary seismic stations on Norwegian territory (Spitsbergen and Jan Mayen) is funded by the Norwegian Ministry of Foreign Affairs. Provided that adequate funding continues to be made available (from the PTS and the Norwegian Ministry of Foreign Affairs), we envisage continuing the provision of data from all Norwegian seismic IMS stations without interruption to the IDC in Vienna.

U. Baadshaug
S. Mykkeltveit
J. Fyen

References

Kradolfer, U. (1993): Automating the exchange of earthquake information. *EOS, Trans., AGU*, 74, 442.

Kradolfer, U. (1996): AutoDRM — The first five years, *Seism. Res. Lett.*, 67, 4, 30-33.

Mykkeltveit, S. & U. Baadshaug (1996): Norway's NDC: Experience from the first eighteen months of the full-scale phase of GSETT-3. *Semiann. Tech. Summ., 1 October 1995 - 31 March 1996*, NORSAR Sci. Rep. No. 2-95/96, Kjeller, Norway.

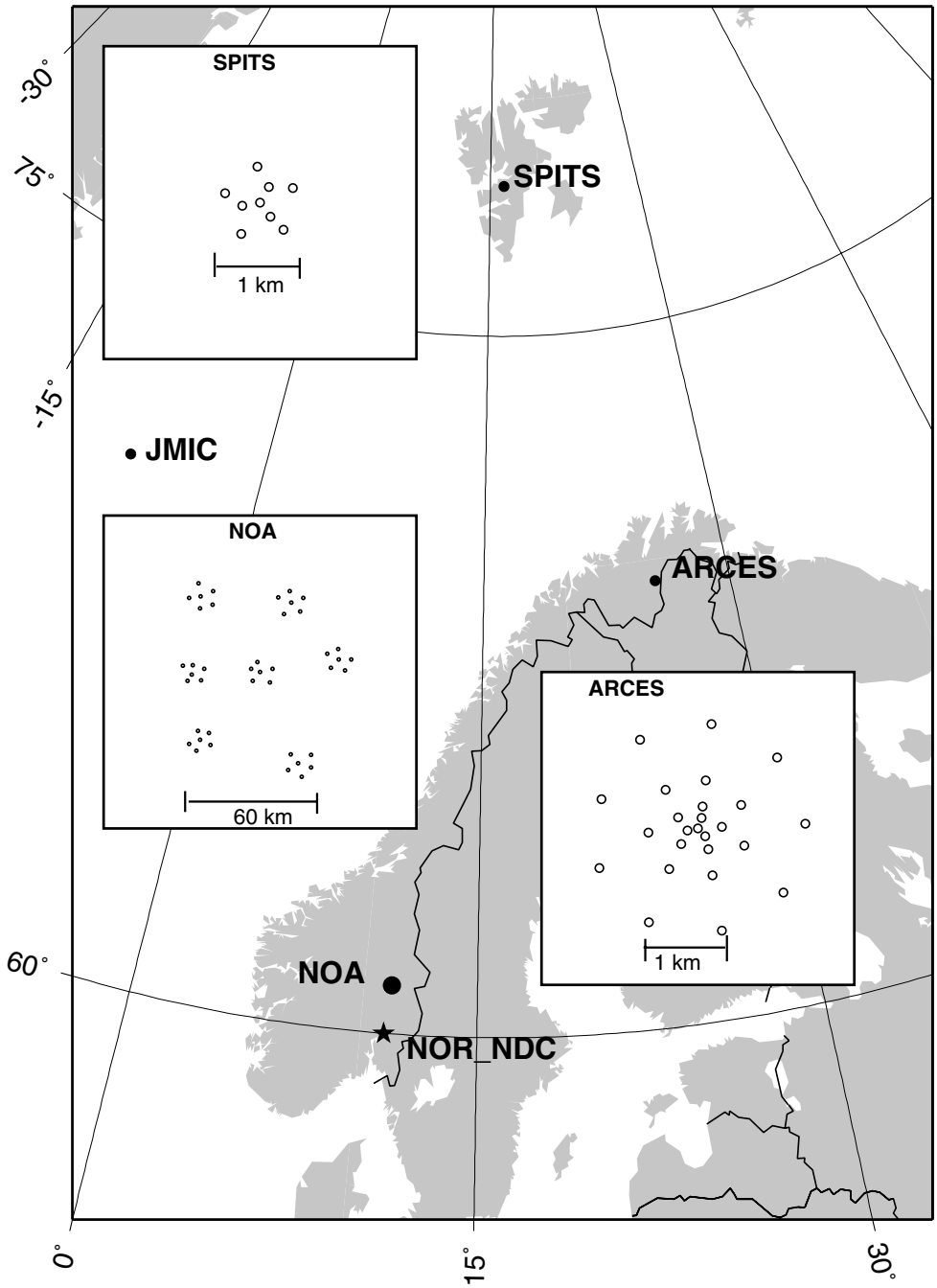

Fig. 4.2.1. The figure shows the locations and configurations of the three Norwegian seismic IMS array stations that provided data to the IDC during the period January - June 2008. The data from these stations and the JMIC three-component station are transmitted continuously and in real time to the Norwegian NDC (NOR_NDC). The stations NOA and ARCES are primary IMS stations, whereas SPITS and JMIC are auxiliary IMS stations.

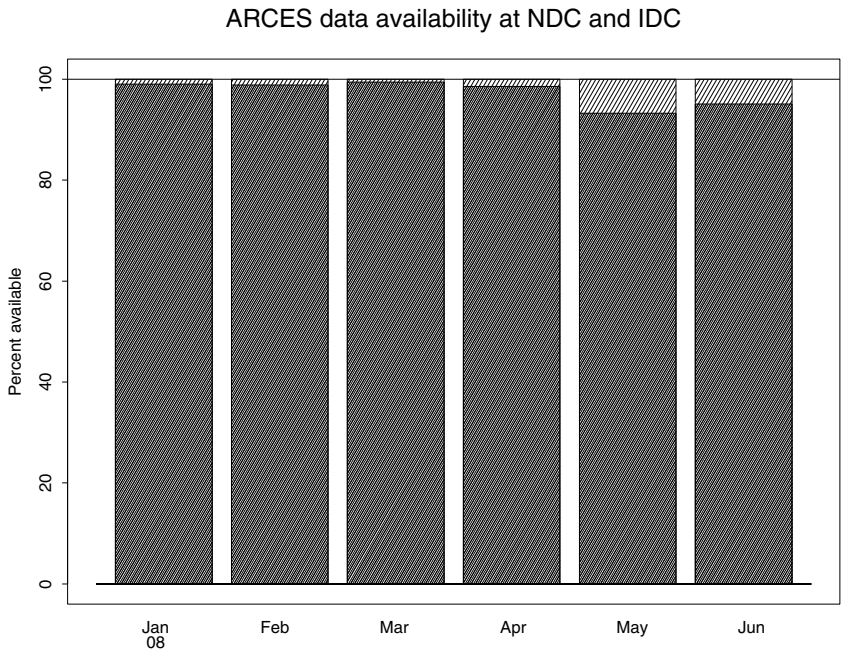

Fig. 4.2.2. The figure shows the monthly availability of ARCES array data for the period January - June 2008 at NOR_NDC and the IDC. See the text for explanation of differences in definition of the term "data availability" between the two centers. The higher values (hatched bars) represent the NOR_NDC data availability.

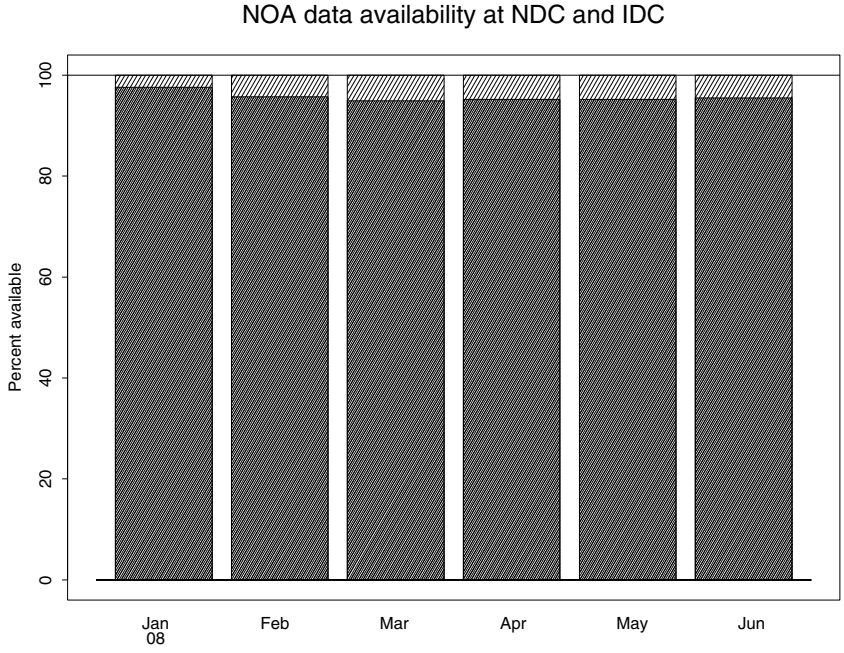

Fig. 4.2.3. The figure shows the monthly availability of NORSAR array data for the period January - June 2008 at NOR_NDC and the IDC. See the text for explanation of differences in definition of the term "data availability" between the two centers. The higher values (hatched bars) represent the NOR_NDC data availability.

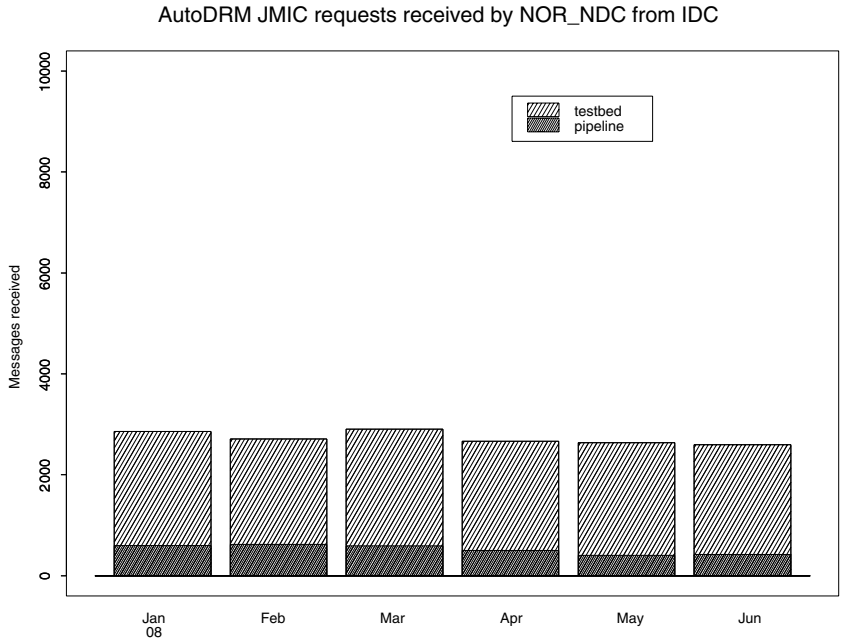

Fig. 4.2.4. The figure shows the monthly number of requests received by NOR_NDC from the IDC for JMIC waveform segments during January - June 2008.

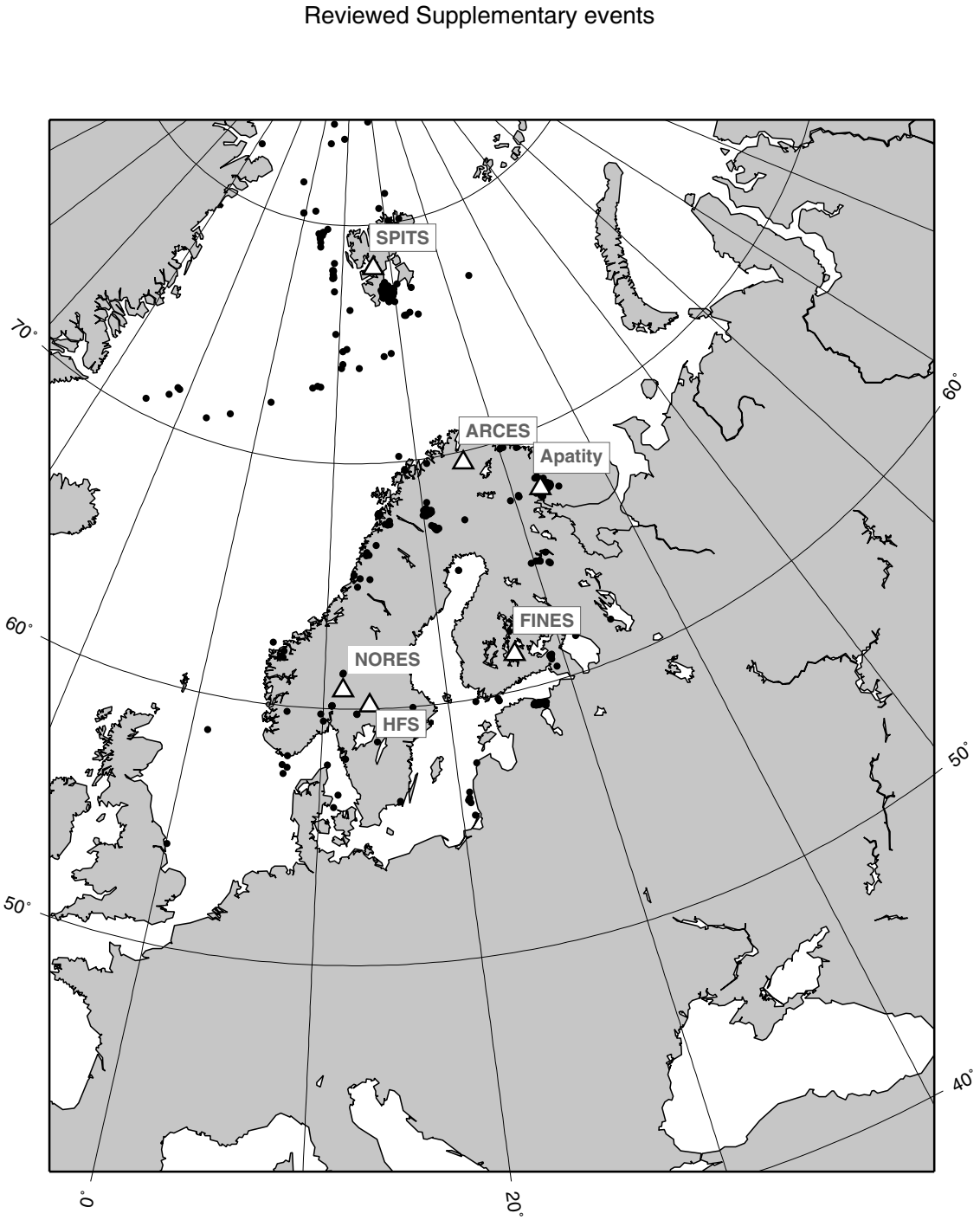

Fig. 4.2.5. The map shows the 705 events in and around Norway contributed by NOR_NDC during January - June 2008 as supplementary (Gamma) events to the IDC, as part of the Nordic supplementary data compiled by the Finnish NDC. The map also shows the main seismic stations used in the data analysis to define these events.

4.3 Field Activities

The activities at the NORSAR Maintenance Center (NMC) at Hamar currently include work related to operation and maintenance of the following IMS seismic stations: the NOA teleseismic array (PS27), the ARCES array (PS28) and the Spitsbergen array (AS72). Some work has also been carried out in connection with the seismic station on Jan Mayen (AS73), the radionuclide station at Spitsbergen (RN49), and preparations for the infrasound station at Karasjok (IS37). NORSAR also acts as a consultant for the operation and maintenance of the Hagfors array in Sweden (AS101).

NORSAR carries out the field activities relating to IMS stations in a manner generally consistent with the requirements specified in the appropriate IMS Operational Manuals, which are currently being developed by Working Group B of the Preparatory Commission. For seismic stations these specifications are contained in the Operational Manual for Seismological Monitoring and the International Exchange of Seismological Data (CTBT/WGB/TL-11/2), currently available in a draft version.

All regular maintenance on the NORSAR field systems is conducted on a one-shift-per-day, five-day-per-week basis. The maintenance tasks include:

- Operating and maintaining the seismic sensors and the associated digitizers, authentication devices and other electronics components.
- Maintaining the power supply to the field sites as well as backup power supplies.
- Operating and maintaining the VSATs, the data acquisition systems and the intra-array data transmission systems.
- Assisting the NDC in evaluating the data quality and making the necessary changes in gain settings, frequency response and other operating characteristics as required.
- Carrying out preventive, routine and emergency maintenance to ensure that all field systems operate properly.
- Maintaining a computerized record of the utilization, status, and maintenance history of all site equipment.
- Providing appropriate security measures to protect against incidents such as intrusion, theft and vandalism at the field installations.

Details of the daily maintenance activities are kept locally. As part of its contract with CTBTO/PTS NORSAR submits, when applicable, problem reports, outage notification reports and equipment status reports. The contents of these reports and the circumstances under which they will be submitted are specified in the draft Operational Manual.

P.W. Larsen
K.A. Løken

5 Documentation Developed

Gibbons, S.J., F. Ringdal & T. Kværna (2008): Detection and characterization of seismic phases using continuous spectral estimation on incoherent and partially coherent arrays. Geophys. J. Int., 172, 405-421.

Pirli, M. & J. Schweitzer (2008): Continued overview of NORSAR system responses: The NORES and ARCES arrays. In: Semiannual Technical Summary, 1 January - 30 June 2008, NORSAR Sci. Rep. 2-2008, Kjeller.

Ringdal, F., T. Kværna & S.J. Gibbons (2008): Initial studies of high-frequency signals recorded at ARCES. In: Semiannual Technical Summary, 1 January - 30 June 2008, NORSAR Sci. Rep. 2-2008, Kjeller.

Ringdal, F., T. Kværna & S.J. Gibbons (2008): Initial studies of signals recorded by ARCES infrasound sensors. In: Semiannual Technical Summary, 1 January - 30 June 2008, NORSAR Sci. Rep. 2-2008, Kjeller.

Roth, M., J. Fyen & P.W. Larsen (2008): Setup of an experimental infrasound deployment within the ARCES array. In: Semiannual Technical Summary, 1 January - 30 June 2008, NORSAR Sci. Rep. 2-2008, Kjeller.

6 Summary of Technical Reports /Papers Published

6.1 Initial studies of high-frequency signals recorded at ARCES

Sponsored by US Army Space and Missile Defence Command, Contract No. W9113M-05-C-0224

1. Introduction

Over the years, the regional processing system at NORSAR has detected a number of small seismic events on or near Novaya Zemlya. As estimated by Ringdal (1997), the threshold of the array network to confidently detect and locate seismic events in this region is about magnitude 2.5. The two regional arrays Spitsbergen and ARCES are by far the most sensitive monitoring stations for Novaya Zemlya and adjacent regions, and these two arrays therefore effectively determine the monitoring capability of the network for that area.

Until 2005, the sampling rates of the Spitsbergen and ARCES arrays were 40 Hz, which limited the frequency range of recorded signals to less than the Nyquist frequency of 20 Hz. Nevertheless, several studies have been carried out emphasizing the outstanding quality of high-frequency seismic recordings and the potential usefulness of such recordings, in particular for the Spitsbergen array. This includes several contributions in previous NORSAR Semiannual Technical Summaries, as well as a publication by Bowers et. al. (2001).

The upgrade in 2005 of the Spitsbergen array, which included the installation of five new three-component seismometers as well as an increase of the sampling rate from 40 to 80 Hz, has resulted in a significant improvement in the processing at Spitsbergen of seismic events at regional distances (Ringdal et al., 2007). For example, S-phase detection at the array has been significantly improved as a result of the data provided by the new three-component seismometers. Furthermore, the increased sample rate has made possible studies of high-frequency propagation up to a Nyquist frequency of 40 Hz. During 2006 and 2007 we recorded four small seismic events close to Novaya Zemlya, and with the increased sampling rate, this enabled us to study the high-frequency propagation across the Barents Sea from Novaya Zemlya to Spitsbergen in some detail. These studies showed that significant signal energy could be observed at frequencies well above 20 Hz, which is remarkable for low-magnitude events (in the range m_b=2.2 to 2.7) at an epicentral distance of more than 1000 km.

One of the recommendations made as a result of these studies was to increase the sampling rate of the ARCES array in order to investigate if the high-frequency propagation could match that observed at Spitsbergen. While this has not been done fully, a recent development has been the installation of additional recording equipment at the center broadband element of ARCES. This new equipment comprises a Guralp digitizer, with a sampling rate of 100 Hz, applied to all three components of the broadband seismometer installation. These data are extracted in parallel with the regular broadband data, which are digitized at a 40 Hz rate, using a Nanometrics digitizer. The high-frequency data have been available at the NORSAR data center since 23 March 2008.

2. High-frequency ARCES recordings

We have carried out an initial investigation of recordings of high-frequency seismic waves at the ARCES array. This contribution describes initial results from these studies. We have analyzed in detail a number of seismic events at regional distances from ARCES, with epicentral distances ranging from 270 to about 1300 km, and assessed the amount of high-frequency signal energy observed at the station.

In the following paragraphs, we discuss in detail some of these observations. The events discussed here are listed in Table 6.1.1, and the locations are shown in Figure 6.1.1. We begin with the closest events, and then proceed to increasing distances.

Event 1: Troms, Norway (Distance 270 km).

This is a small earthquake (magnitude 2.71) at a relatively close distance to ARCES (270 km) and results from processing this event are shown in Figure 6.1.2. Not surprisingly, there is a large amount of signal energy at all frequencies up to the 50 Hz Nyquist frequency. From the filtered time-domain plots, we note that the phases Pg and Lg are most pronounced in the lower frequency bands. In contrast, Pn and Sn are not visible with the 1-2 Hz filter but become successively more pronounced in the higher frequency filter bands. It is also noteworthy, and in fact relatively typical for all the events analyzed so far, that the signal becomes more emergent and with less distinctive onset of secondary phases at the highest frequencies.

With regard to signal-to-noise ratio (SNR), we can see from the spectra that the best SNR for the Pn phase is in the 8-16 Hz band. Therefore, the introduction of high frequency sensors would not appear to improve the detection thresholds for earthquakes at these distances, but would be expected to be useful for event characterization.

Events 2 and 3: Kiruna, Sweden (Distance 280 km).

Figure 6.1.3 shows two events (events 2 and 3 in Table 6.1.1) associated with the Kiruna iron ore mine in northern Sweden. These two events occurred only two minutes apart. In both cases, there is observable energy in all the frequency bands shown, but the first (smaller) event, with magnitude only 1.82, has a low SNR in the 30-45 Hz band. The events occurred at a time of day (near 01 a.m. local time) which is characteristic for the explosion practice for this mine, but there is also a known rockburst activity in this underground mine. The second event (magnitude 2.45) is larger than the typical explosions in this mine. It is therefore possible that this event may have been a rockburst, but we have not received confirmation from the mine authorities as of the time of preparing this report.

Event 4: Malmberget/Aitik, Sweden (Distance about 330 km).

Figure 6.1.4 shows another mining event, this time from the Malmberget/Aitik area in northern Sweden. Malmberget is an underground iron ore mine, whereas Aitik is a nearby open-pit copper mine. The timing and size of the event is consistent with the explosion practice at Aitik, although we have not received confirmation from the mine authorities. A particularly interesting observation is madefrom the spectrogram of this event, which shows distinct spectral lines, which is a characteristic feature for many ripple-fired explosions. It appears that the large band-

width provided by the high-frequency recordings could be helpful in some cases identifying ripple-fired mining exposions.

Event 5: Khibiny, Kola Peninsula, Russia (Distance about 400 km).

Figure 6.1.5 shows a typical, large explosion in the Khibiny mine on the Kola Peninsula. The magnitude is 2.53 and the distance to ARCES is about 400 km. Again, we see significant energy well above 30 Hz, mainly for the Pn and Sn phases. At the lowest frequencies, all four phases (Pn, Pg, Sn, Lg) can be observed. The best SNR for the Pn phase in this case is in the 4-8 Hz band. All of the large mining explosions in Khibiny are ripple-fired, and there are indications of banding in the spectrogram, although not as clear as for Event 4.

Event 6: Steigen, northern Norway (Distance about 460 km).

This is an earthquake (magnitude 3.6 as reported by the IDC) in an area known for numerous earthquake sequences in the past. We note in particular the very strong Pg and Lg phases in the two lowest filter bands on Figure 6.1.6. At the higher frequencies, the Pn and Sn phases become increasingly dominant. Again we see significant energy almost up to the Nyquist frequency of 50 Hz, mainly for the Pn and Sn phases.

Event 7: Storfjorden-Heerland, Spitsbergen (Distance about 860 km).

The remaining three cases are at considerably greater distances than the first five. Case 6 is one example of an earthquake in a large earthquake aftershock sequence south of Spitsbergen. The main shock occurred on 21 February 2008 at 02.46.17 GMT. The magnitude of this earthquake was 6.2, making it the largest instrumentally recorded intraplate earthquake in Norway and surrounding areas. An illustration of the heavy aftershock activity is shown on Figure 6.1.7, which is a simulated helicorder plot covering a full day (25 February). Figure 6.1.8 corresponds to one of the aftershocks occurring after the high-frequency system was installed at ARCES. The event magnitude is 4.0 as reported by the IDC. Like for the shorter epicentral distances, we note that there is significant signal energy even above 40 Hz. Again, the Pn and Sn phases are dominant. However, in the 1-2 Hz filter there is a clear Lg phase. This is surprising since we have previously observed that Lg is generally blocked for most paths crossing the Barents Sea. However, the vespagram shown on Figure 6.1.9 leaves no doubt that this is indeed an Lg phase.

Event 8: Knipovich Ridge (Distance about 960 km).

This earthquake, with magnitude 4.1 as reported by the IDC, is the only non-intraplate earthquake in our data set. It is located on the northern Atlantic ridge system, and could be expected to have more dominant low-frequency energy than the other events. We note from Figure 6.1.10 that there is no visible signal in the 30-45 Hz band, but somewhat surprisingly, we note from the waveform plots and the spectra that there is considerable SNR both for Pn and Sn at frequencies as high as the 16-32 Hz band. The best SNR is found between 3 and 10 Hz.

Event 9: North of Svalbard (Distance about 1290 km).

This event, which is shown on Figure 6.1.11, is the event with the greatest epicentral distance (1290 km) from the ARCES array in the data set analyzed. It is an intraplate earthquake,

located on the continental slope north of Spitsbergen, with a travel path crossing the Svalbard archipelago as well as the western Barents Sea. Somewhat surprisingly, even this small earthquake (IDC magnitude 3.8) at such a large distance shows significant high frequency signal energy in the 30-45 Hz band, especially for the Sn phase. Just like for the Storfjorden-Heerland event, we see clear evidence of the Lg phase in the lowest frequency band (1-2 Hz), which is also surprising. The presence of the Lg phase is confirmed in the vespagram shown in Figure 6.1.12, although it is not quite as pronounced as for Event 7.

3. Conclusions

We have carried out an initial study of seismic events at regional distances recorded by the ARCES high-frequency seismic system, which was installed on 23 March 2008. The main conclusion is that these new observations consistently show remarkably efficient propagation at frequencies up to 30 Hz and above. This result is similar to what has been previously observed at the Spitsbergen array for paths from Novaya Zemlya crossing the Barents Sea. The Spitsbergen studies showed that energy exceeding 20 Hz can be recorded with good signal-to-noise ratio even for small events at epicentral distances as large as 1000 km and we see the same result in this study.

We would like at this point to give some additional comments about the advantage of high-frequency recordings. Among the filter bands studied here, the best filter band for event detection across intraplate paths generally appears to be either 4-8 Hz or 8-16 Hz. However, the most remarkable feature in this study is the strong SNR even at the highest frequencies (15-30 and 30-45 Hz). While such frequency bands would not be used for detection purposes, the high frequency data could be very important for signal characterization, as also pointed out by Bowers et. al. (2001) in their paper discussing the level of deterrence to possible CTBT violations in the Novaya Zemlya region provided by data from the Spitsbergen array. Another example would be to assist in identifying ripple-fired mining explosions.

We should note that the available high-frequency data so far does not include events to the east and north-east of the ARCES array, and the high-frequency propagation from the Novaya Zemlya region to ARCES is therefore still unknown. As more data is accumulated, we may be in a position to carry out a more detailed study of the propagation characteristics for additional paths in the region, and make a more systematic study of the benefits from combining the high-frequency observations from Spitsbergen and ARCES. The usefulness of the horizontal components for high-frequency S-phase detection, already demonstrated for the Spitsbergen array, is also an area that needs further study for ARCES.

Frode Ringdal
Tormod Kværna
Steven J. Gibbons

References

Bowers, D., P. D. Marshall, and A. Douglas (2001). The level of deterrence provided by data from the SPITS seismometer array to possible violations of the Comprehensive Test Ban in the Novaya Zemlya region, *Geophys. J. Int.*, 146, pp. 425-438.

Ringdal, F. (1997). Study of low-magnitude seismic events near the Novaya Zemlya nuclear test site. *Bull. Seism. Soc. Am.*, **87**, 1563-1575

Ringdal, F., T. Kværna, S. Mykkeltveit, S.J. Gibbons & J. Schweitzer (2007): Basic research on seismic and infrasonic monitoring of the European Arctic. In: Proceedings 29th Monitoring Research Review, Denver, Co., 26-28 September 2007.

Table 1: Events analyzed in this study. Magnitudes are those of the IDC REB where available, otherwise the GBF values automatically calculated at NORSAR are used.

Nr	Date	Origin time	Lat	Lon	Dkm	Region	Magnitude
1	2008/04/24	115-17:14:56.0	69.59	18.57	270.3	Troms, Norway	2.71 (GBF)
2	2008/04/12	103-23:17:05.0	67.77	20.41	285.2	Kiruna, Sweden	1.82 (GBF)
3	2008/04/12	103-23:19:21.0	67.77	20.41	285.2	Kiruna, Sweden	2.45 (GBF)
4	2008/04/01	092-17:08:10.0	67.03	21.09	333.5	Malmberget/Aitik, Sweden	2.12 (GBF)
5	2008/03/23	083-03:24:44.9	67.62	33.72	397.0	Kola Peninsula, Russia	2.53 (GBF)
6	2008/04/11	102-06:02:55.1	67.90	15.09	458.8	Steigen, Nordland, Norway	3.6 (IDC)
7	2008/04/10	101-06:20:00.1	77.02	18.59	863.0	Storfjorden, Svalbard	4.0 (IDC)
8	2008/04/07	098-23:51:14.2	76.38	7.24	961.4	Knipovich Ridge	4.1 (IDC)
9	2008/03/24	084-18:28:18.1	80.89	15.84	1292.5	North of Svalbard	3.8 (IDC)

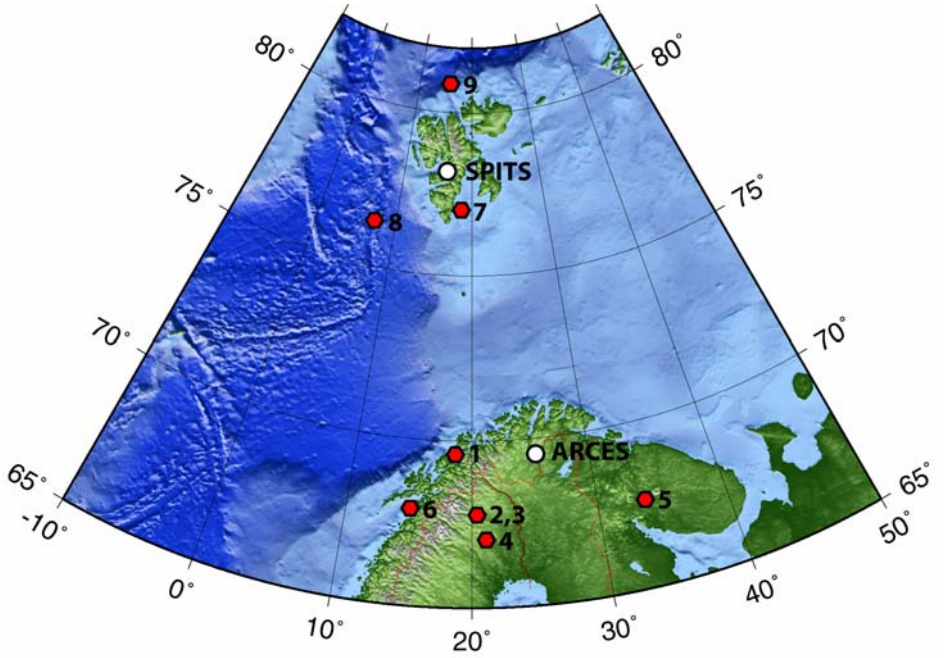

Figure 6.1.1 Map of the European Arctic showing the location of the seismic events discussed in the text, together with the location of the ARCES and Spitsbergen arrays.

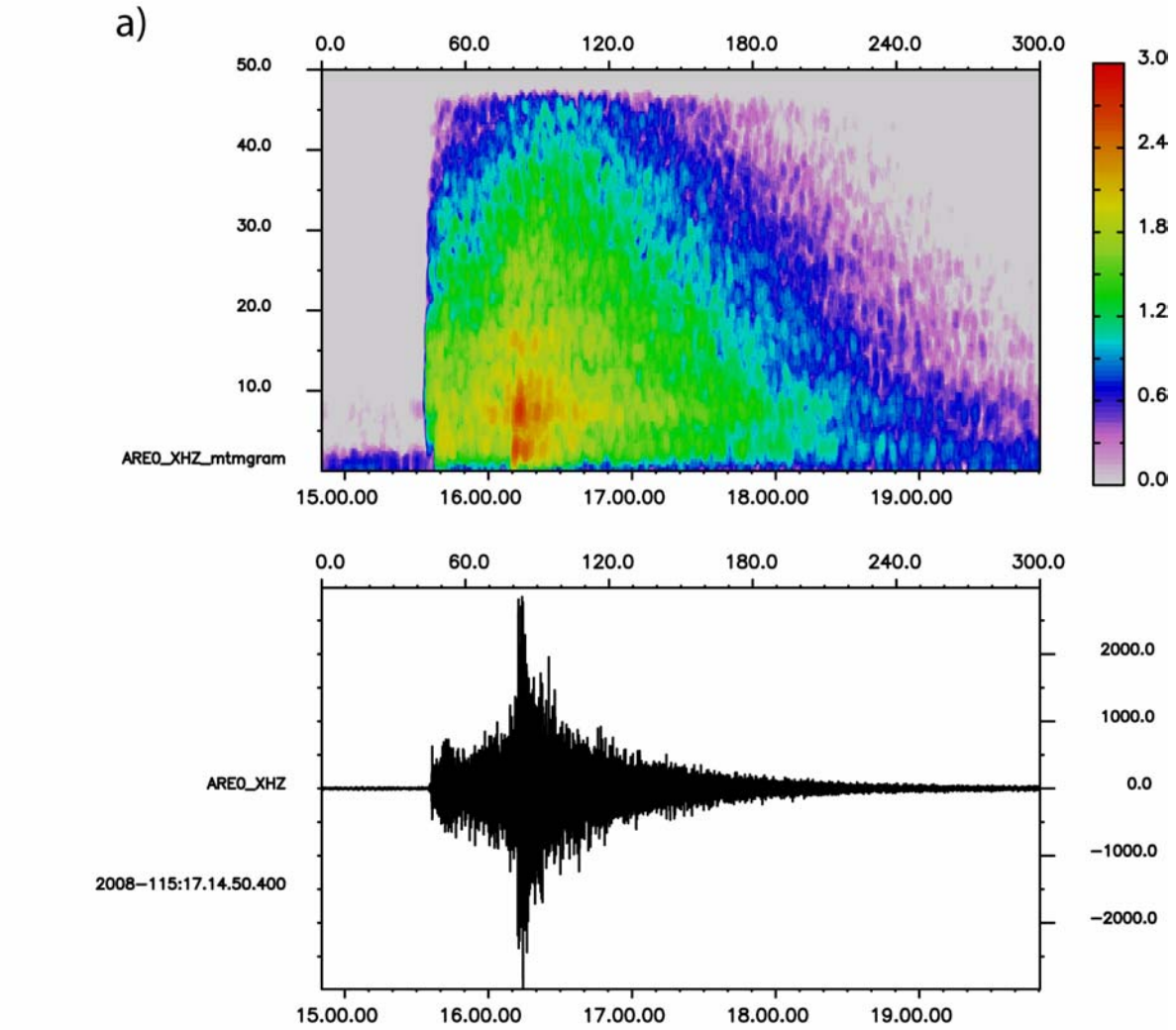

Figure 6.1.2 This page and the next page contain panels showing various displays representing the vertical component of the ARCES high-frequency seismometer for Event 1 (Troms, Norway, at a distance of about 270 km): a) Displays of 5 minutes of spectrogram and waveform plot filtered with a 2.2 Hz high-pass filter. b) Waveform plot filtered in 6 different frequency bands, with the main regional phases indicated. c) Amplitude spectra of noise and the phases indicated in the waveform plot: Noise (magenta), Pn (blue), Lg (green). See text for details.

b)

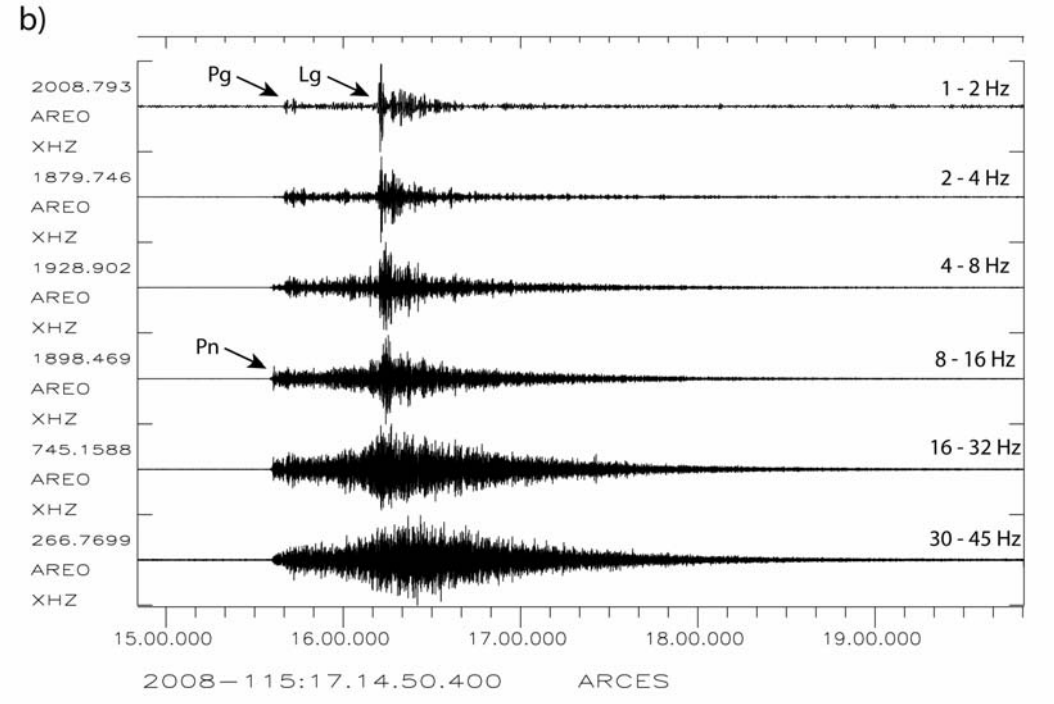
Pg
Lg
Pn
2008.793
AREO
XHZ
1879.746
AREO
XHZ
1928.902
AREO
XHZ
1898.469
AREO
XHZ
745.1588
AREO
XHZ
266.7699
AREO
XHZ
1 - 2 Hz
2 - 4 Hz
4 - 8 Hz
8 - 16 Hz
16 - 32 Hz
30 - 45 Hz
15.00.000
16.00.000
17.00.000
18.00.000
19.00.000
2008—115:17.14.50.400
ARCES

c)

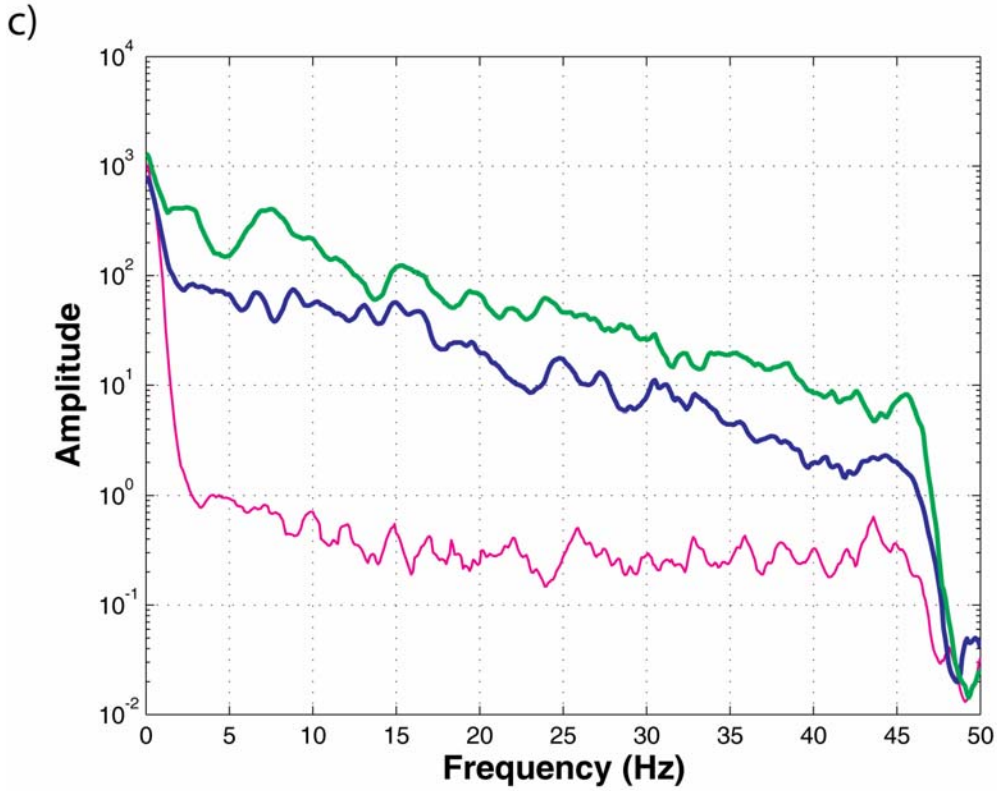
Amplitude
Frequency (Hz)
10^4
10^3
10^2
10^1
10^0
10^{-1}
10^{-2}
0
5
10
15
20
25
30
35
40
45
50

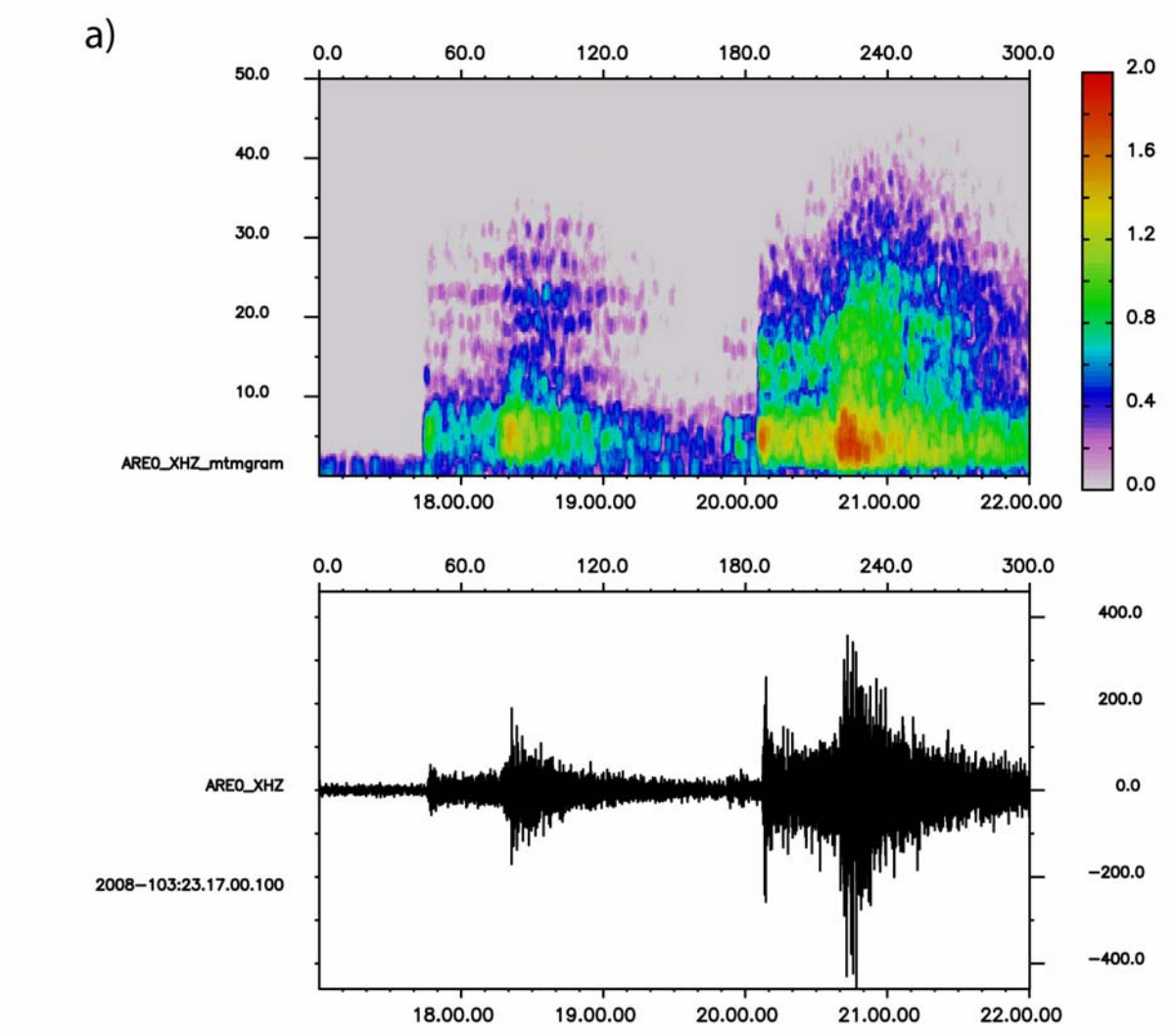

Figure 6.1.3 This page and the next page contain panels showing various displays representing the vertical component of the ARCES high-frequency seismometer for Events 2 and 3 (Kiruna, Sweden, at a distance of about 285 km): a) Displays of 5 minutes of spectrogram and waveform plot filtered with a 2.2 Hz high-pass filter. b) Waveform plot filtered in 6 different frequency bands, with the main regional phases indicated. c) Amplitude spectra for the two events of noise and the phases indicated in the waveform plot: Noise (magenta), Pn (blue), Sn (green). See text for details.

b)

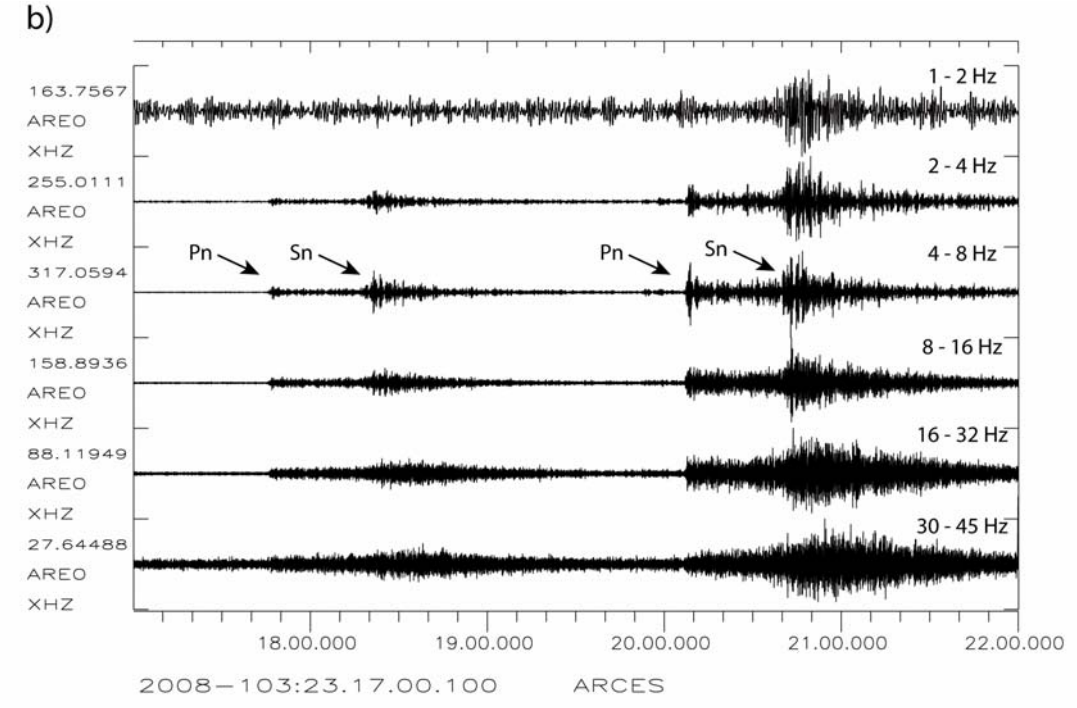
163.7567
AREO
XHZ
255.0111
AREO
XHZ
317.0594
AREO
XHZ
158.8936
AREO
XHZ
88.11949
AREO
XHZ
27.64488
AREO
XHZ
1 - 2 Hz
2 - 4 Hz
4 - 8 Hz
8 - 16 Hz
16 - 32 Hz
30 - 45 Hz
Pn
Sn
Pn
Sn
18.00.000
19.00.000
20.00.000
21.00.000
22.00.000
2008—103:23.17.00.100 ARCES

c)

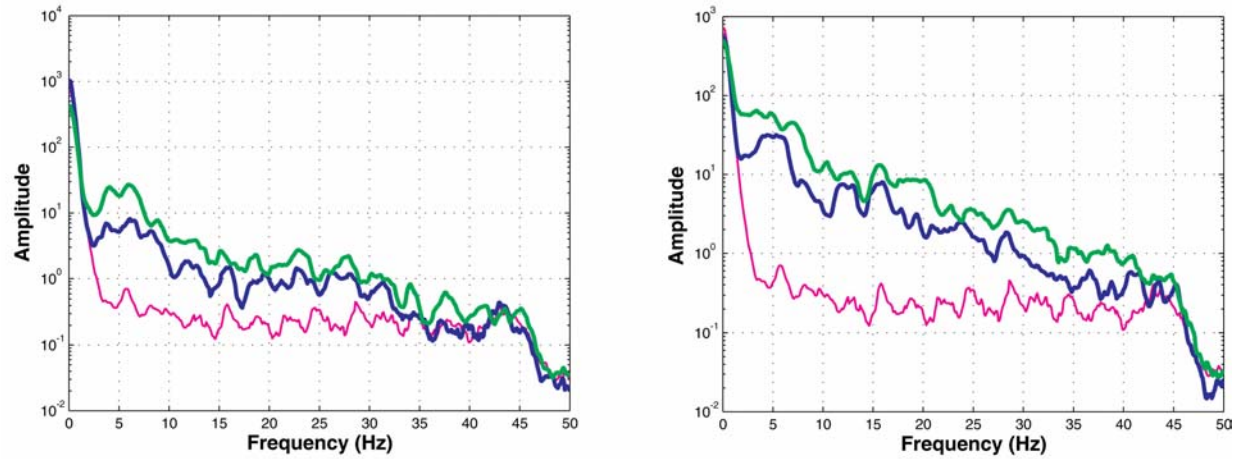
Amplitude
Frequency (Hz)
Amplitude
Frequency (Hz)

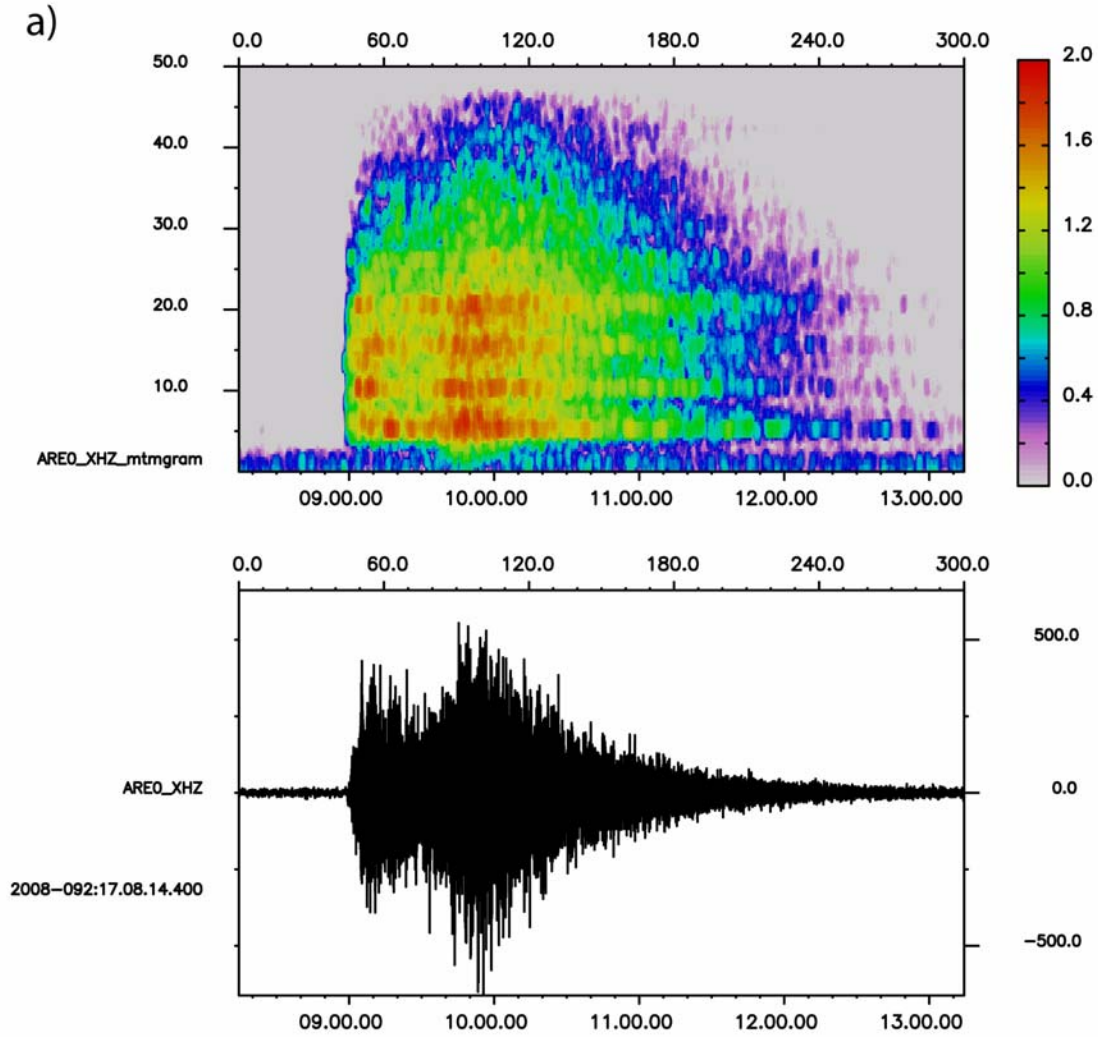

Figure 6.1.4 This page and the next page contain panels showing various displays representing the vertical component of the ARCES high-frequency seismometer for Event 4 Malmberget/ Aitik, Sweden, at a distance of about 330 km): a) Displays of 5 minutes of spectrogram and waveform plot filtered with a 2.2 Hz high-pass filter. b) Waveform plot filtered in 6 different frequency bands, with the main regional phases indicated. c) Amplitude spectra of noise and the phases indicated in the waveform plot: Noise (magenta), Pn (blue), Sn (green). See text for details.

b)

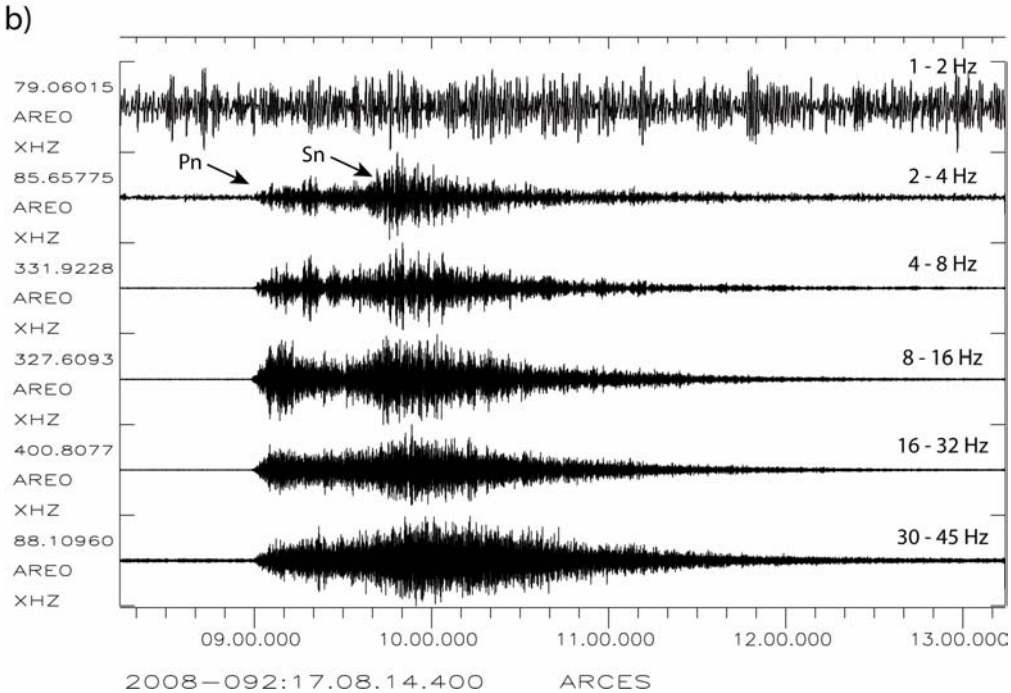
79.06015
AREO
XHZ
85.65775
AREO
XHZ
331.9228
AREO
XHZ
327.6093
AREO
XHZ
400.8077
AREO
XHZ
88.10960
AREO
XHZ
Pn
Sn
1 - 2 Hz
2 - 4 Hz
4 - 8 Hz
8 - 16 Hz
16 - 32 Hz
30 - 45 Hz
09.00.000
10.00.000
11.00.000
12.00.000
13.00.000
2008–092:17.08.14.400 ARCES

c)

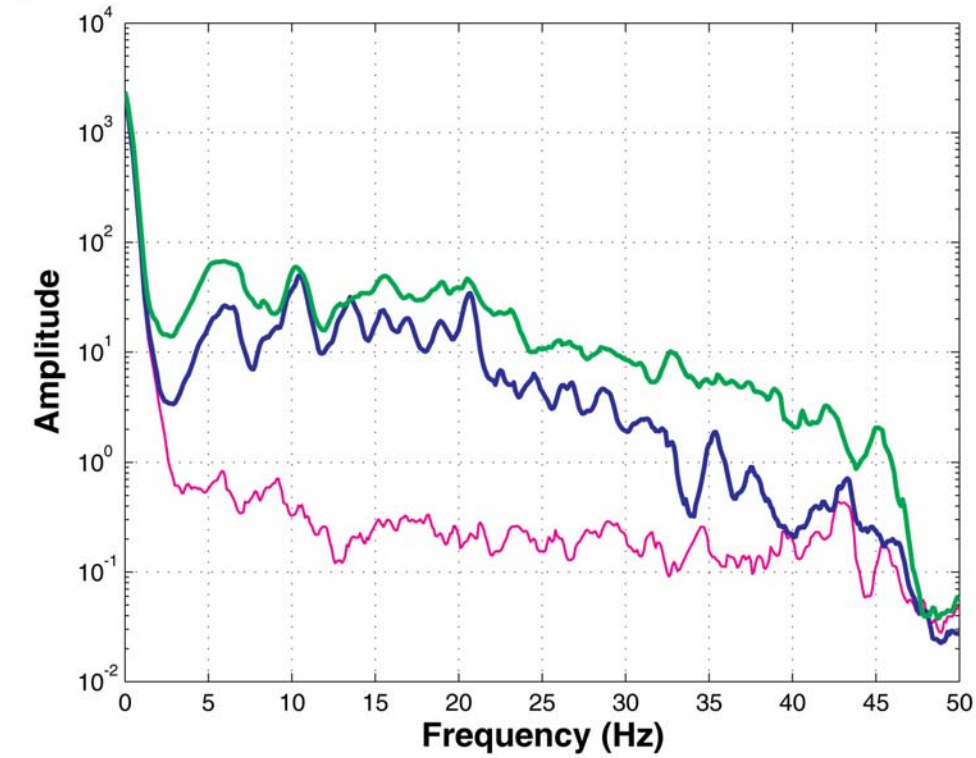
Amplitude
Frequency (Hz)
10^4
10^3
10^2
10^1
10^0
10^{-1}
10^{-2}
0
5
10
15
20
25
30
35
40
45
50

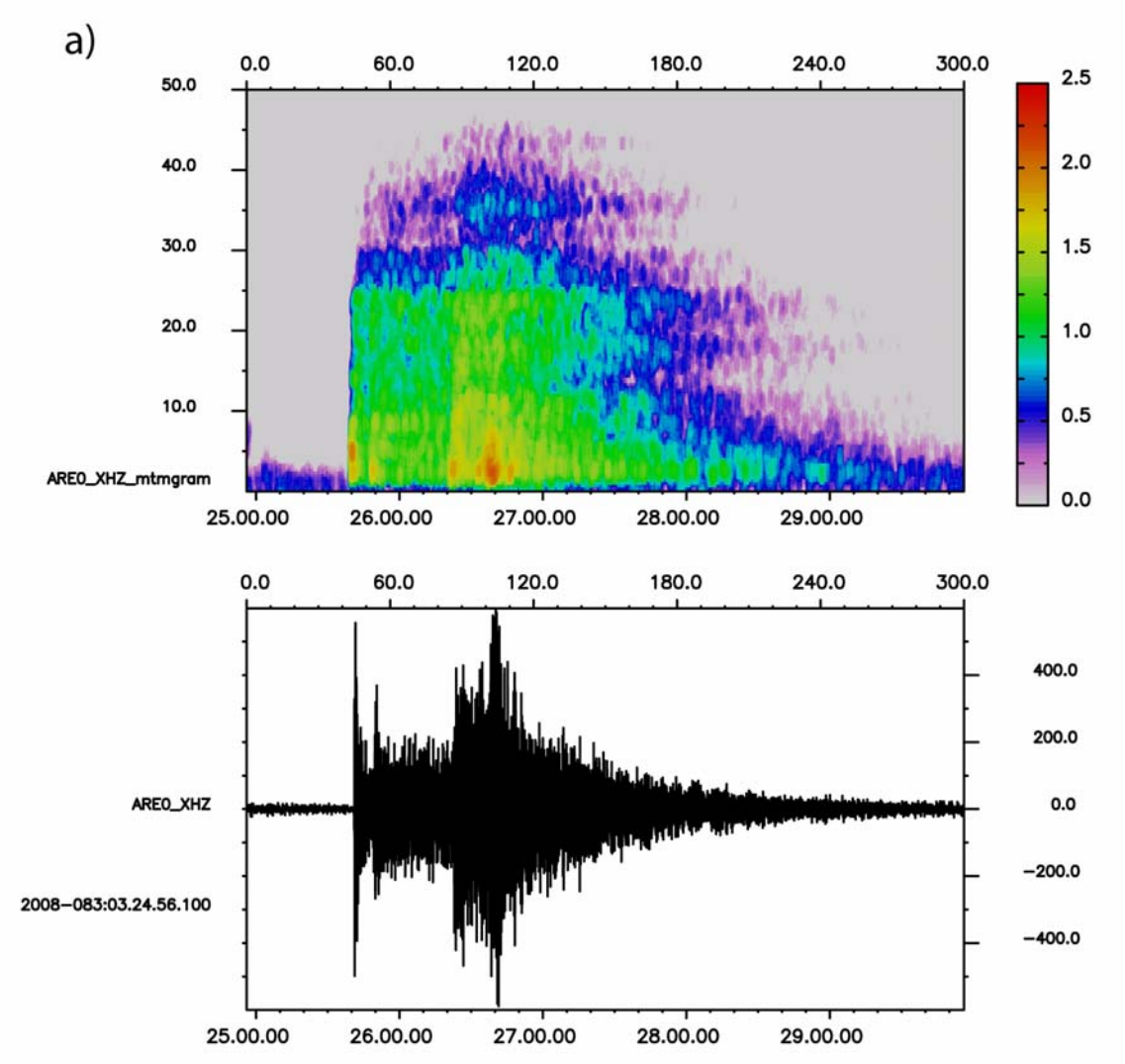

Figure 6.1.5 This page and the next page contain panels showing various displays representing the vertical component of the ARCES high-frequency seismometer for Event 5 (Khibiny, Kola Peninsula, Russia, at a distance of about 400 km): a) Displays of 5 minutes of spectrogram and waveform plot filtered with a 2.2 Hz high-pass filter. b) Waveform plot filtered in 6 different frequency bands, with the main regional phases indicated. c) Amplitude spectra of noise and phases indicated in the waveform plot: Noise (magenta), Pn (blue), Sn (green). See text for details.

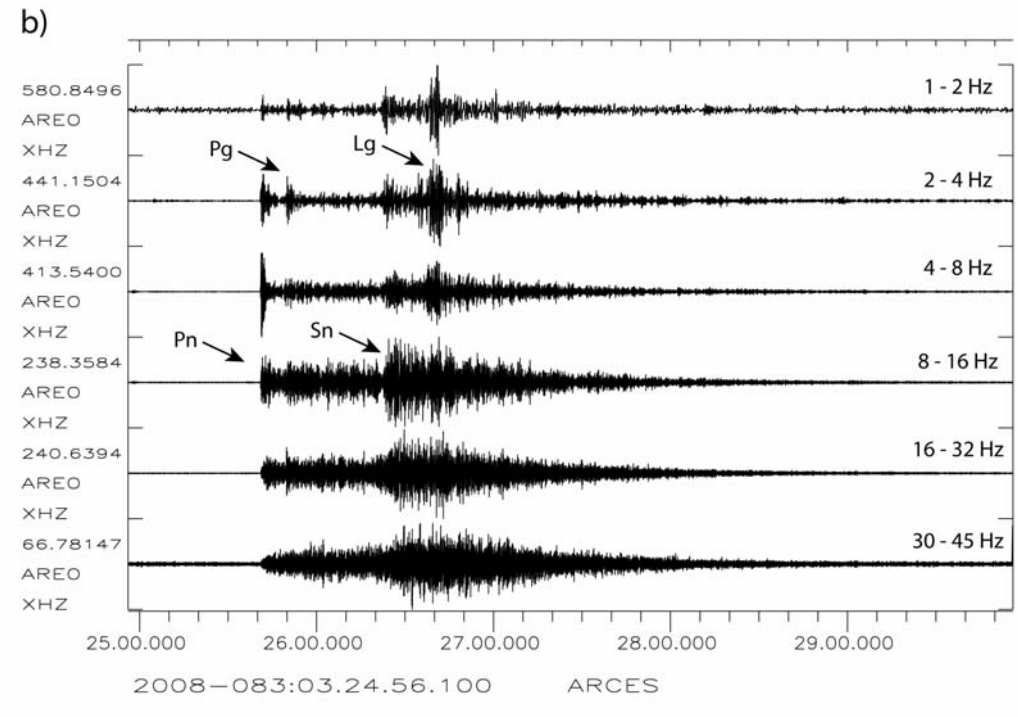
b)
580.8496
AREO
XHZ
441.1504
AREO
XHZ
413.5400
AREO
XHZ
238.3584
AREO
XHZ
240.6394
AREO
XHZ
66.78147
AREO
XHZ
Pg
Lg
Pn
Sn
1 - 2 Hz
2 - 4 Hz
4 - 8 Hz
8 - 16 Hz
16 - 32 Hz
30 - 45 Hz
25.00.000
26.00.000
27.00.000
28.00.000
29.00.000
2008–083:03.24.56.100 ARCES

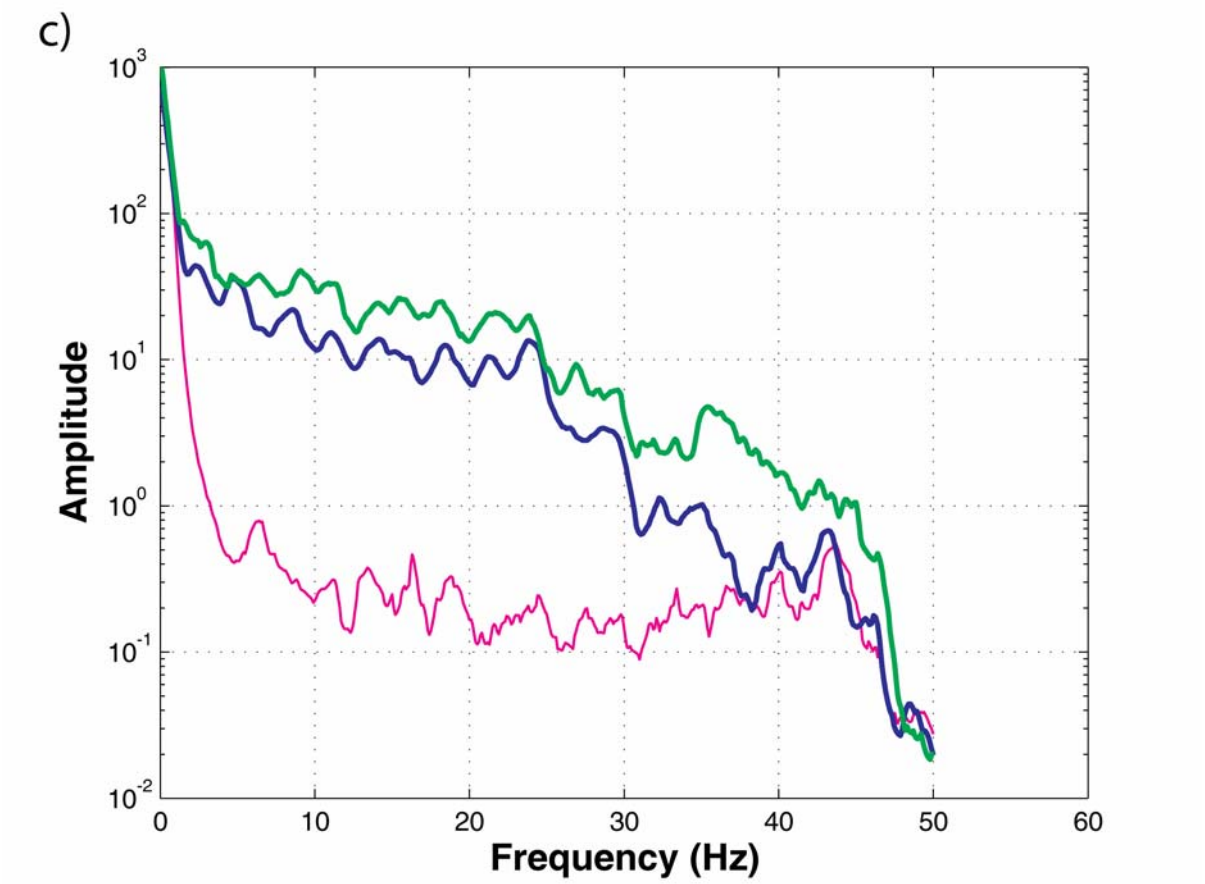
c)
Amplitude
10^3
10^2
10^1
10^0
10^{-1}
10^{-2}
0
10
20
30
40
50
60
Frequency (Hz)

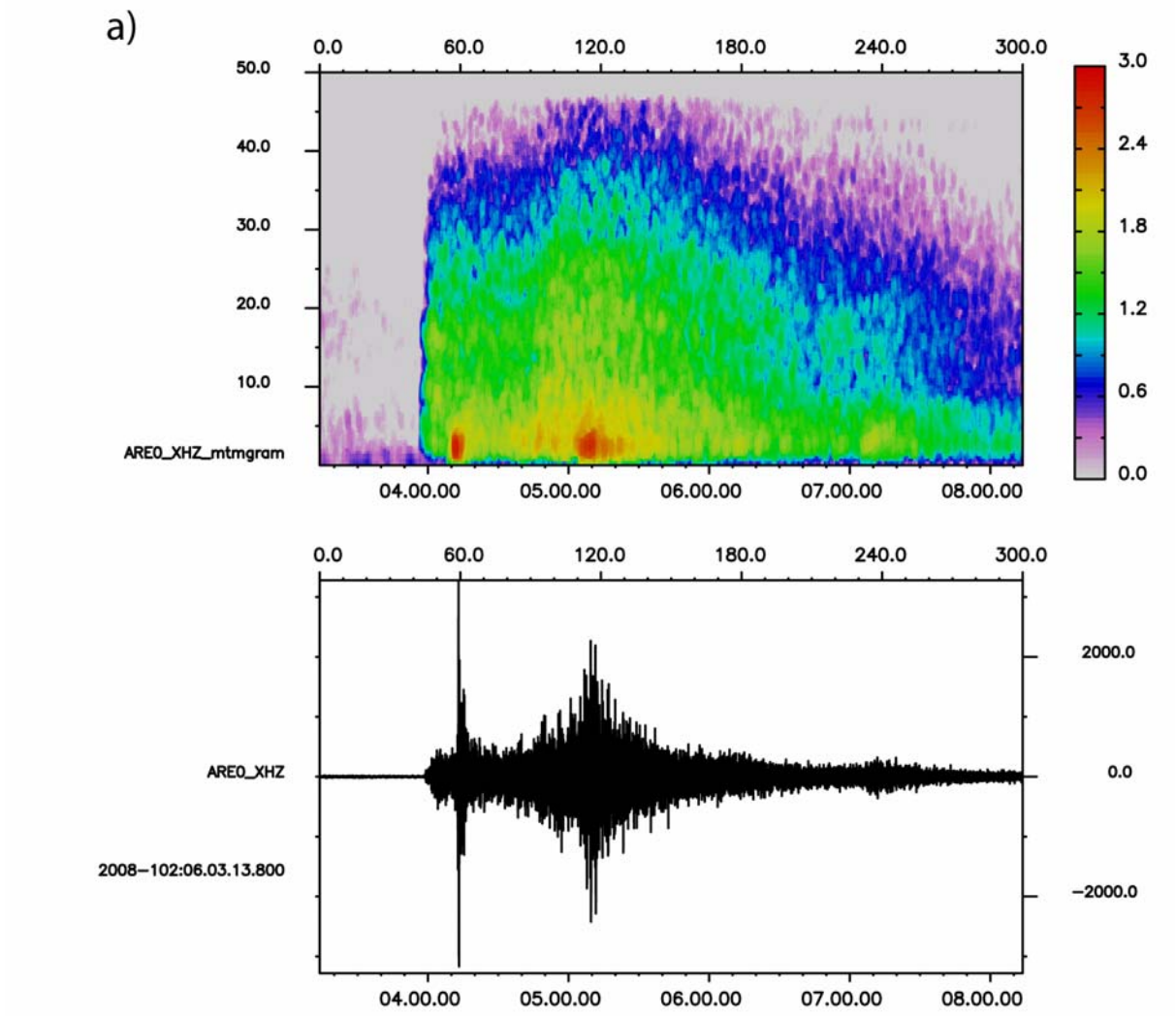

Figure 6.1.6 This page and the next page contain panels showing various displays representing the vertical component of the ARCES high-frequency seismometer for Event 6 (Steigen, Norway, at a distance of about 460 km): a) Displays of 5 minutes of spectrogram and waveform plot filtered with a 2.2 Hz high-pass filter. b) Waveform plot filtered in 6 different frequency bands, with the main regional phases indicated. c) Amplitude spectra of noise and tphases indicated in the waveform plot: Noise (magenta), Pn (blue), Sn (green), Lg (red). See text for details.

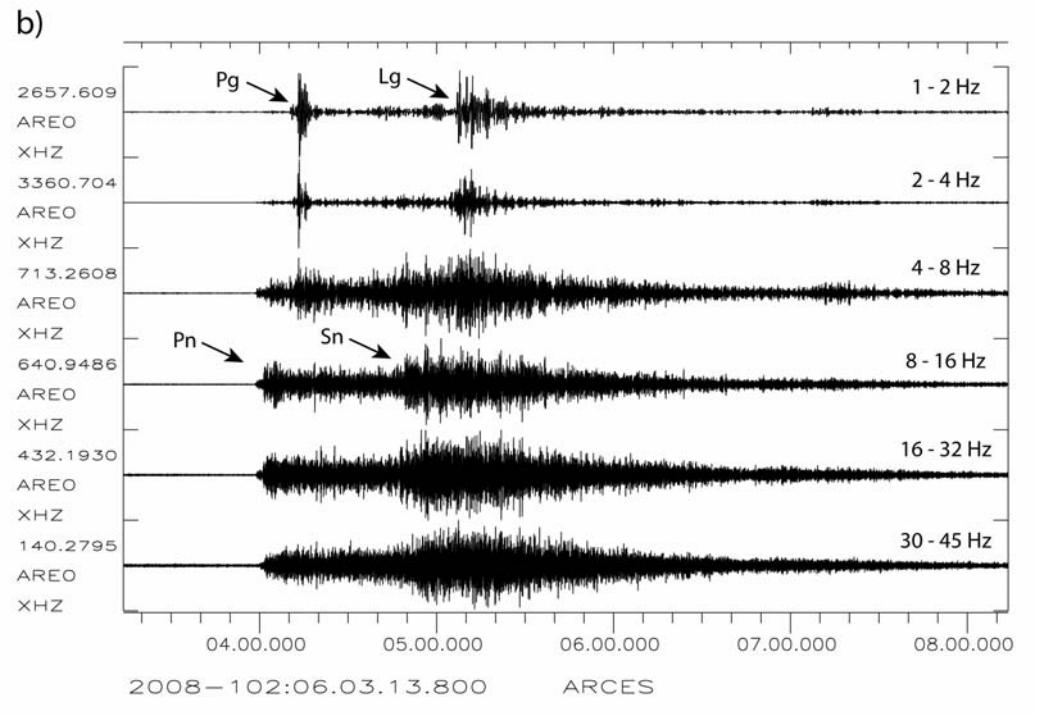
b)
Pg
Lg
Pn
Sn
2657.609
AREO
XHZ
3360.704
AREO
XHZ
713.2608
AREO
XHZ
640.9486
AREO
XHZ
432.1930
AREO
XHZ
140.2795
AREO
XHZ
1 - 2 Hz
2 - 4 Hz
4 - 8 Hz
8 - 16 Hz
16 - 32 Hz
30 - 45 Hz
04.00.000
05.00.000
06.00.000
07.00.000
08.00.000
2008–102:06.03.13.800
ARCES

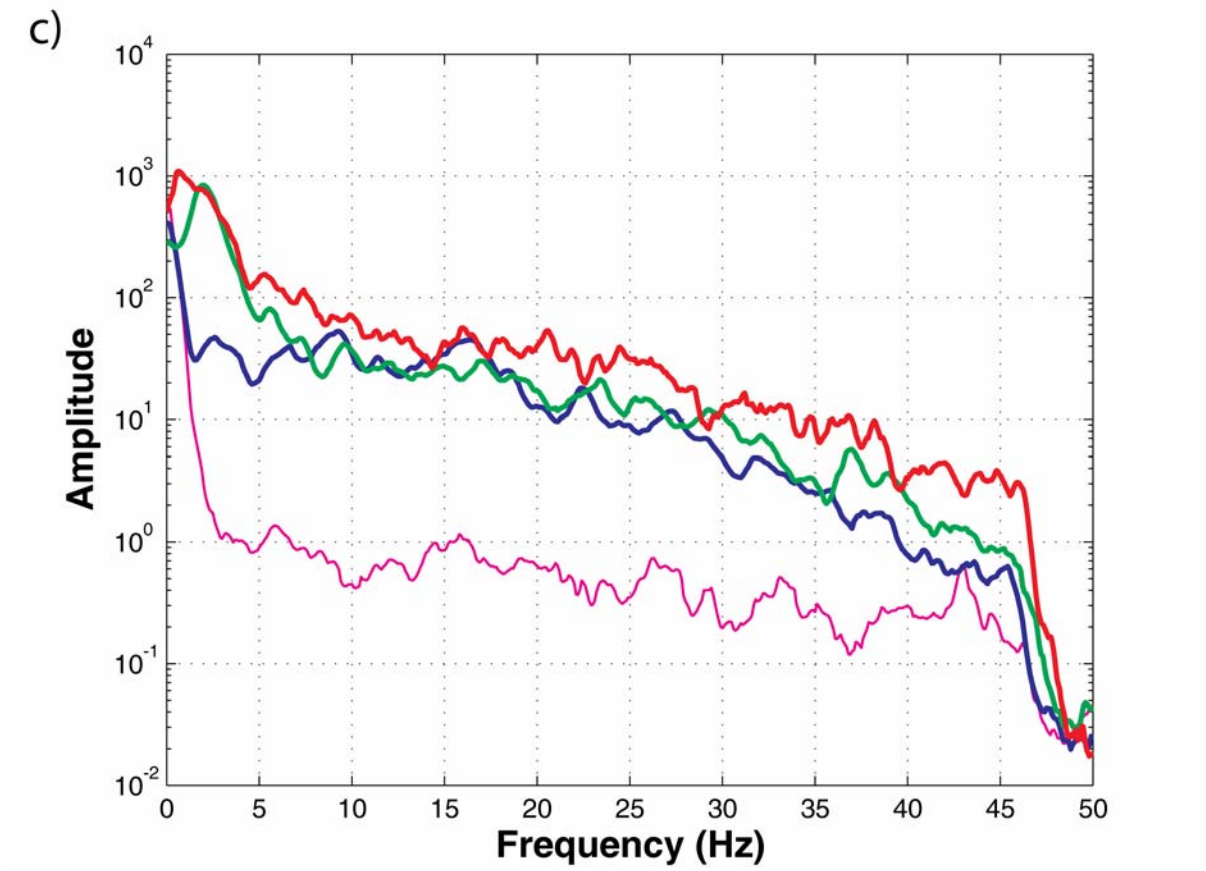
c)
Amplitude
Frequency (Hz)
10^4
10^3
10^2
10^1
10^0
10^{-1}
10^{-2}
0
5
10
15
20
25
30
35
40
45
50

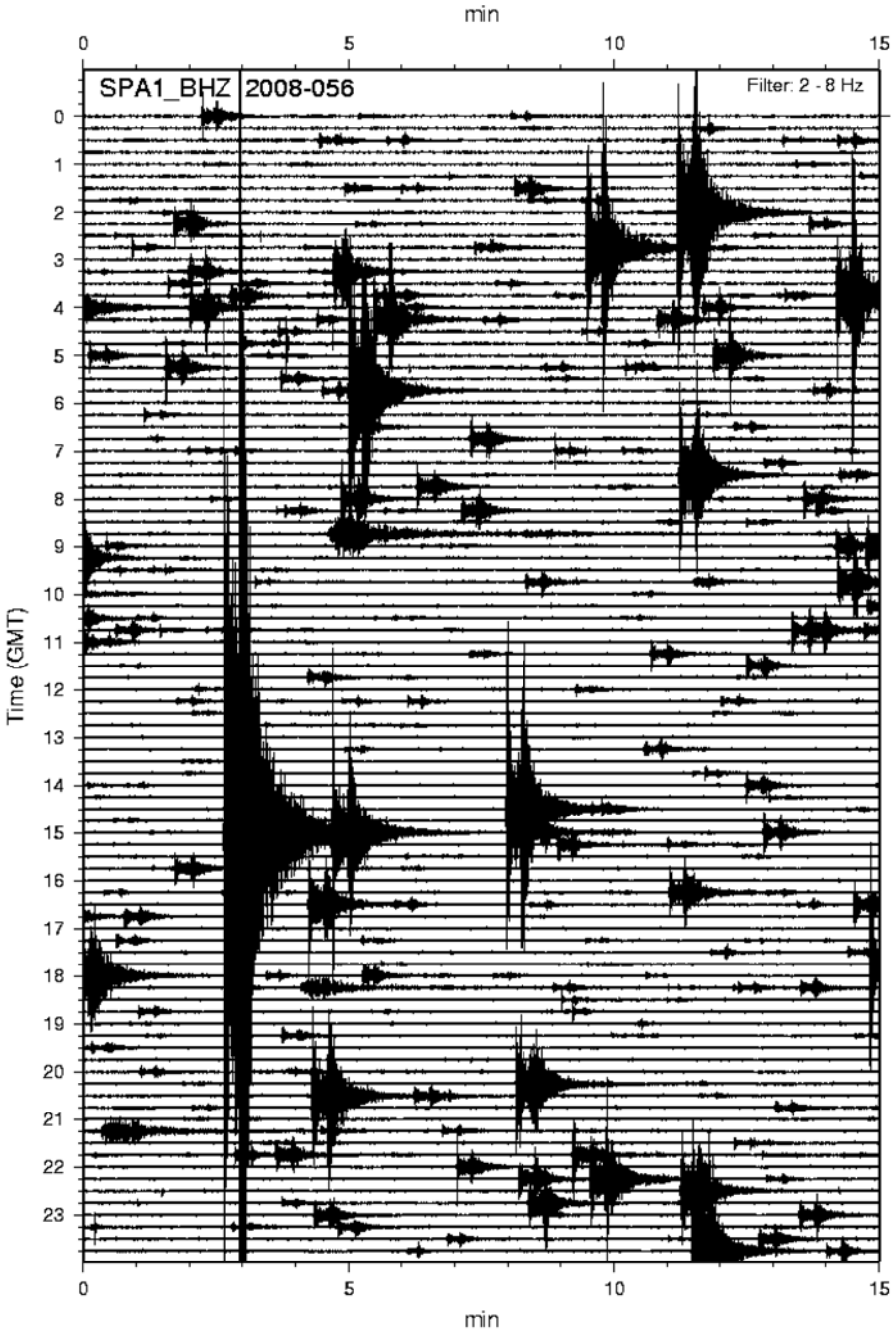

Figure 6.1.7 This figure shows a simulated helicorder plot of one day's data (25 February 2008) as recorded by the Spitsbergen array central vertical component seismometer, filtered in the band 2-8 Hz. This is the fifth day following the large earthquake on 21 February, but as is apparent from the plot, the aftershock activity is still intense.

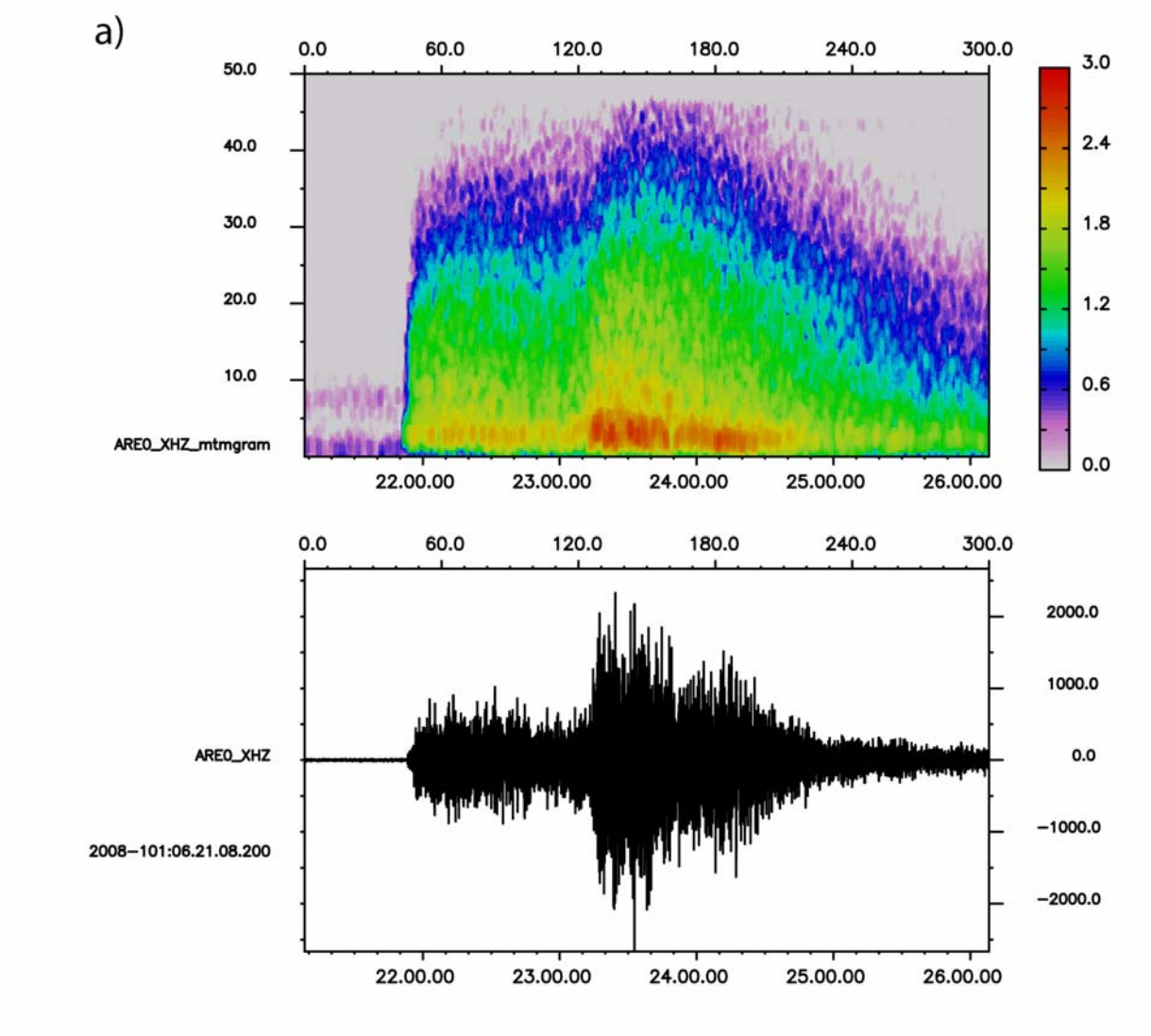

Figure 6.1.8 This page and the next page contain panels showing various displays representing the vertical component of the ARCES high-frequency seismometer for Event 7 (Storfjorden, Svalbard, Norway, at a distance of about 860 km): a) Displays of 5 minutes of spectrogram and waveform plot filtered with a 2.2 Hz high-pass filter. b) Waveform plot filtered in 6 different frequency bands, with the main regional phases indicated. c) Amplitude spectra of noise and tphases indicated in the waveform plot: Noise (magenta), Pn (blue), Sn (green). See text for details.

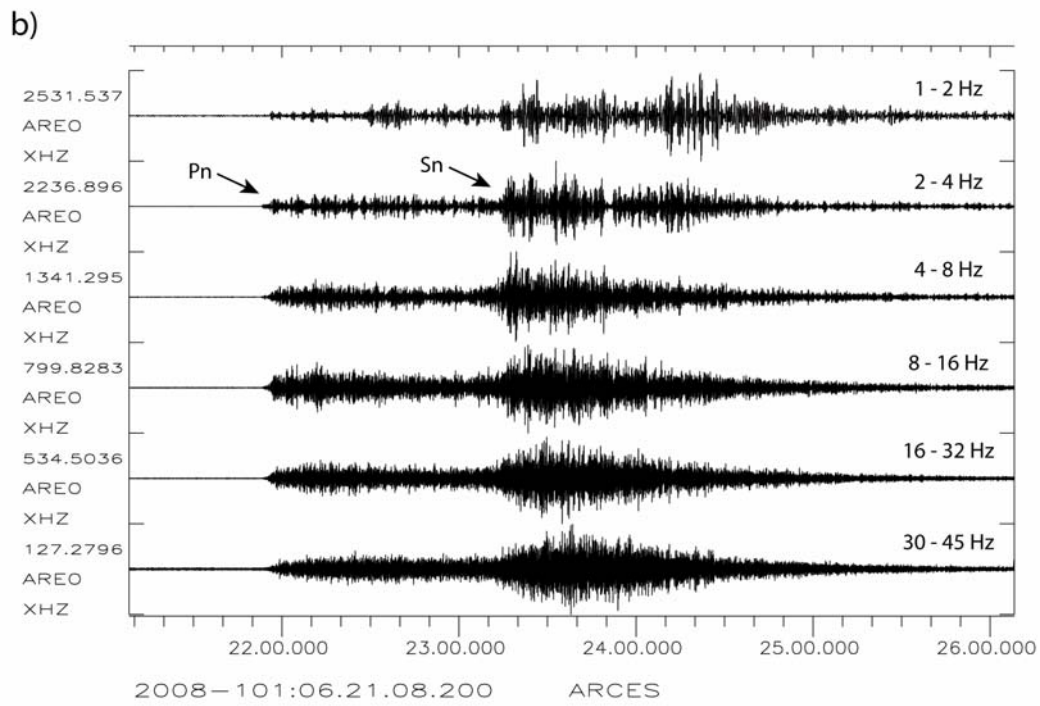
b)
2531.537
AREO
XHZ
2236.896
AREO
XHZ
1341.295
AREO
XHZ
799.8283
AREO
XHZ
534.5036
AREO
XHZ
127.2796
AREO
XHZ
Pn
Sn
1 - 2 Hz
2 - 4 Hz
4 - 8 Hz
8 - 16 Hz
16 - 32 Hz
30 - 45 Hz
22.00.000
23.00.000
24.00.000
25.00.000
26.00.000
2008–101:06.21.08.200 ARCES

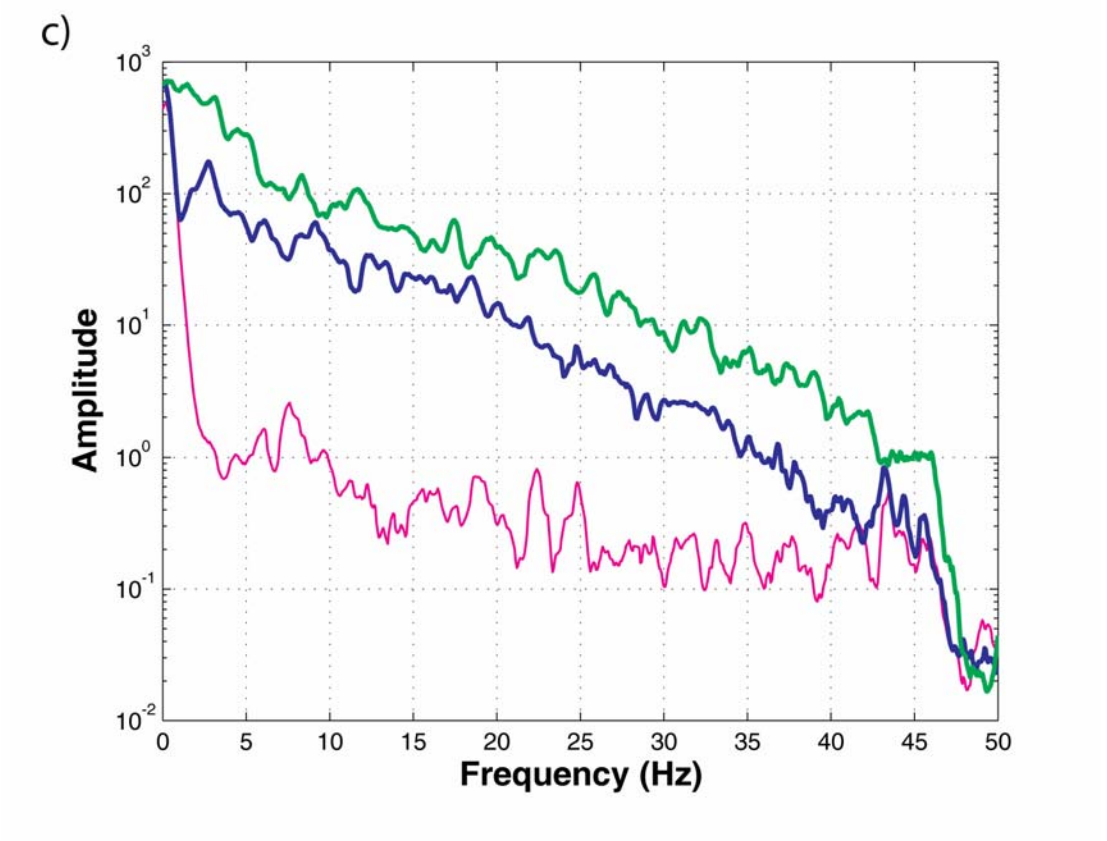
c)
Amplitude
Frequency (Hz)

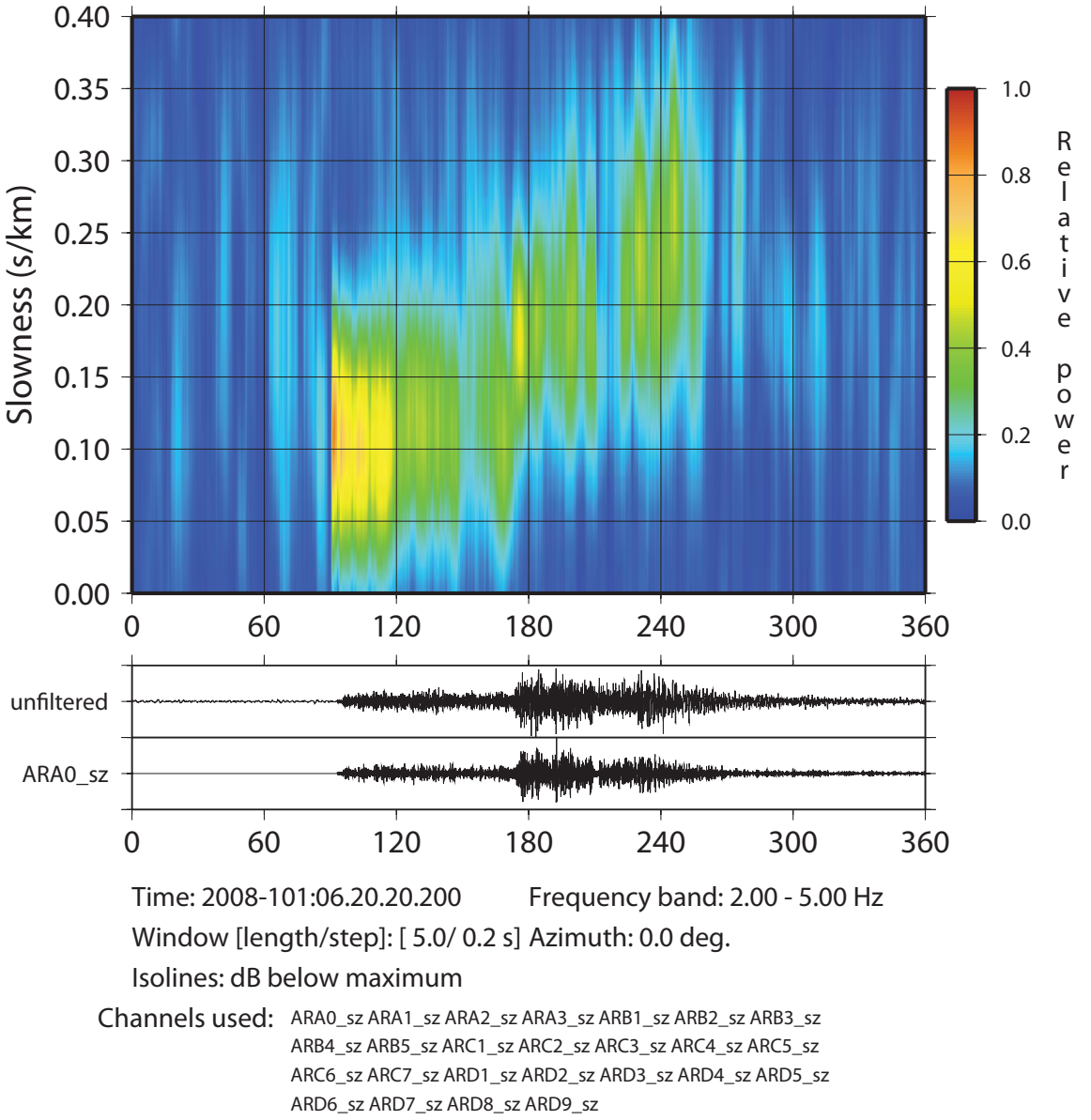

Figure 6.1.9 Vespagram of the ARCES array at the time of Event 7. The beam is steered due North. There are clear indications of Pn (slowness 0.1 s/km), Sn (slowness 0.15-0.20 s/km) and Lg (about 0.25 s/km).

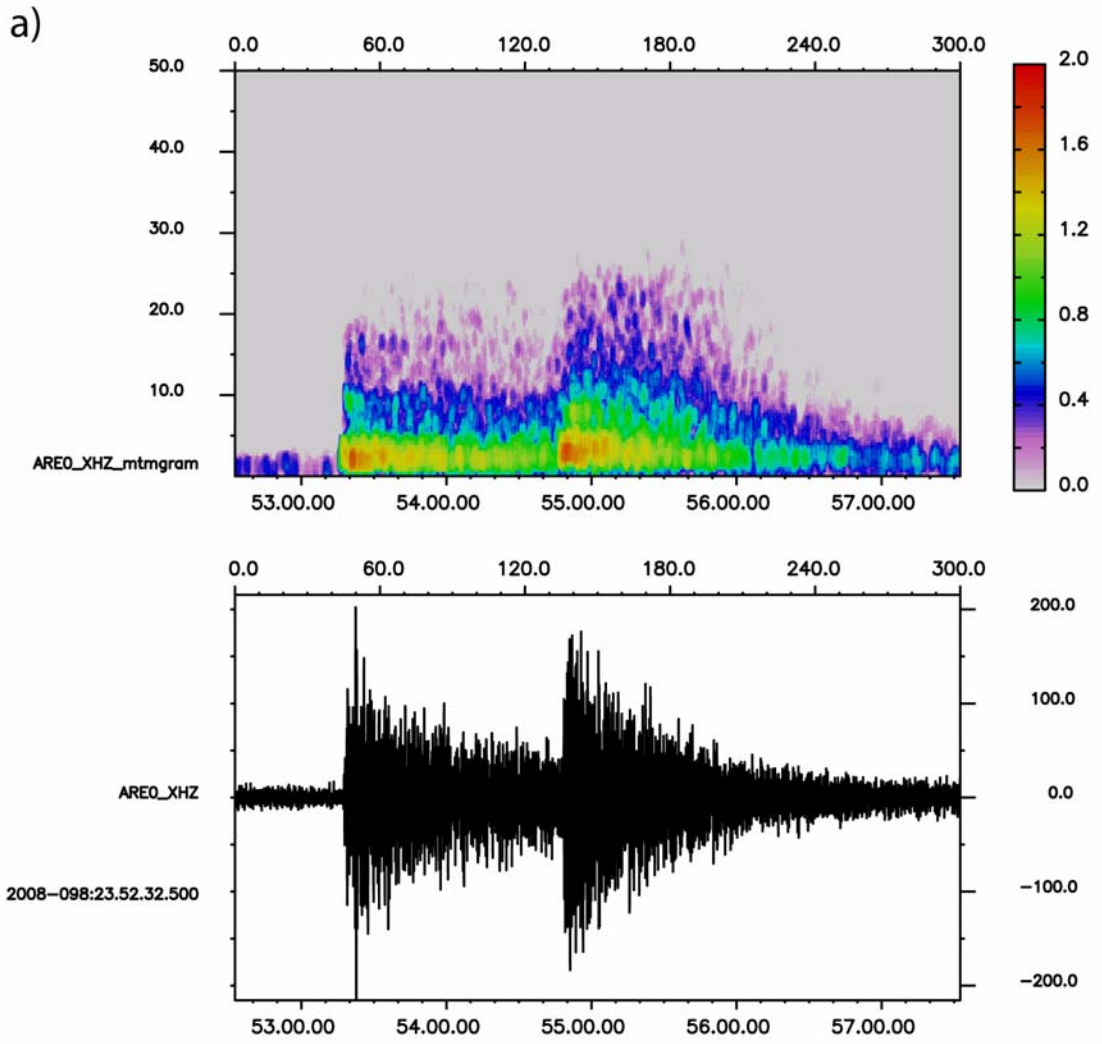

Figure 6.1.10 This page and the next page contain panels showing various displays representing the vertical component of the ARCES high-frequency seismometer for Event 8 (Knipovich Ridge, at a distance of about 960 km): a) Displays of 5 minutes of spectrogram and waveform plot filtered with a 2.2 Hz high-pass filter. b) Waveform plot filtered in 6 different frequency bands, with the main regional phases indicated. c) Amplitude spectra of noise and tphases indicated in the waveform plot: Noise (magenta), Pn (blue), Sn (green). See text for details.

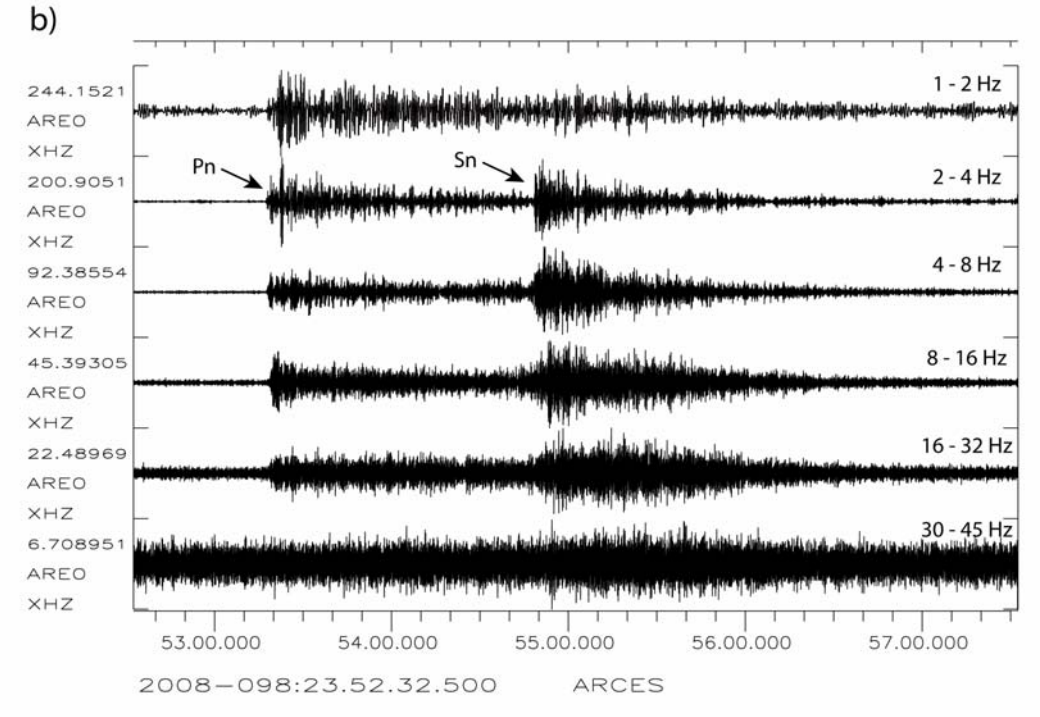
b)
244.1521
AREO
XHZ
200.9051
AREO
XHZ
92.38554
AREO
XHZ
45.39305
AREO
XHZ
22.48969
AREO
XHZ
6.708951
AREO
XHZ
Pn
Sn
1 - 2 Hz
2 - 4 Hz
4 - 8 Hz
8 - 16 Hz
16 - 32 Hz
30 - 45 Hz
53.00.000
54.00.000
55.00.000
56.00.000
57.00.000
2008–098:23.52.32.500
ARCES

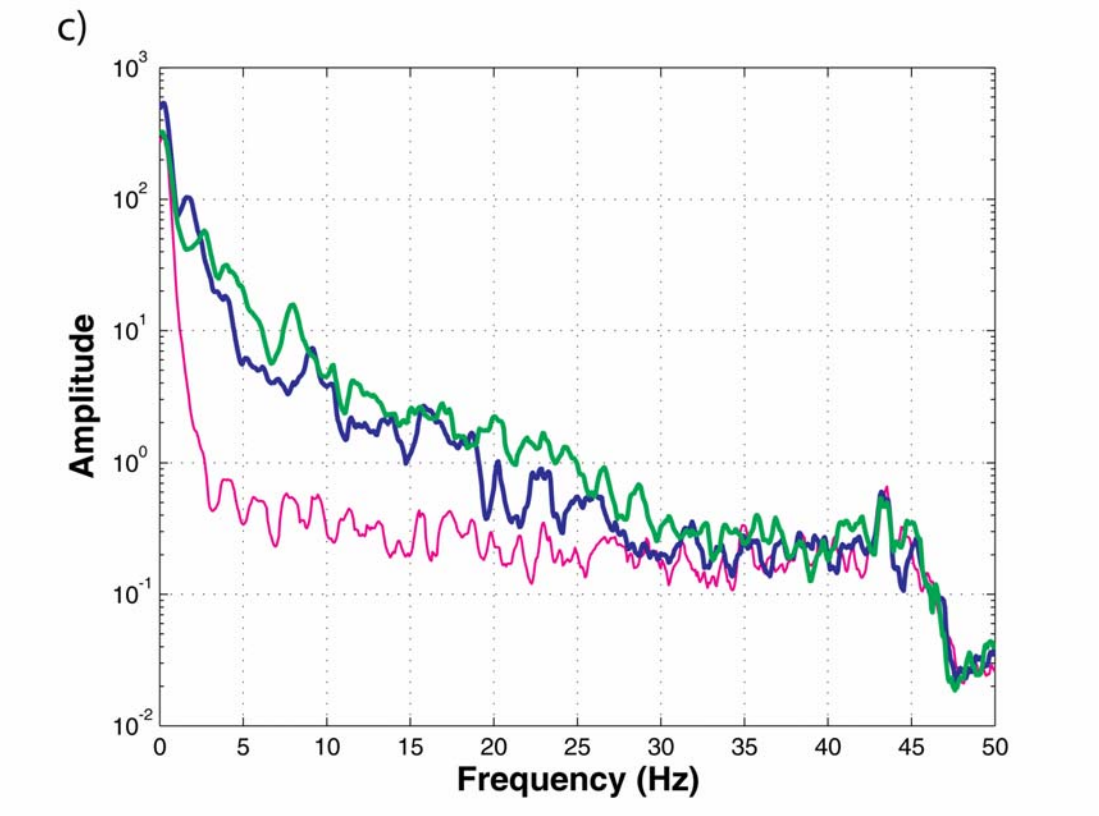
c)
Amplitude
Frequency (Hz)

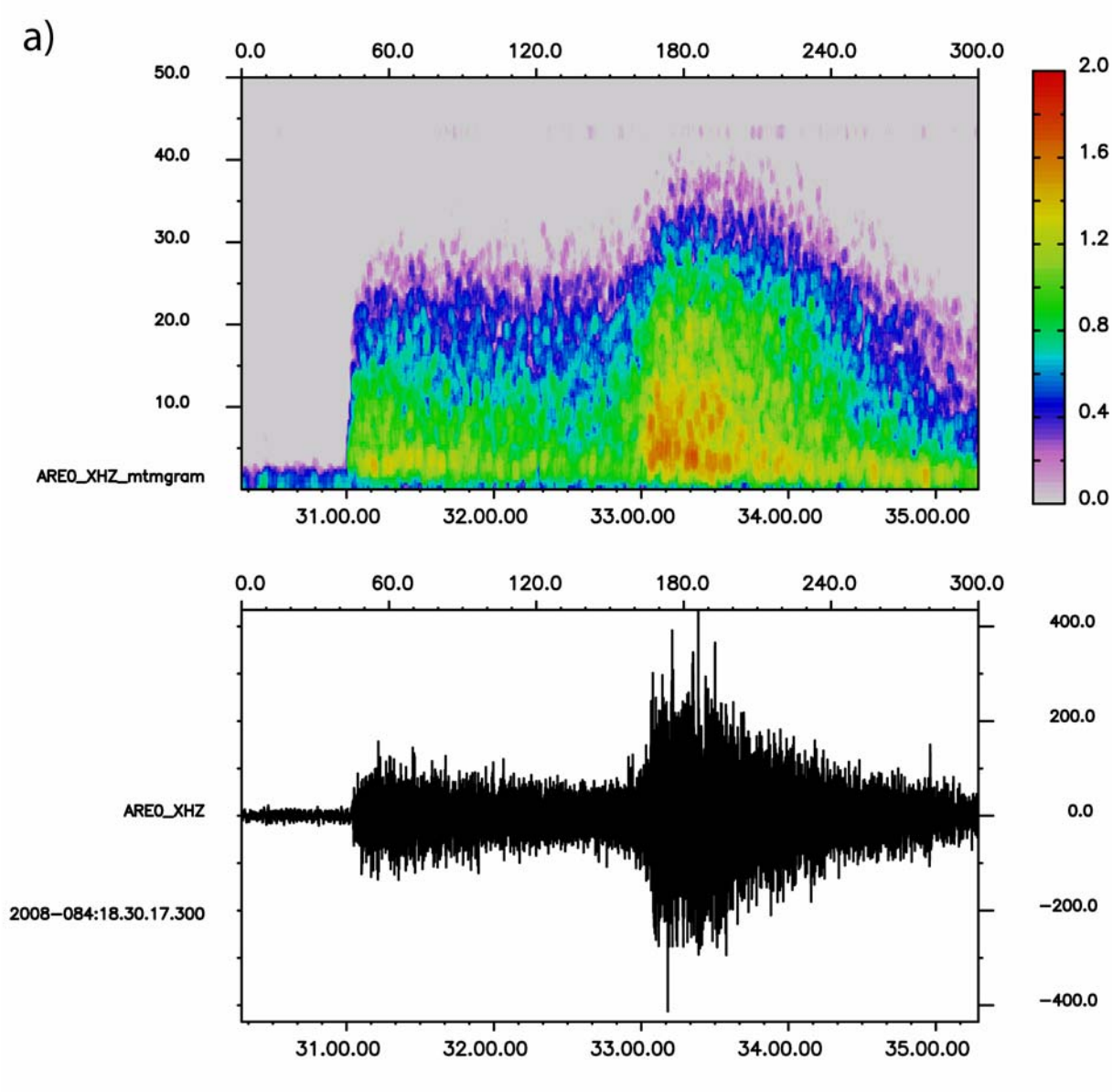

Figure 6.1.11 This page and the next page contain panels showing various displays representing the vertical component of the ARCES high-frequency seismometer for Event 9 (North of Svalbard, at a distance of about 1290 km): a) Displays of 5 minutes of spectrogram and waveform plot filtered with a 2.2 Hz high-pass filter. b) Waveform plot filtered in 6 different frequency bands, with the main regional phases indicated. c) Amplitude spectra of noise and tphases indicated in the waveform plot: Noise (magenta), Pn (blue), Sn (green). See text for details.

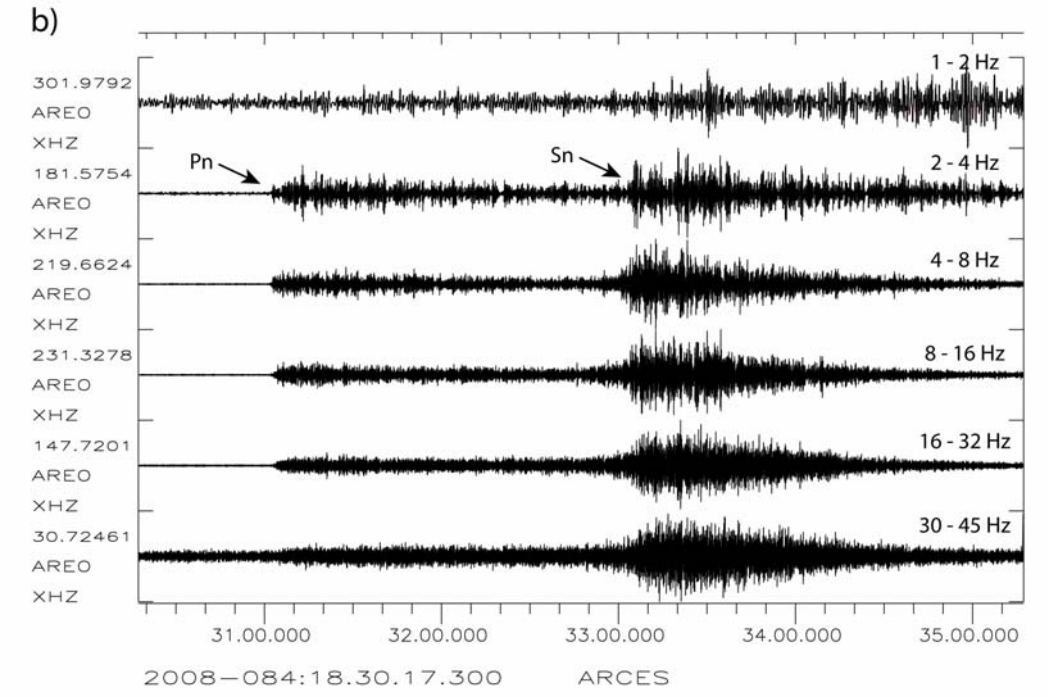
b)
301.9792
AREO
XHZ
181.5754
AREO
XHZ
219.6624
AREO
XHZ
231.3278
AREO
XHZ
147.7201
AREO
XHZ
30.72461
AREO
XHZ
Pn
Sn
1 - 2 Hz
2 - 4 Hz
4 - 8 Hz
8 - 16 Hz
16 - 32 Hz
30 - 45 Hz
31.00.000
32.00.000
33.00.000
34.00.000
35.00.000
2008—084:18.30.17.300
ARCES

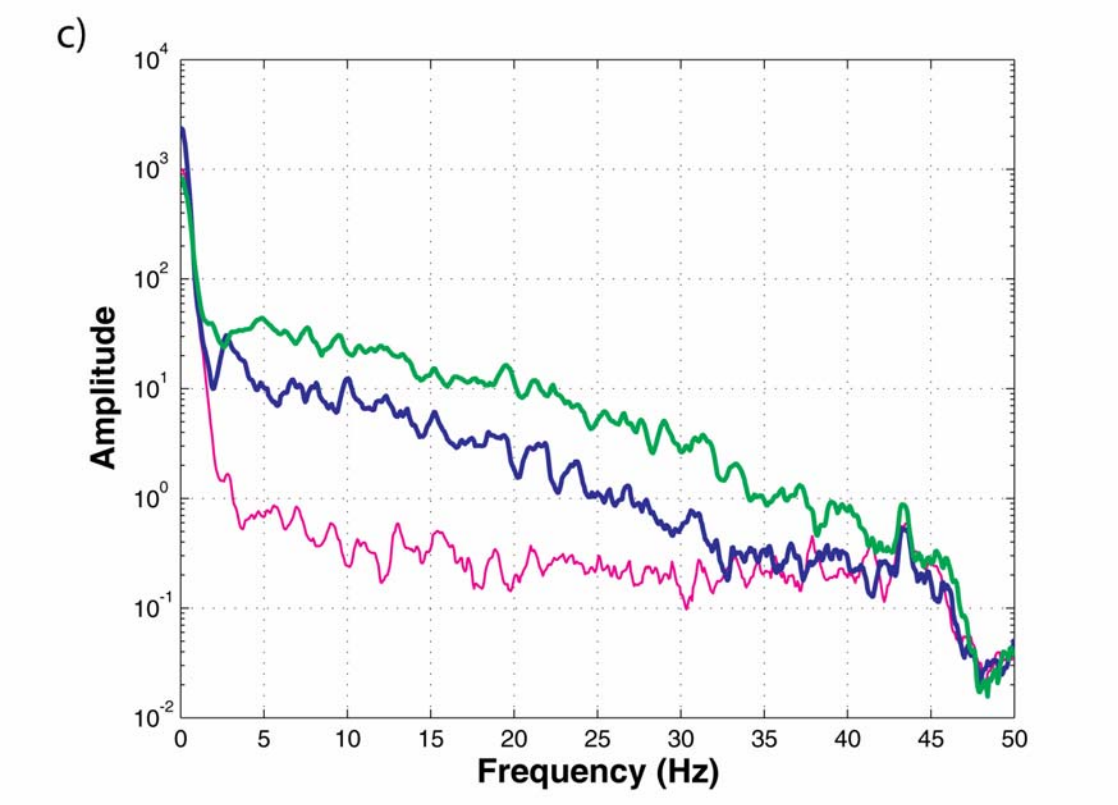
c)
Amplitude
Frequency (Hz)
10^4
10^3
10^2
10^1
10^0
10^{-1}
10^{-2}
0
5
10
15
20
25
30
35
40
45
50

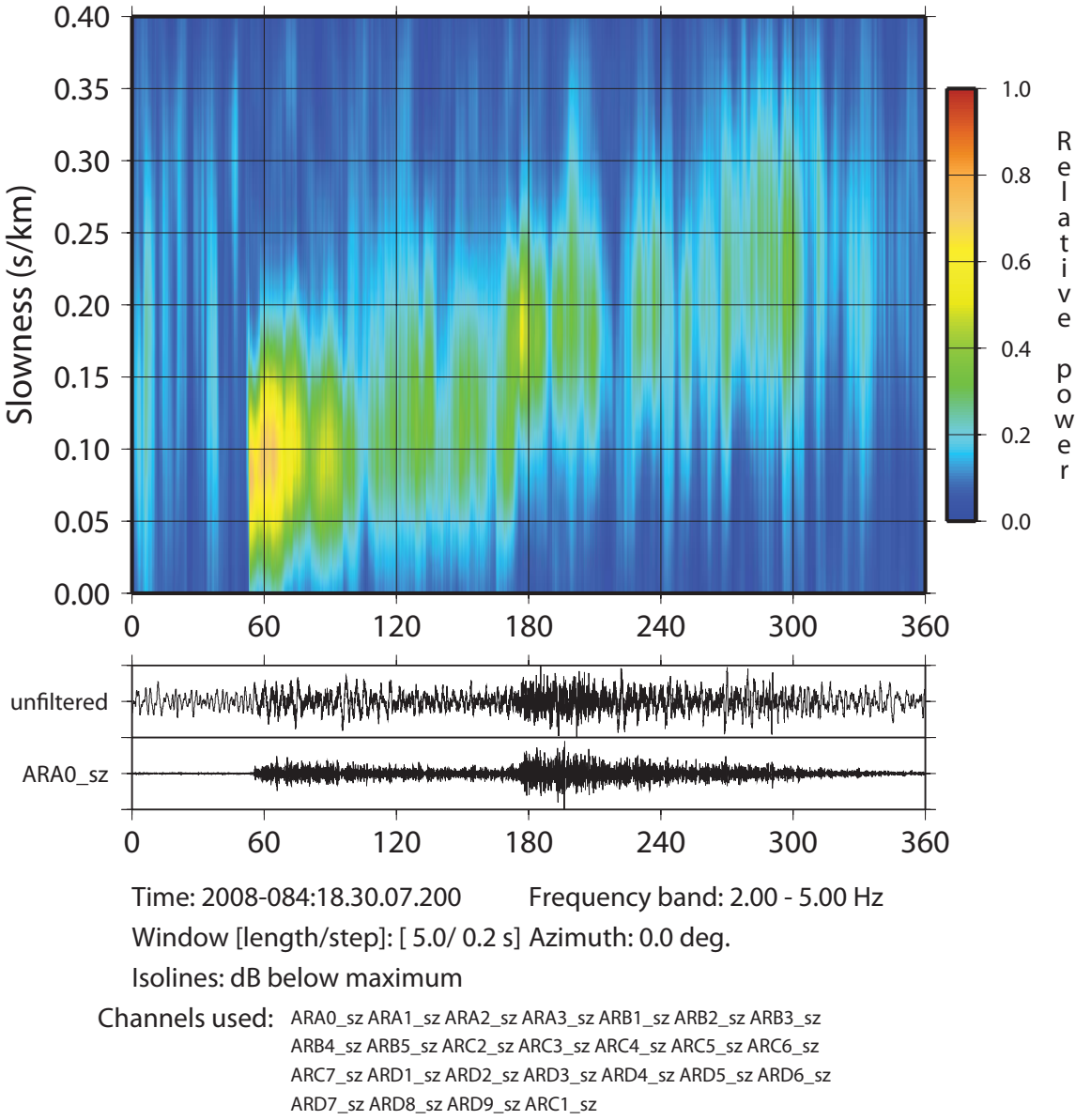

Figure 6.1.12 Vespagram of the ARCES array at the time of Event 9. The beam is steered due North. There are clear indications of Pn (slowness 0.1 s/km) and Sn (slowness 0.15-0.20 s/km). There is also evidence of the Lg phase (slowness about 0.25 s/km).

6.2 Setup of an experimental infrasound deployment within the ARCES array

In mid-March 2008 NORSAR carried out an experimental installation of three micro-barometers at the stations ARA1, ARA2 and ARB2 of the ARCES seismic array near Karasjok, northern Norway. The purpose of this experiment was to compare the performance of microbarographs to that of the seismometers with regard to recording infrasonic signals. The full ARCES array has a diameter of about 3 km, whereas the distances between the three infrasound station is about 200 -300 m, as shown in Figure 6.2.1.

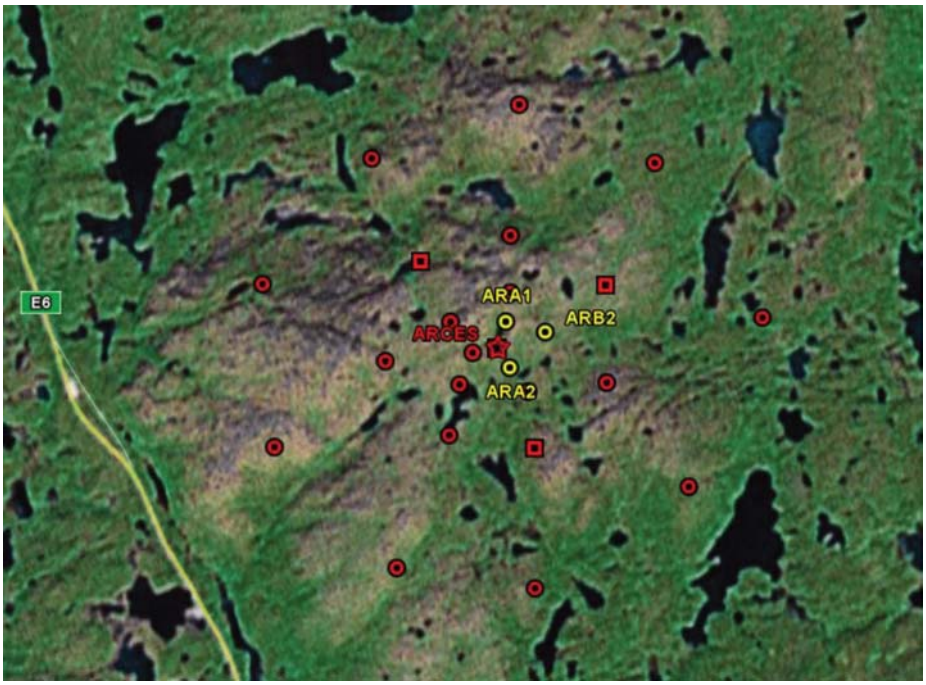

Figure 6.2.1. Map of the ARCES array with three infrasound sensors collocated with the seismic stations ARA1, ARA2, ARB2.

The microbarometers used in the experimental infrasound array are Martec MB2500 instruments with a bandwidth from 0.01 – 27 Hz and a sensitivity of 20 mV/Pa. Each barometer is about 35 cm high with a diameter of 15 cm and a weight of 7 kg (see Figure 6.2.2). The lower part of the instrument is the measurement chamber containing a barometric aneroid bellow, which is deformed by small variations of atmospheric pressure. The deformation of the bellow in turn is measured by a displacement transducer.

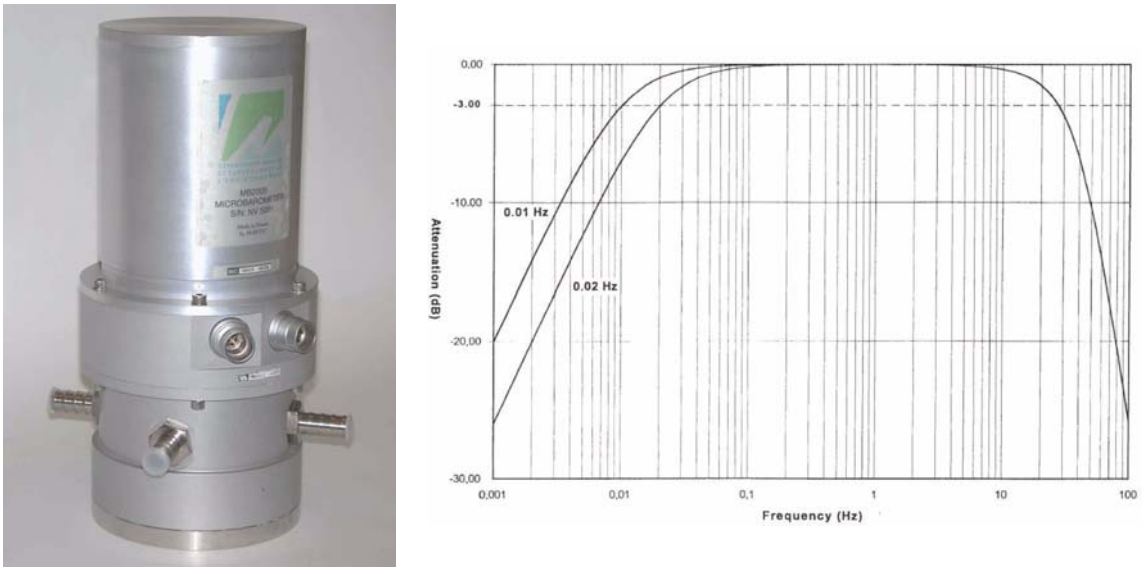

Figure 6.2.2. Martec MB2500 (left) and instrument response (right).

The microbarometers are installed in the very same pit as the seismometers (see Figure 6.2.3), and the analog signals are digitized in the pit at an 80 Hz rate using a Guralp DM24. The digital data (seismic and acoustic) are transmitted by an optical fiber cable to the central station at ARCES and from there by a VSAT satellite link to the NORSAR data processing center in real-time.

Figure 6.2.3. Pit containing a vertical seismometer with a Nanometrix digitizer and the microbarometer (middle) together with the Guralp digitizer (black box). A single inlet connects the barometer with the porous hoses arranged around the pit.

In order to suppress wind noise the decision was made to use porous hoses. At each pit four 12 m long porous hoses were installed in a cross-type layout (see Figure 6.2.4). The hoses are connected to a manifold outside of the pit, and therefore only one inlet penetrates the vault and connects to the barometer. For stations ARA1 and ARB2 we used only the porous hoses, for station ARA2 we additionally encased the hose by a plastic drainage pipe. At the time of the installation we still had a snow cover of up to 1.5 m depths. At all stations the hoses/pipes have been buried as deep into the snow as possible. The deployment is illustrated in Figures 6.2.5 and 6.2.6.

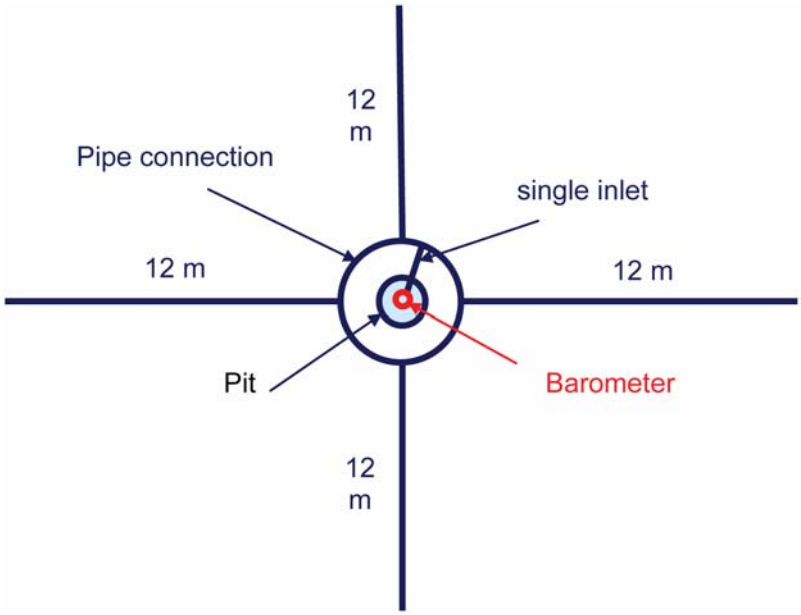

Figure 6.2.4. Sketch of the porous hose layout for wind noise reduction.

Figure 6.2.5. Porous hose (left) and porous hose in a drainage pipe (right) before deployment.

Figure 6.2.6. Burying the pipes.

Figure 6.2.7 shows the power spectral density of the three infrasound stations under calm conditions (May 1, 2008) and during a strong breeze (May 15, 2008) with average wind speed of 0.3 m/s and 8.8 m/s, respectively. During calm conditions the stations ARA1 and ARA2 have very similar spectra, whereas ARB2 has higher amplitudes (~ factor of 2) for frequencies below 2 Hz. All stations have a frequency peak around 2.3 Hz during quiet conditions. This peak is most probably an issue of the digitizers, and we will have to investigate the reasons more closely. During a strong breeze the noise level of stations ARA1 and ARA2 increase by about a factor of 10; for station ARB2 the effect is much more dramatic having an increase of about 3 orders of magnitude.

The reason for the blatant difference between the stations ARA1/ARA2 on one hand and ARB2 on the other hand, became obvious when we visited the ARCES in the beginning of June 2008. Once the snow had disappeared the hoses at ARB2 are lying on the bare rock directly exposed to the wind. In contrast, stations ARA1 and ARA2 are somewhat in the lee, and additionally, the hoses/pipes are protected from the wind by low brushes.

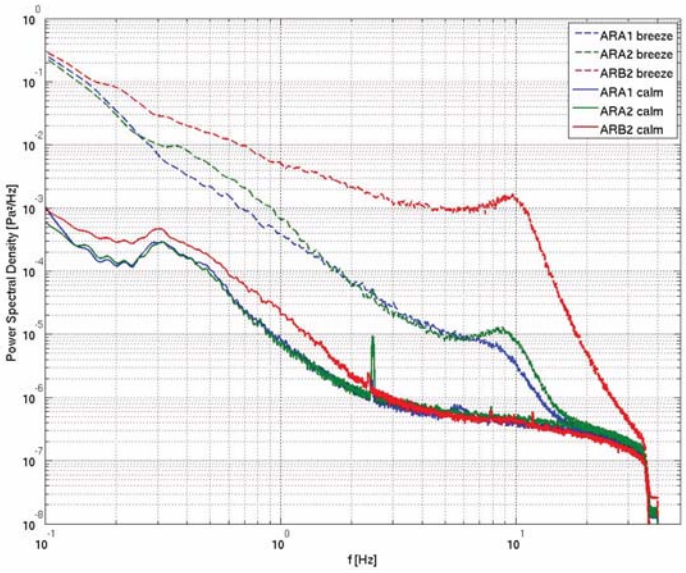

Figure 6.2.7. Power density spectra for the infrasound stations for calm conditions (continuous) and during a strong breeze (dashed). The spectra are computed for a 2-hour window.

Figure 6.2.8 (a-b) shows the infrasound records under calm conditions for two different time windows during May 15, 2008. The first plot (Fig 6.2.8a) highlights the ambient noise associated with shear-generated gravity waves with periods in the range of minutes. Fig 6.2.8b shows a 2-minute zoom of the first part of Fig. 6.2.8a, and shows microbaroms (generated by the interaction of sea waves with the atmosphere) with periods between 5-8 seconds together with a clear infrasound signal. Figure 6.2.9 shows results of slowness analysis of the infrasound signal which has an apparent velocity of 340 m/s and a backazimuth of 237 deg.

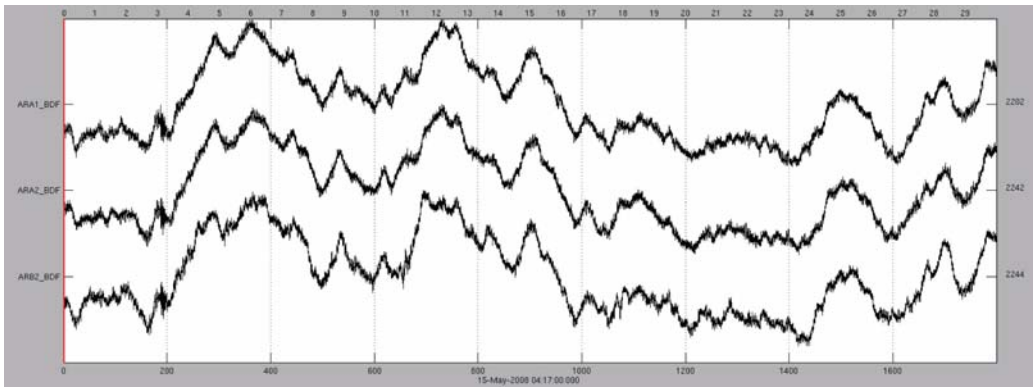

Figure 6.2.8a. A 30-minute time window.

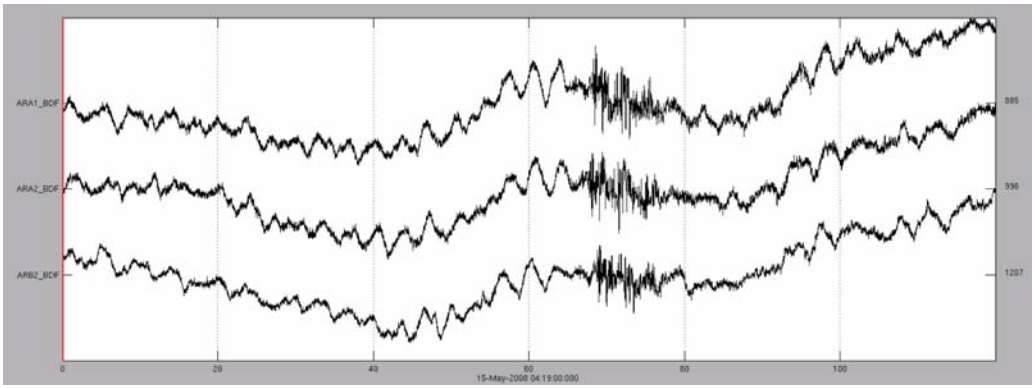

Figure 6.2.8b. A 2-minute time window taken from the first part of Fig 6.2.8a.

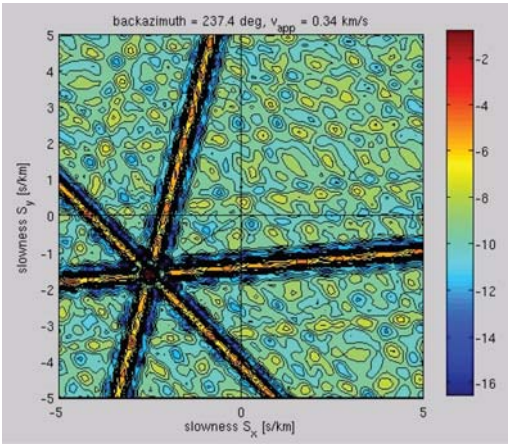

Figure 6.2.9. Slowness analysis of the infrasound event in Fig 6.2.8b.

Figures 6.2.10-6.2.12 illustrate some additional results for an event on May 22, 2008. This event is probably an explosion carried out by the Russian military with the purpose of destroying old, outdated ammunition. The infrasonic waves for this event were recorded both by the microbarographs (Figure 6.2.10) and the seismometers (Figure 6.2.11).

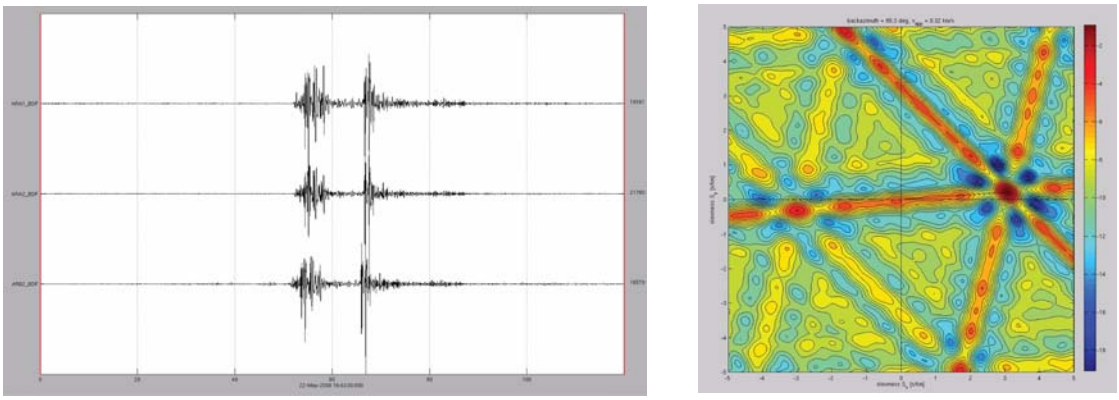

Figure 6.2.10. Barometer recordings (2-10 Hz), backazimuth 86.3 deg, apparent velocity 320 m/s..

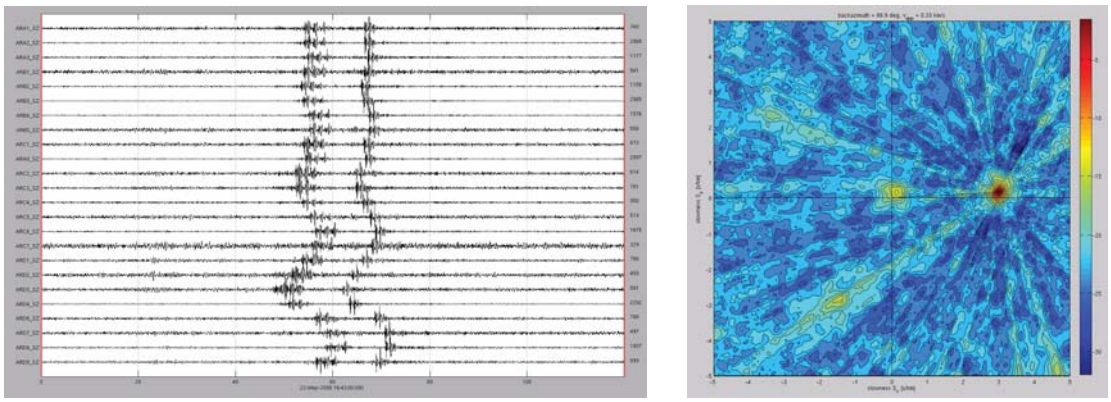

Figure 6.2.11. Seismometer recordings (2-10 Hz), backazimuth 86.9 deg, apparent velocity 330 m/s.

Figure 6.2.12 shows a pairwise comparison of the recordings by collocated microbarographs and seismometers. It is seen that the infrasonic signals are essentially identical on each pair of collocated instruments. We also note that the signal-to-noise ratio is significantly better on the microbarographs as compared to the seismometer recordings.

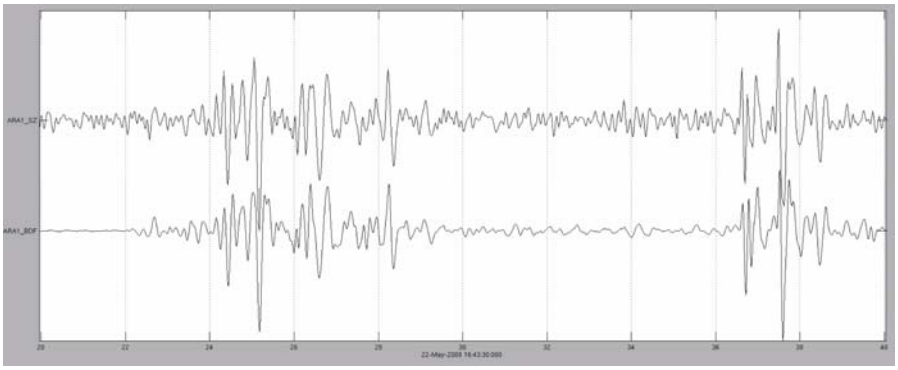

Figure 6.2.12a. Infrasound signal recorded with seismometer (top) and microbarometer (bottom) collocated in ARA1 (20 s time window, 2-10 Hz)

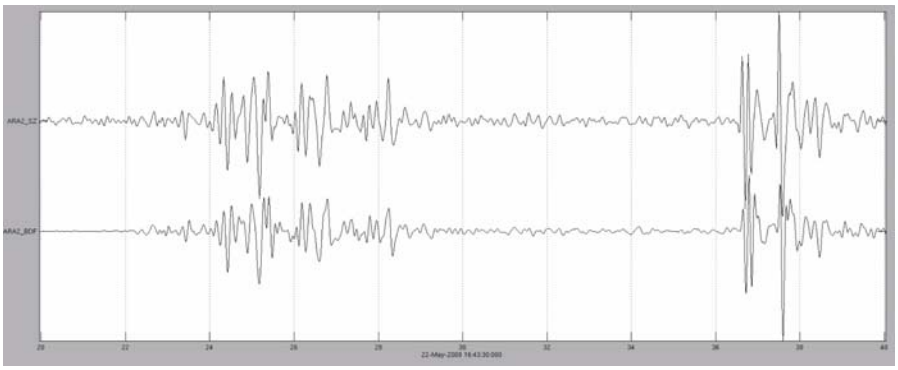

Figure 6.2.12b. Infrasound signal recorded with seismometer (top) and microbarometer (bottom) collocated in ARA2 (20 s time window, 2-10 Hz)

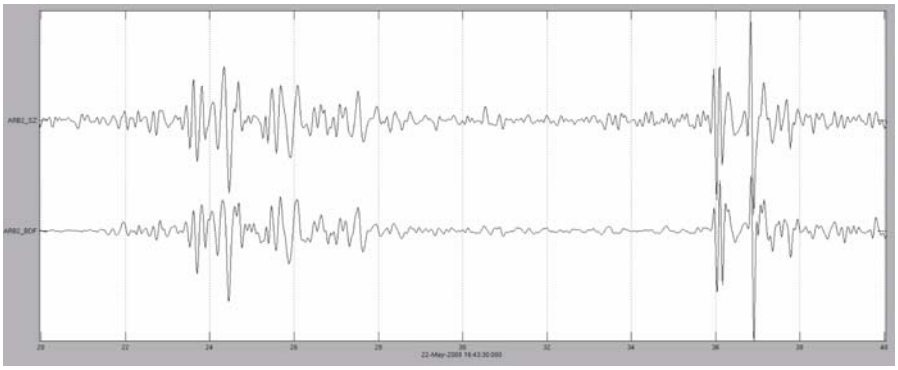

Figure 6.2.12c. Infrasound signal recorded with seismometer (top) and microbarometer (bottom) collocated in ARB2 (20 s time window, 2-10 Hz)

Michael Roth
Jan Fyen
Paul W. Larsen

6.3 Initial studies of signals recorded by ARCES infrasound sensors

Sponsored by US Army Space and Missile Defence Command, Contract No. W9113M-05-C-0224

6.3.1 Introduction

An important aspect of the infrasonic studies is the availability of data from a distributed network of arrays. The Swedish infrasound array network provides a useful supplement to the seismic and infrasonic arrays in Norway and NW Russia. The Apatity infrasound array is a three-element array co-located with the nine-element Apatity short-period regional seismic array, which was installed in 1992 on the Kola Peninsula, Russia by the Kola Regional Seismological Centre (KRSC). For further details see Baryshnikov (2004). The 25 element ARCES array is a short-period regional seismic array, located in northern Norway. ARCES has no infrasound sensors, but because of special near surface installation conditions, many of its seismic sensors are also sensitive to infrasound signals (see e.g., Ringdal & Schweitzer, 2005). The Swedish Infrasound Network (Liszka, 2007) has been in operation since the beginning of the 1970s. Operated by the Swedish Institute of Space Physics, the network has until recently comprised four infrasound stations: Kiruna, Jämtön, Lycksele and Uppsala. The station in Uppsala was moved to Sodankylä, Finland, during the summer of 2006. The currently available network of arrays for infrasound processing in the Nordic region is shown in Figure 6.3.1.

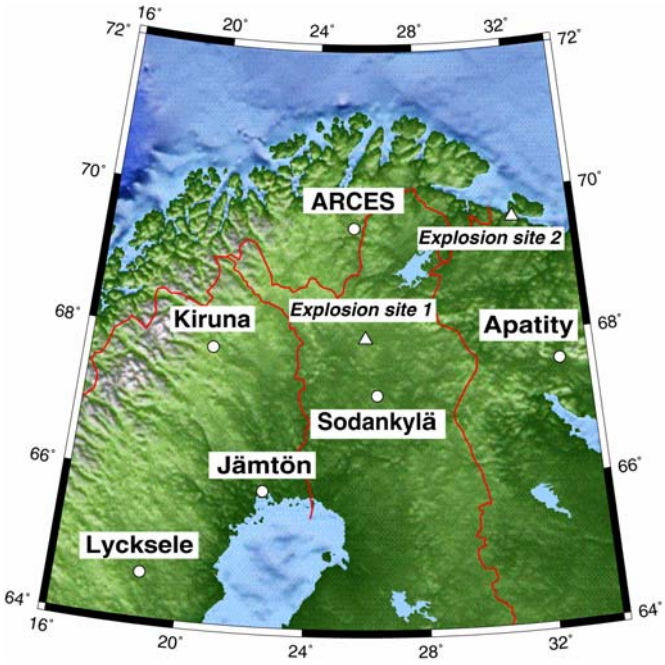

Figure 6.3.1. Locations of the arrays used for infrasonic processing in the Nordic countries. The site of the explosions in northern Finland discussed in previous papers (Explosion site 1) and the location of the presumed explosion in NW Russia discussed in detail in this paper (Explosion site 2) are marked on the map.

6.3.2 Experimental deployment of microbarographs within ARCES

The NORSAR staff has expended much effort during the past several years to determine a site for the projected IMS infrasound station near the ARCES array. Although these efforts until now have not been successful, we have made some progress in evaluating the infrasonic recording possibilities using dedicated infrasound sensors (as compared to using the seismic sensors of the ARCES array for infrasound recording). A recent development has been the installation of additional infrasonic recording equipment at three element near the center of ARCES, as illustrated in Figure 6.3.2. The data are digitized at a 40 Hz rate and extracted in parallel with the regular seismic data. The data from the infrasound sensors have been available at the NORSAR data center since about 1 April 2008.

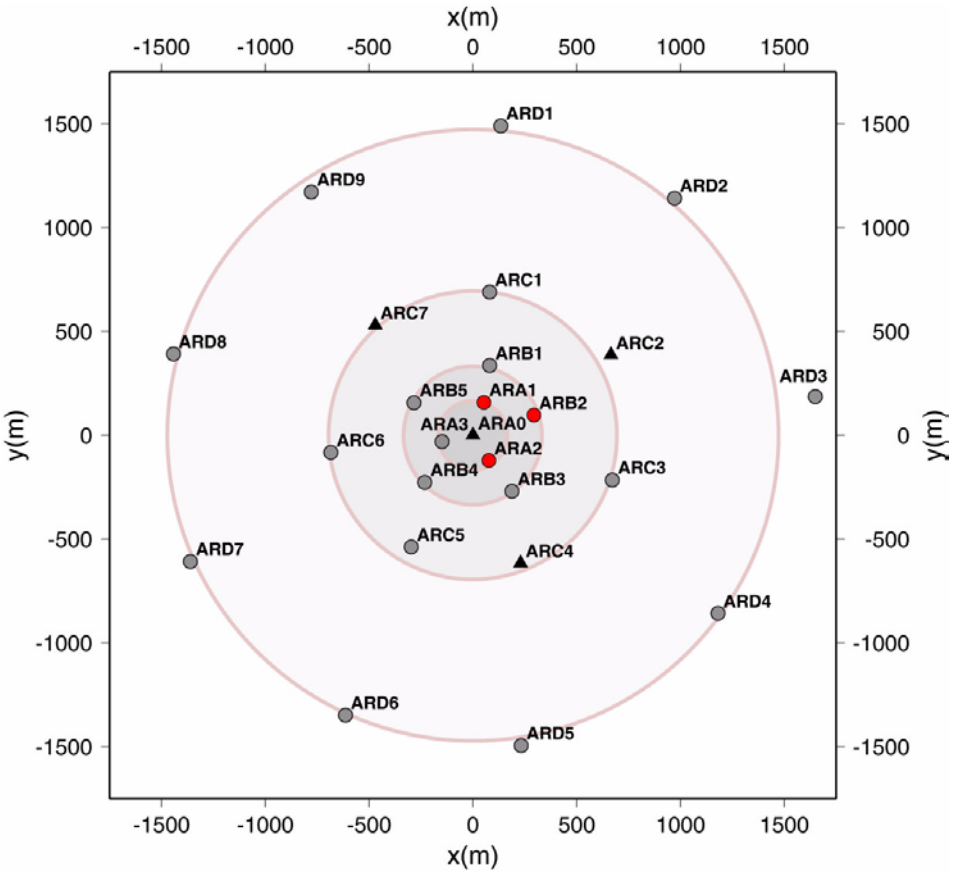

Figure 6.3.2. Configuration of the ARCES array. The filled circles denote vertical-component seismometers, and the triangles denote three-component seismometers. The three filled red circles represent the sites where infrasound sensors have been experimentally installed in addition to the seismic sensors. Also note that an experimental high-frequency seismic element has recently been installed at the center (ARA0) of the array.

6.3.3 Seismometers versus microbarographs for infrasound recording

We have begun an investigation aimed at comparing the quality of recording of infrasound signals when using seismometers versus recordings using microbarographs. Even taking into account the very efficient recording of such signals by the ARCES seismometers, our expectation would be that significant improvement would be obtained when using microbarographs. Nevertheless, the much larger number of seismic sensors would be a factor that should also be taken into account.

Figure 6.3.3 shows two waveforms covering 20 minutes of ARCES array data and representing the presumed explosion in NW Russia mentioned above. The top waveform shows seismometer data (ARA2) and the bottom waveform shows microbarograph data from the same site. We note that the seismometer data shows P and S phases from the presumed explosion as well as P and S phases from an unrelated seismic event (a mining event near Kiruna, Sweden). The infrasonic signal is very clear on both the traces and looks quite similar on the two sensors.

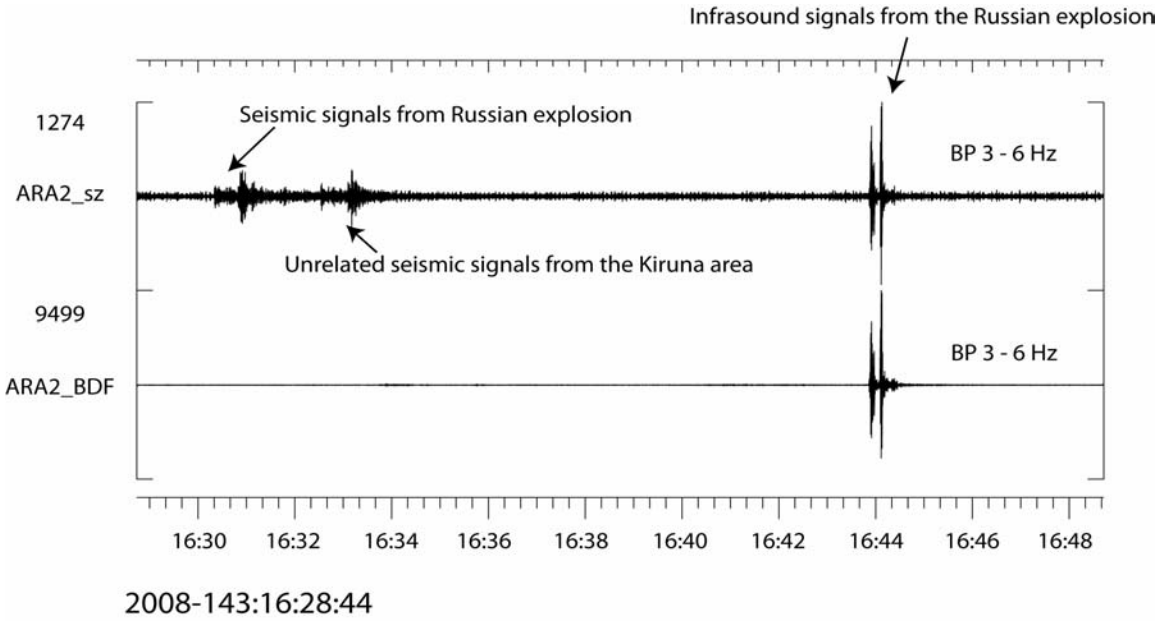

Figure 6.3.3. The figure shows two waveforms covering 20 minutes of ARCES array data and representing a presumed explosion in NW Russia on 22 May 2008. The data are filtered in a 3-6 Hz frequency band.

One interesting observation from Figure 6.3.3 is the differences in signal-to-noise ratio (SNR) between the two traces. While the SNR of the infrasonic signal is high in both cases, it is clearly superior for the microbarograph. This is by no means surprising; in fact, the most surprising feature is that the seismic trace is so close to the microbarograph trace in terms of both SNR and waveform characteristics. Also note that “noise” on the seismic trace comprises both the usual “background noise” and the actual seismic signals, which naturally are not visible on the microbarograph trace.

The similarity of the infrasonic signals on the two sensors is further illustrated in Figure 6.3.4, which shows an expanded plot in a somewhat broader frequency band (1.5-6 Hz). This similarity is even more clearly shown in Figure 6.3.5, where the two sensor traces are plotted together in the same coordinate system.

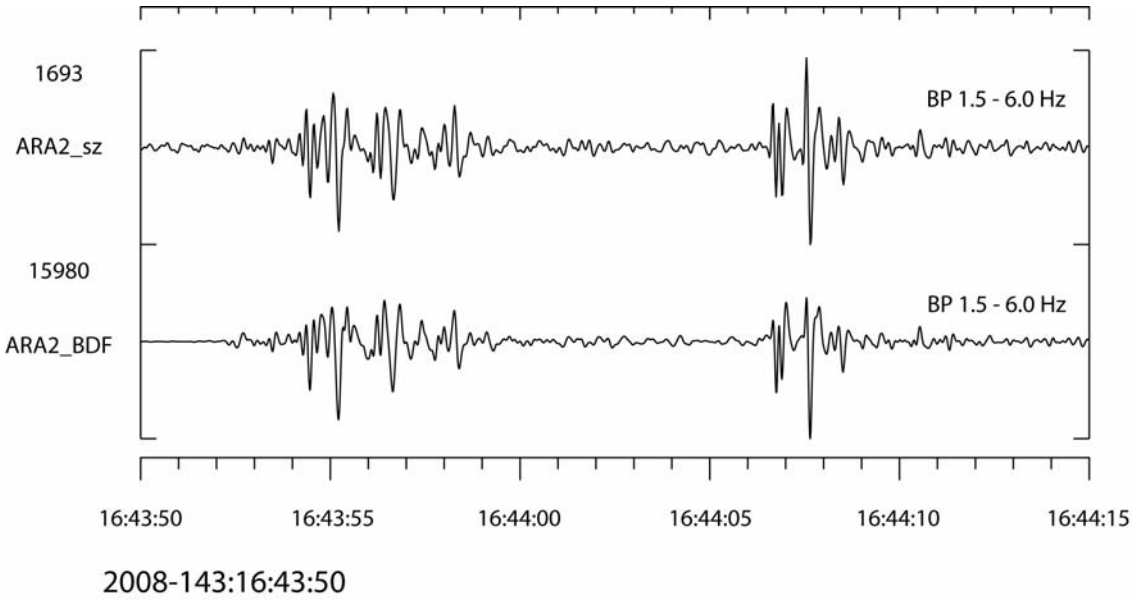

Figure 6.3.4. Expanded plot of the infrasonic signals shown in Figure 6.3.3, filtered in the1.5-6.0 Hz frequency band. Note the similarity of the signals recorded by the seismometer (top) and the microbarograph (bottom).

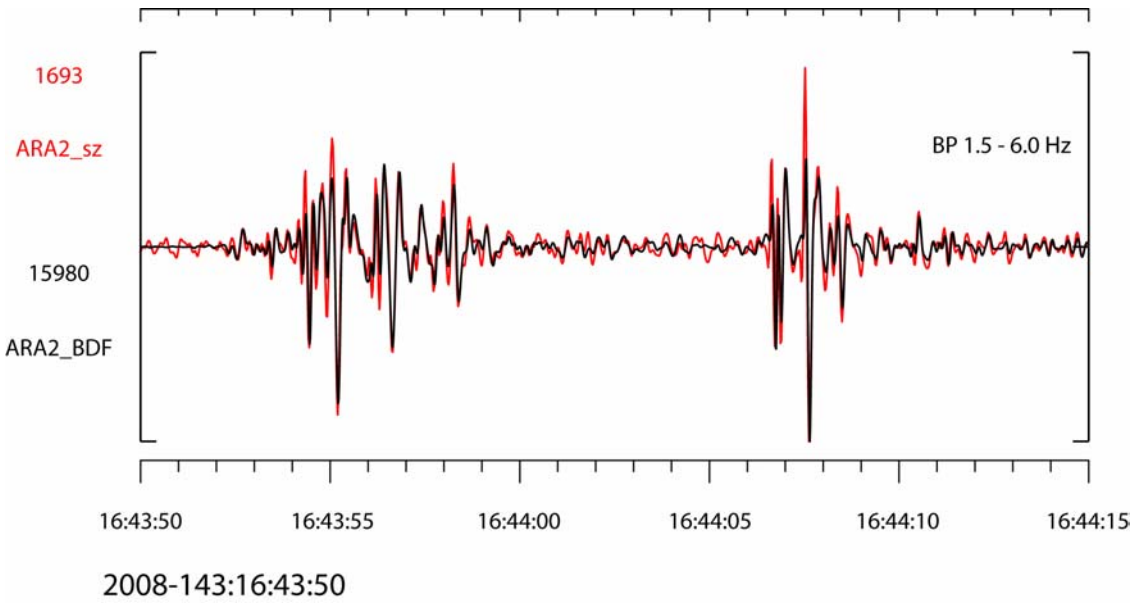

Figure 6.3.5. Same as Figure 6.3.4, but with the two sensor traces plotted in the same coordinate system.

In Figure 6.3.6, we show for comparison the infrasonic data recorded by a seismometer in the Apatity array, together with data recorded by a co-located microbarograph. Again, the similarity between the two sensors is remarkable, but in this case there is a phase delay of about 0.03 seconds between the two sensor types. This is probably due to a small difference in sensor location (of the order of 10 meters), and is in any case insignificant for our purposes.

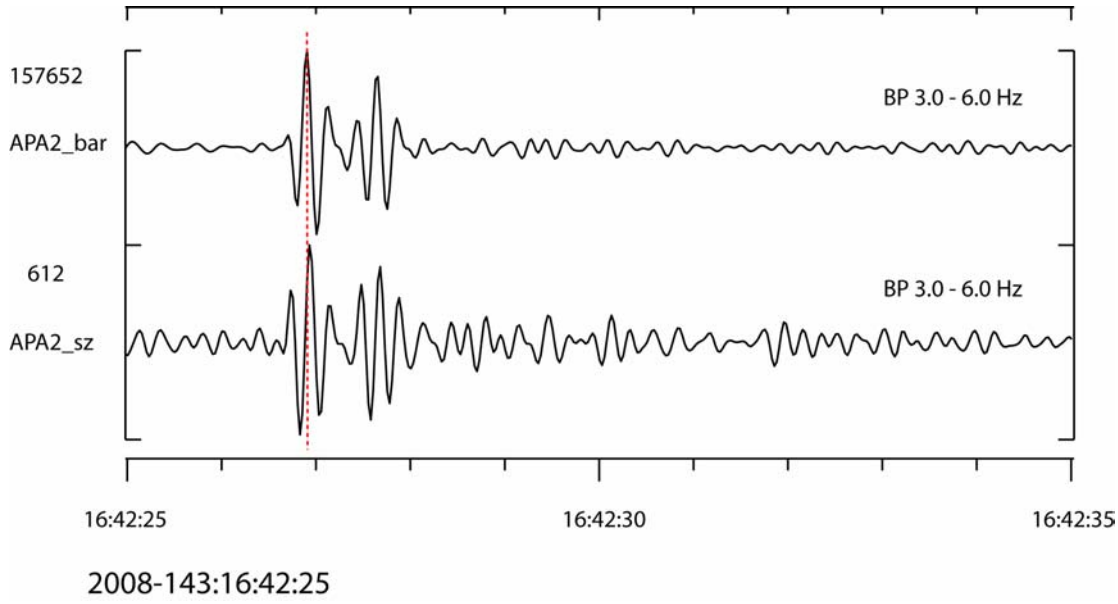

Figure 6.3.6. Recordings of the infrasonic phase at the Apatity array for the previously discussed presumed explosion in NW Russia. The traces are from a seismometer (top) and a co-located microbarograph (bottom). Note the slight phase shift between the traces.

We mention one additional feature, which is characteristic for many infrasound recordings. This feature is the presence of more than one infrasonic phase for the same event. It is well known that under various atmospheric conditions, the temporal characteristics and amplitudes of the various infrasonic phases can show great differences, even between explosions conducted in the same place and with the same source characteristics. This fact is discussed in detail by Gibbons et al. (2007) for a set of explosion from a site in northern Finland (Explosion site 1 in Figure 6.3.1).

In the example studied in the present paper, the ARCES data appears to show two infrasonic phases, separated by about 10 seconds. This might initially be interpreted as representing two separate explosions. However, by vespagram analysis of the ARCES signals (see Figure 6.3.7), it is quite clear that there is in fact only one event that causes these phase recordings.

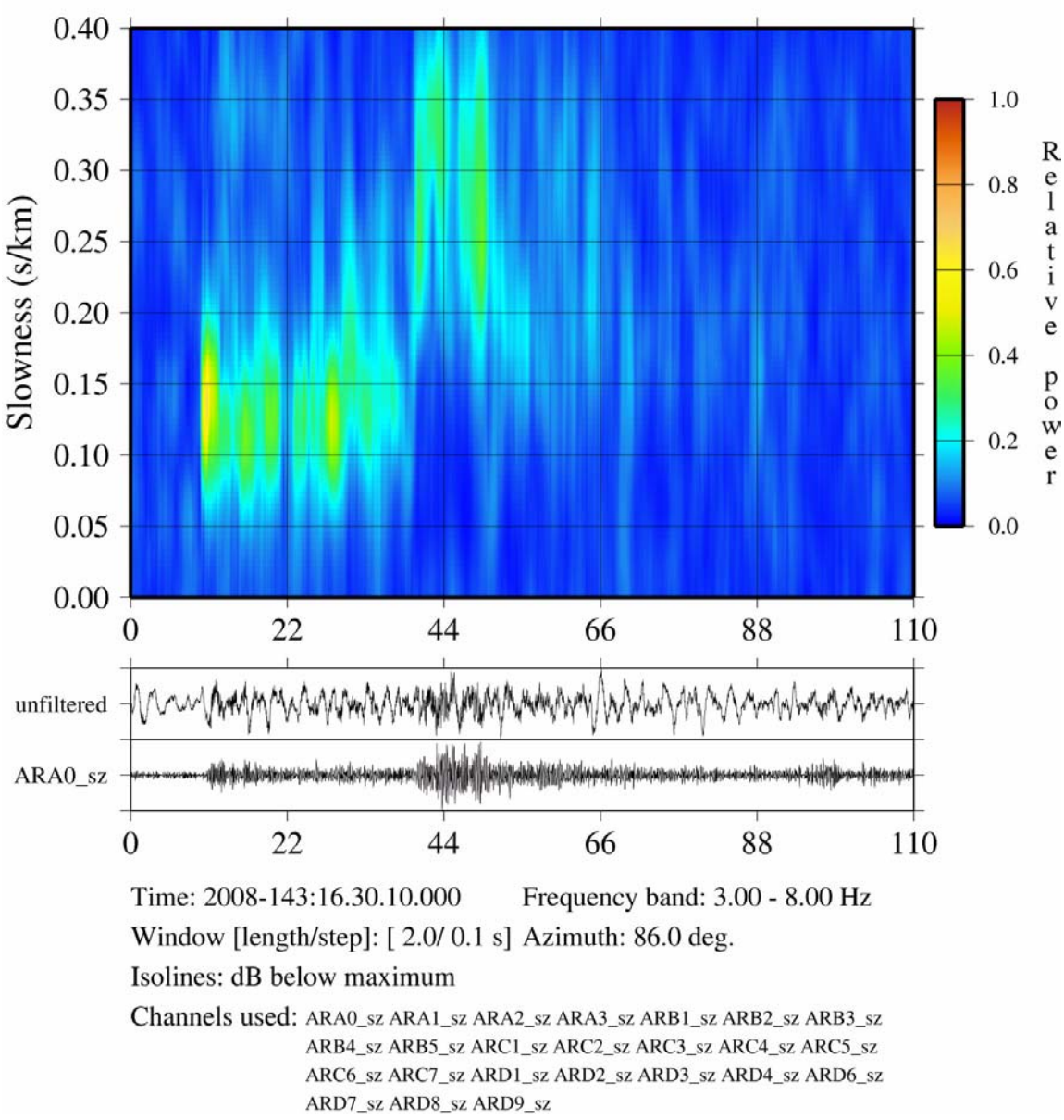

Figure 6.3.7. Vespagram of the ARCES array, steered to 86 degrees, for the time of the seismic phase recordings of the NW Russia presumed explosion. The plot indicates one P-phase and one S-phase, with no clear evidence of a second onset.

6.3.4 Slowness estimation

Figure 6.3.8 shows ARCES full seismic array slowness estimate, using 25 SPZ seismometers, for the infrasound phase of the NW Russia event discussed in this paper. The method of Frankel et al. (1991) is used for this and other slowness estimates in this paper. Figure 6.3.9 shows the slowness estimates using only the three microbarographs.

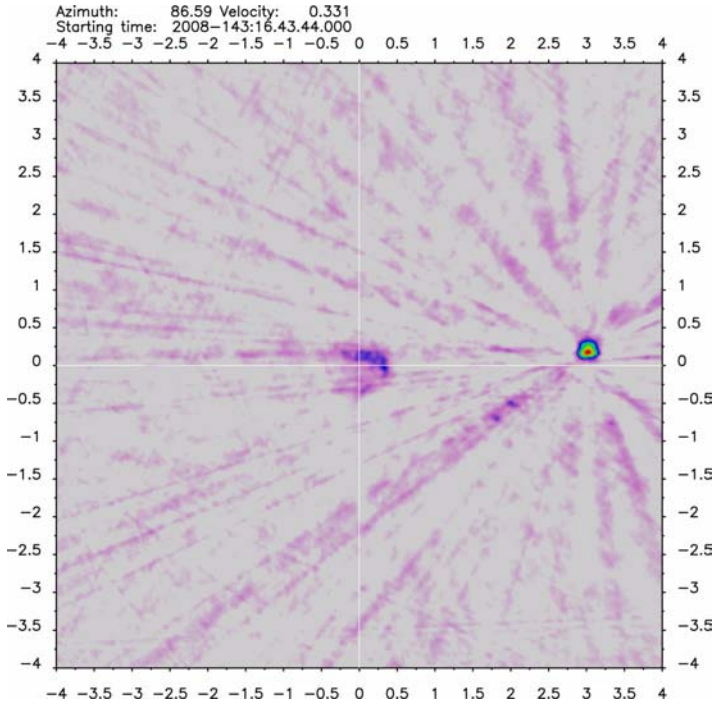

Figure 6.3.8. Slowness estimate of the infrasonic phase of the NW Russia presumed explosion, using the 25 vertical-component seismometers of the ARCES array.

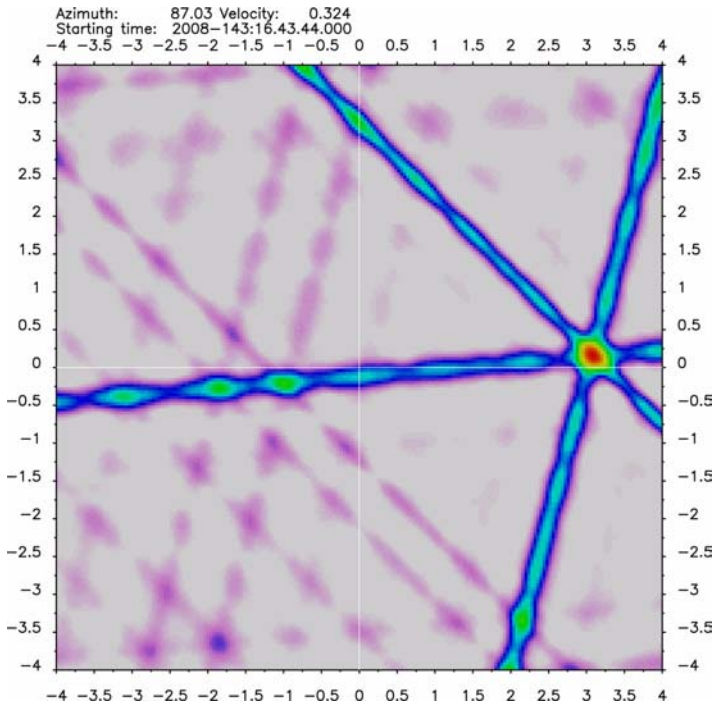

Figure 6.3.9. Slowness estimate of the NW Russia event, using only the three ARCES microbarographs.

We note that the estimated azimuth is 86.59 degrees, and the estimated velocity is 331 m/s for the full 25-element seismic array (Figure 6.3.8). For comparison, the estimated azimuth is 87.03 degrees, and the estimated velocity is 324 m/s using the three microbarographs only. Thus, the difference is very small, although the peak of the seismic plot is somewhat sharper than for the microbarograph plot. The cross-like sidelobe pattern of Figure 6.3.9 is typical of the slowness plots for a three-element array.

Figure 6.3.10 shows the slowness estimate by the Apatity microbarograph array for the infrasound phase recorded at Apatity. The sharpness of the peak is similar to that of ARCES (Figure 6.3.9), which reflects a similar array aperture (about 300 m) and a similar frequency content of the infrasonic signals. The estimated azimuth is 348.23 degrees and the estimated velocity is 340 m/s in this case. Again these are quite close to the (assumed) true values.

A noteworthy feature of Figure 6.3.10 is the color difference (green) of one of the "arms" of the cross-pattern. This occurs because one of the three microbarograph had a hardware (filter) problem at the time of the event, and therefore showed considerably poorer SNR than the other instruments. Nevertheless, the slowness estimate does not deteriorate significantly, although the effect would be more severe for lower SNR signals.

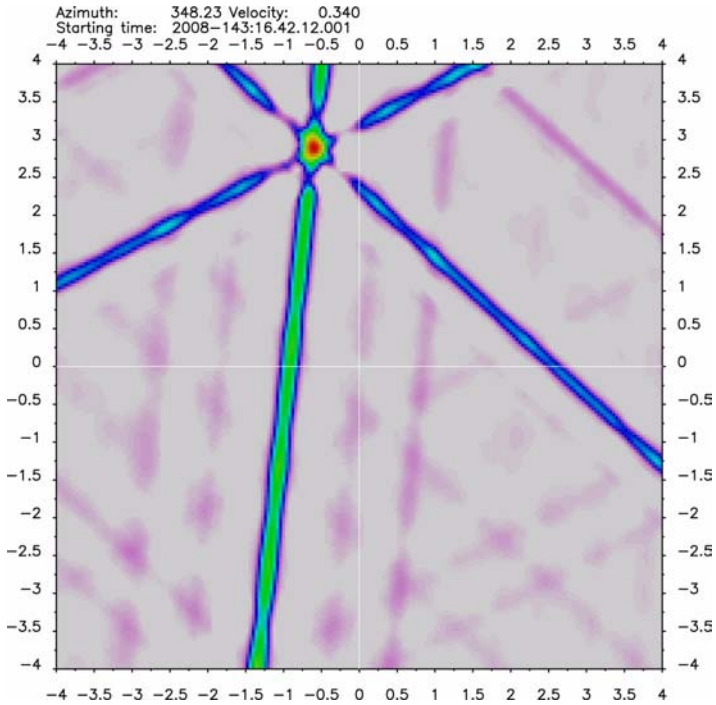

Figure 6.3.10. Slowness estimate of the NW Russia event, using the three Apatity microbarographs.

6.3.5 Swedish/Finnish network data

The Swedish/Finnish infrasound network comprises much smaller arrays than ARCES and Apatity. It could be of interest to compare the results using these arrays to what we have shown before. Figure 6.3.11a shows the waveforms recorded by the Kiruna infrasound array in northern Sweden. The SNR is in fact quite good, and the signals are not clipped (this is sometimes a problem for these arrays, which have a much more limited dynamic range than ARCES and Apatity).

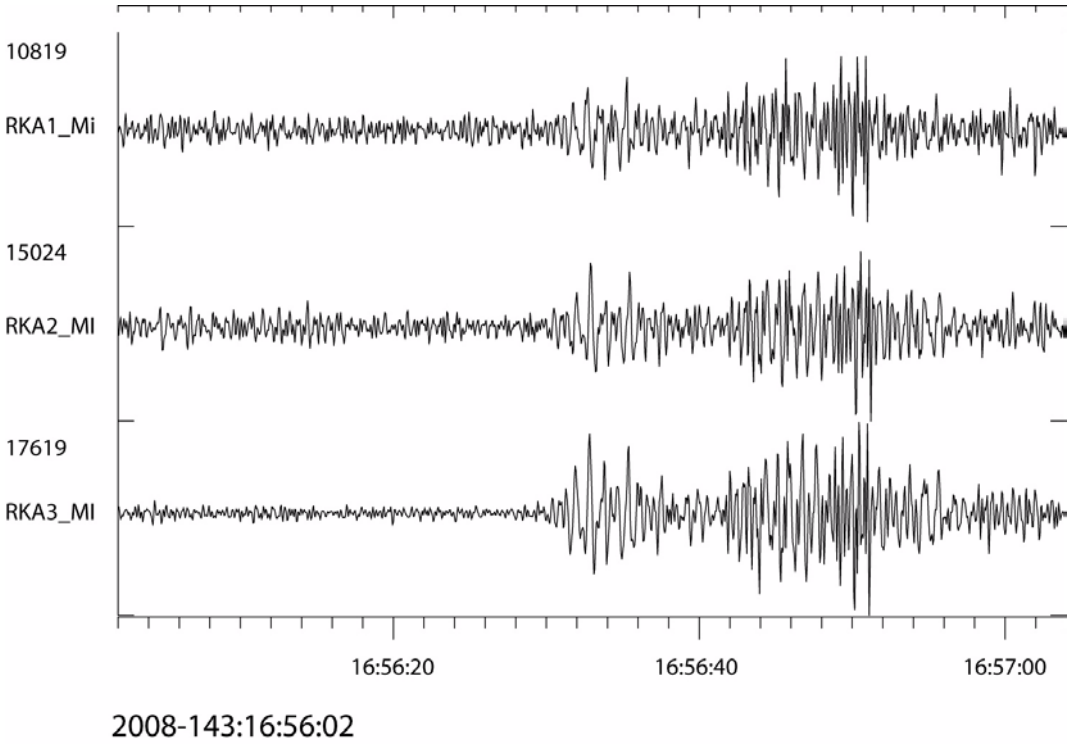

Figure 6.3.11a. Waveforms recorded by the Kiruna infrasound array in northern Sweden for the NW Russia event.

Figure 6.3.11b shows slowness estimate for the infrasound phase using data from the Kiruna infrasound array. The azimuth (81.01 degrees) is quite close to the assumed true azimuth, whereas the phase velocity (296 m/s) is somewhat lower than expected. Here, it must be remembered that the Swedish arrays have an aperture of only 75 meters, which is much less than even the small ARCES and Apatity microbarograph arrays. This causes the peak of the plot shown in Figure 6.3.11a to be much less sharp than what was seen for the ARCES and Apatity microbarograph arrays.

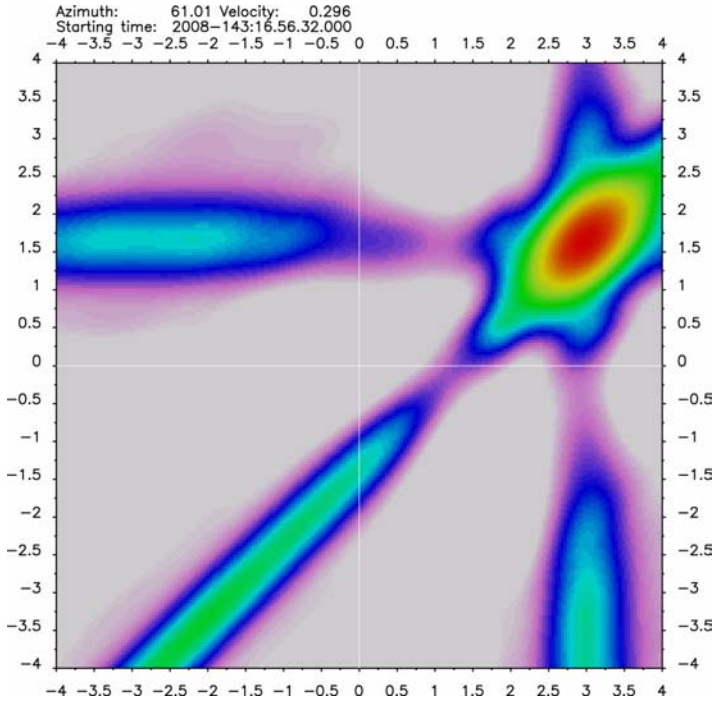

Figure 6.3.11b. Slowness estimate of the NW Russia event, using the Kiruna infrasound array.

6.3.6 Detector performance

In the 1 April - 30 June 2006 Quarterly R&D Status Report we described a slowness-based algorithm for detecting infrasound signals at the ARCES seismic array. Using the seismic sensors of A- and B-rings of the ARCES array, we ran broad-band slowness analysis (Kværna and Doornbos, 1986) with a sampling interval of 2 seconds and a window length of 10 seconds in the 2-5- Hz frequency band. We have now applied this algorithm time interval April - June 2008, and we show in Figure 6.3.12 the results for 22 May 2008. The processing algorithm can be summarized as follows:

1. Only consider slowness estimates in the velocity range 0.25-0.66 km/s (sound velocities).
2. Form groups of consecutive slowness estimates with sound velocities, with the restriction that the azimuth estimates are within 10 degrees of the first azimuth estimate of the group.
3. An infrasound detection is declared if a group has three or more elements (i.e. a duration of 6 seconds or more), and the highest slowness peak of the group is more than 0.9 dB above the 2nd peak.

We have experienced that infrasound signals almost without exceptions yields three or more consecutive slowness estimates with comparable azimuths. This restriction also prevents erroneous declarations of infrasound detections caused by spurious slowness estimates. In the cases with data quality problems (gaps, spikes) on one or more array channels, we may experience a

few ‘false’ consecutive slowness estimates with sound velocities and comparable azimuths. However, under such circumstances the maximum slowness peak is usually not well defined, so we have introduced the additional criterion requiring that the highest slowness peak of the group is more than 0.9 dB above the 2nd peak.

The red data points of Figure 6.3.12 show slowness estimates belonging to groups with three or more elements, formed as described above. The lower panel shows the number of slowness estimates chained together. Notice that for the two signals around 10:06 the numbers are 5 and 15, respectively. For the signal at 16:43, the number is 19.

Details about the 22 May 2008 infrasound detections at the ARCES seismic array are given in Table 6.3.1.

Table 6.3.1. Infrasound detections on the ARCES seismic array, 22 May 2008

Start Time	Duration	App. vel. (km/s)	Back-azi, (deg.)	Rel. Power	SNR (dB)
2008-143:10.06.06.000	8.0	0.337	166.74	0.563	4.22
2008-143:10.06.26.000	28.0	0.337	166.81	0.611	5.74
2008-143:16.43.50.000	36.0	0.329	85.56	0.749	20.93

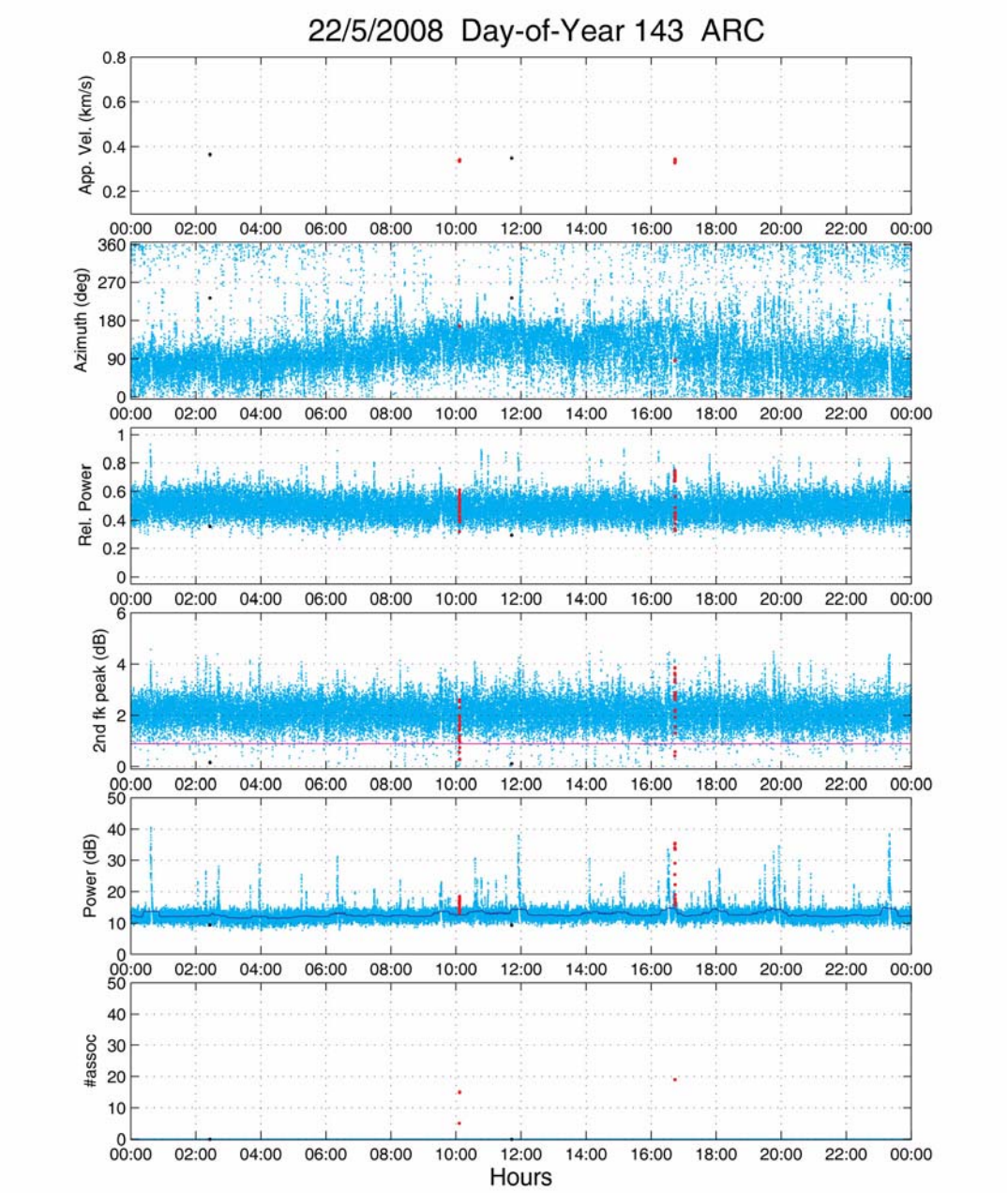

Figure 6.3.12. Processing results from continuous slowness analysis of the ARCES A- and B-ring seismic sensors for 22 May 2008. The red points represent slowness estimates from candidate infrasound signals.
1st panel: Apparent velocity. Seismic velocities fall outside the axis.
2nd panel: Back-azimuth.
3rd panel: The relative power of the slowness maximum (a coherency measure).
4th panel: The difference in decibels between the slowness maximum and the 2nd slowness peak.
5th panel: The absolute power of the slowness maximum (a signal amplitude measure). The blue line represents a smoothed average over the time interval.
6th panel: The number of slowness estimates chained together.

We have adopted a similar procedure for processing of the three ARCES microbarographs. The 22 May 2008 processing results for the ARCES microbarographs are displayed in Figure 6.3.13. Different from processing of the seismic sensors, we now almost always show get slowness estimates with sound velocities, and we had to introduce some changes to the algorithms for forming infrasound detection groups. Another issue with the microbarograph data is that we quite often have large amplitudes at only one of the sensors, probably caused by local wind or other very local noise sources. In order to identify such instances, we introduced the amplitude ratio

$$\frac{Max(a_i)}{Min(a_i)} \; i = 1,3$$

where a_i is the short-term average at sensor i. This ratio yields high values when one of the microbarographs has anomalous values. The processing algorithm applied to the microbarographs can be summarized as follows:

1. Only consider slowness estimates where $\frac{Max(a_i)}{Min(a_i)} < 3.16$ (or $log_{10} \frac{Max(a_i)}{Min(a_i)} < 0.5$)

   See 6th panel of Figure 6.3.13.

2. Only consider slowness estimates in the velocity range 0.25-0.66 km/s (sound velocities). See 1st panel of Figure 6.3.13.

3. Calculate the relative power median and the inter-quartile range (iqr) for the entire time interval. Only consider slowness estimates with relative power values exceeding the median + 1.5 *iqr. This threshold is shown by the red line in the 3rd panel of Figure 6.3.13.

4. Form groups of consecutive slowness estimates with sound velocities, with the restriction that the azimuth estimates are within 10 degrees of the first azimuth estimate of the group.

5. An initial infrasound detection is declared if a group has four or more elements. See 7th panel of Figure 6.3.13.

6. Calculate the amplitude SNR of the individual slowness estimates using the long-term average of the absolute slowness power as the reference (see 5th panel of Figure 6.3.13). For definition of infrasound detection groups having a short duration, we required an SNR of about 4 dB, shown by the red line in the 5th panel of Figure 6.3.13.

Details about the 22 May 2008 infrasound detections at the ARCES microbarographs are given in Table 6.3.2, and we see a much higher number of detections than for the ARCES seismic sensors. The microbarograph infrasound detections corresponding to those found on the seismic sensors (see Table 6.3.1) are marked red. For readability the infrasound detection falling within one-hour intervals are highlighted.

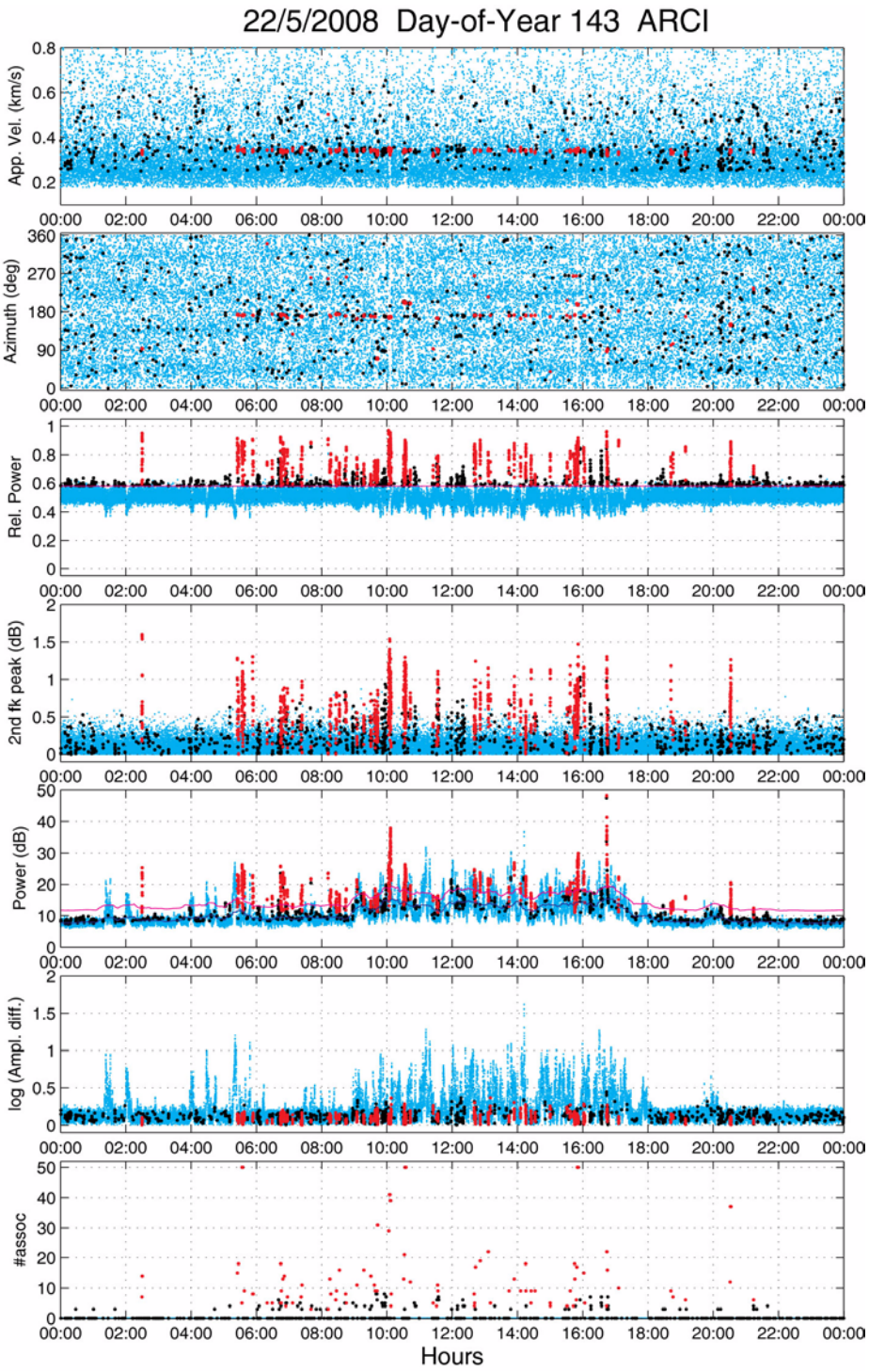

Figure 6.3.13. Processing results from continuous slowness analysis of the three ARCES microbarograph sensors for 22 May 2008. The red points represent slowness estimates from candidate infrasound signals.
1st panel: Apparent velocity.
2nd panel: Back-azimuth.
3rd panel: The relative power of the slowness maximum (a coherency measure).

4th panel: The difference in decibels between the slowness maximum and the 2nd slowness peak.
5th panel: The absolute power of the slowness maximum (a signal amplitude measure). The blue line represents a smoothed average over the time interval.
6th panel: Maximum amplitude difference among the three microbarograph sensors.
7th panel: The number of slowness estimates chained together.

Table 6.3.2. Infrasound detections on the ARCES microbarographs, 22 May 2008

Start Time	Duration	App. vel. (km/s)	Back-azi, (deg.)	Rel. Power	SNR (dB)
2008-143:02.29.26.000	12.0	0.332	93.51	0.729	4.44
2008-143:02.29.50.000	26.0	0.326	93.69	0.950	16.79
2008-143:05.24.54.000	28.0	0.342	172.11	0.913	11.47
2008-143:05.26.48.000	34.0	0.339	171.02	0.864	11.09
2008-143:05.33.24.000	8.0	0.344	170.16	0.857	6.78
2008-143:05.33.36.000	104.0	0.340	171.05	0.892	14.58
2008-143:05.37.44.000	16.0	0.340	172.91	0.884	13.48
2008-143:05.53.04.000	14.0	0.343	171.32	0.907	13.49
2008-143:05.54.04.000	14.0	0.344	171.28	0.822	9.78
2008-143:06.19.42.000	8.0	0.343	340.46	0.749	6.51
2008-143:06.29.00.000	8.0	0.342	174.24	0.759	7.69
2008-143:06.44.26.000	8.0	0.335	174.07	0.922	16.19
2008-143:06.44.38.000	34.0	0.332	173.72	0.898	13.18
2008-143:06.45.40.000	8.0	0.339	170.09	0.714	4.35
2008-143:06.45.54.000	16.0	0.340	170.39	0.645	3.87
2008-143:06.48.32.000	24.0	0.336	173.37	0.883	14.15
2008-143:06.51.12.000	26.0	0.336	172.72	0.837	12.41
2008-143:06.54.04.000	6.0	0.337	168.58	0.701	4.62
2008-143:06.56.58.000	12.0	0.337	165.26	0.833	8.84
2008-143:07.06.30.000	8.0	0.347	127.73	0.707	5.00
2008-143:07.22.08.000	12.0	0.336	168.25	0.770	8.01
2008-143:07.23.46.000	20.0	0.346	167.22	0.852	10.60
2008-143:07.40.20.000	4.0	0.339	259.74	0.885	12.22
2008-143:08.11.54.000	4.0	0.504	256.97	0.910	14.02
2008-143:08.15.02.000	24.0	0.342	171.19	0.755	7.02
2008-143:08.16.42.000	14.0	0.336	168.01	0.804	8.93
2008-143:08.25.54.000	10.0	0.339	173.35	0.676	5.07
2008-143:08.27.08.000	16.0	0.335	172.25	0.781	8.22
2008-143:08.32.30.000	30.0	0.347	174.22	0.743	7.58
2008-143:08.44.10.000	14.0	0.341	169.06	0.772	6.41
2008-143:08.45.14.000	8.0	0.333	261.08	0.851	9.70
2008-143:09.04.50.000	20.0	0.337	163.02	0.780	8.94

Table 6.3.2. Infrasound detections on the ARCES microbarographs, 22 May 2008

Start Time	Duration	App. vel. (km/s)	Back-azi, (deg.)	Rel. Power	SNR (dB)
2008-143:09.17.24.000	30.0	0.337	168.42	0.736	4.26
2008-143:09.30.18.000	26.0	0.339	169.49	0.662	3.04
2008-143:09.36.50.000	20.0	0.340	168.23	0.753	3.66
2008-143:09.38.18.000	16.0	0.339	168.03	0.760	6.67
2008-143:09.41.38.000	16.0	0.331	69.89	0.712	2.87
2008-143:09.42.24.000	60.0	0.341	68.48	0.762	4.37
2008-143:10.02.58.000	56.0	0.340	167.68	0.969	11.49
2008-143:10.04.30.000	80.0	0.337	166.91	0.907	15.81
2008-143:10.05.54.000	76.0	0.334	166.81	0.955	22.89
2008-143:10.07.18.000	6.0	0.336	165.88	0.706	6.74
2008-143:10.07.46.000	14.0	0.348	166.94	0.814	9.19
2008-143:10.30.38.000	24.0	0.343	201.56	0.795	4.45
2008-143:10.31.50.000	40.0	0.338	201.78	0.799	6.23
2008-143:10.33.04.000	132.0	0.338	201.67	0.900	11.90
2008-143:10.42.56.000	22.0	0.341	201.06	0.692	6.55
2008-143:11.25.00.000	8.0	0.327	92.44	0.725	4.14
2008-143:11.31.14.000	6.0	0.347	164.24	0.783	4.09
2008-143:11.33.04.000	20.0	0.340	164.59	0.722	2.46
2008-143:11.33.38.000	16.0	0.338	164.50	0.793	4.69
2008-143:12.40.24.000	14.0	0.340	171.68	0.855	6.79
2008-143:12.40.48.000	6.0	0.333	264.44	0.829	10.50
2008-143:12.41.18.000	8.0	0.336	264.78	0.872	8.70
2008-143:12.42.34.000	32.0	0.341	170.86	0.822	7.51
2008-143:12.51.16.000	36.0	0.337	170.73	0.901	10.24
2008-143:13.06.06.000	42.0	0.342	215.08	0.814	7.81
2008-143:13.10.10.000	8.0	0.339	171.13	0.752	7.62
2008-143:13.44.22.000	16.0	0.342	170.50	0.827	5.82
2008-143:13.53.54.000	24.0	0.338	172.46	0.877	13.02
2008-143:14.05.48.000	16.0	0.338	163.02	0.786	7.07
2008-143:14.14.50.000	34.0	0.341	170.67	0.850	10.71
2008-143:14.15.28.000	16.0	0.340	171.10	0.870	10.29
2008-143:14.24.50.000	8.0	0.339	171.20	0.744	5.58
2008-143:14.25.06.000	16.0	0.344	170.76	0.794	4.69
2008-143:14.32.16.000	16.0	0.333	170.78	0.661	2.26
2008-143:15.00.08.000	8.0	0.338	167.63	0.711	4.90
2008-143:15.00.18.000	6.0	0.340	39.81	0.804	5.54
2008-143:15.30.44.000	6.0	0.339	171.12	0.648	4.30
2008-143:15.31.26.000	6.0	0.389	206.73	0.748	5.13
2008-143:15.36.54.000	16.0	0.338	168.00	0.822	6.57

Table 6.3.2. Infrasound detections on the ARCES microbarographs, 22 May 2008

Start Time	Duration	App. vel. (km/s)	Back-azi, (deg.)	Rel. Power	SNR (dB)
2008-143:15.42.40.000	6.0	0.338	263.95	0.804	7.17
2008-143:15.44.44.000	34.0	0.342	171.42	0.800	4.81
2008-143:15.45.24.000	24.0	0.343	172.07	0.713	-1.15
2008-143:15.48.08.000	10.0	0.335	263.99	0.862	7.36
2008-143:15.49.00.000	32.0	0.344	198.98	0.740	1.98
2008-143:15.50.00.000	126.0	0.340	197.09	0.917	15.68
2008-143:16.01.42.000	28.0	0.343	170.49	0.848	9.72
2008-143:16.03.44.000	8.0	0.334	169.70	0.732	4.04
2008-143:16.43.52.000	6.0	0.325	86.27	0.961	39.90
2008-143:16.44.02.000	42.0	0.342	85.88	0.935	38.25
2008-143:16.45.00.000	30.0	0.319	92.12	0.781	7.51
2008-143:17.05.50.000	18.0	0.333	182.80	0.900	8.56
2008-143:18.42.02.000	16.0	0.326	101.30	0.784	5.92
2008-143:18.45.54.000	12.0	0.329	104.94	0.809	6.52
2008-143:19.09.00.000	10.0	0.333	168.36	0.853	8.33
2008-143:20.30.56.000	22.0	0.340	149.19	0.753	5.15
2008-143:20.31.32.000	72.0	0.334	148.81	0.889	12.40
2008-143:21.14.10.000	10.0	0.334	234.27	0.721	4.54

Figure 6.3.14 shows more details about the infrasound detections at the ARCES seismic sensor for the time interval 10:00 - 11:00 on 22 May 2008. The two detections at 10:06 have very similar back-azimuths (166 degrees) and apparent velocities (0.337 km/s), and are most likely attributed to the same signal.

The detections at the three ARCES microbarographs for the 10:00 - 11:00 time interval are shown in Figure 6.3.15. The five infrasound detections within the time interval 10:03 - 10:08 have all similar back-azimuths (165-167 degrees) and apparent velocities (0.334-0.348 km/s). The corresponding waveforms are shown in Figure 6.3.16, where the time intervals of the infrasound detections are highlighted red. The waveforms plot clearly show that the declared detections correspond to separate infrasound signal pulses. The group of three infrasound detections between 10:30 and 10:35 show the same type of characteristics with separate signal pulses having similar back azimuths (201 degrees) and apparent velocities (0.338 - 0.343 km/s).

The microbarograph waveform plot of Figure 6.3.16 show several instances where one of the sensors has anomalous amplitudes. However, the previously described method for identifying such instances efficiently prevent any infrasound detections within such time intervals.

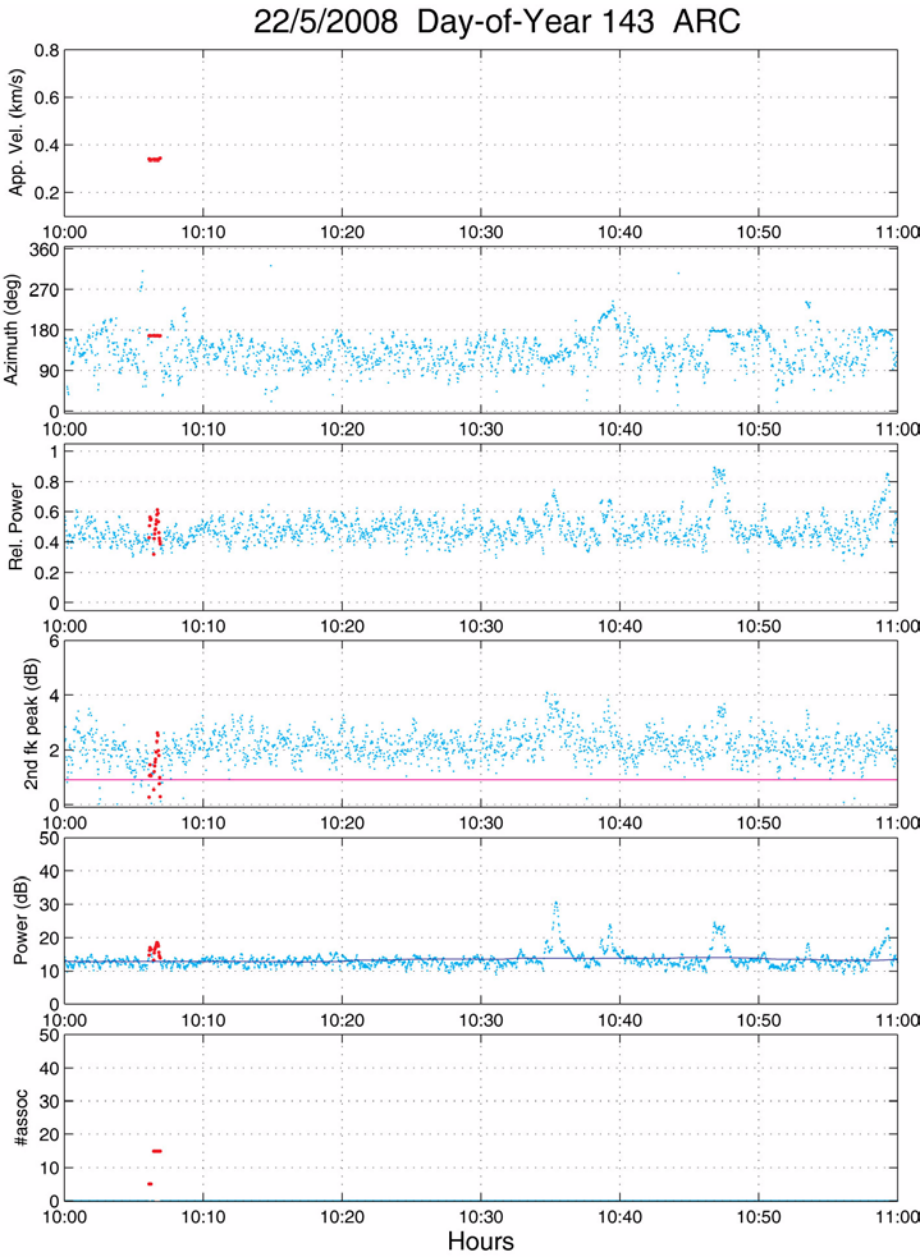

Figure 6.3.14. Processing results from continuous slowness analysis of the ARCES A- and B-ring seismic sensors for 10:00 - 11:00 GMT on 22 May 2008. The red points represent slowness estimates from candidate infrasound signals. See caption of Figure 6.3.12 for details.

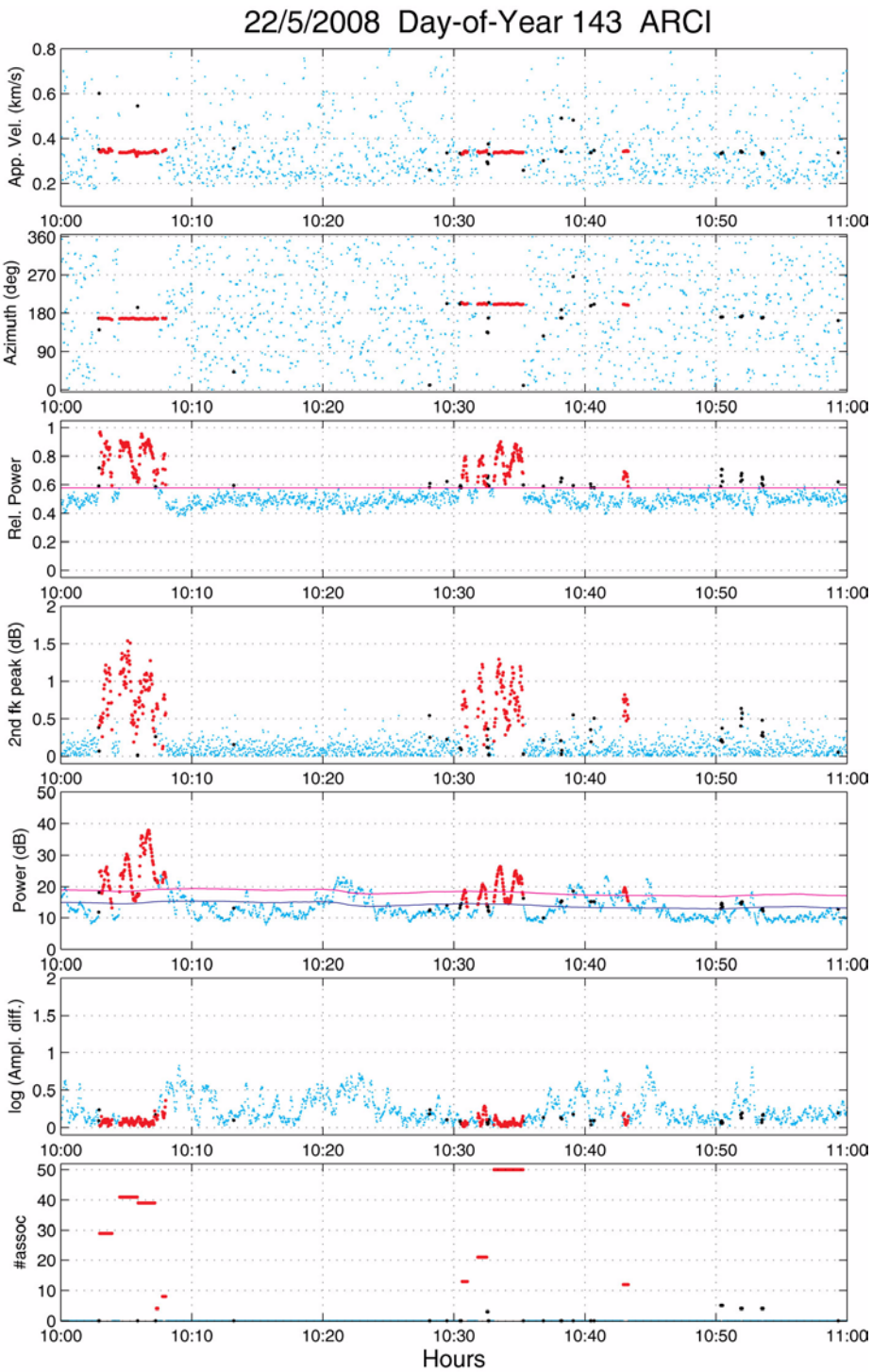

Figure 6.3.15. Processing results from continuous slowness analysis of the three ARCES microbarograph sensors for 10:00 -11:00 on 22 May 2008. The red points represent slowness estimates from candidate infrasound signals. See caption of Figure 6.3.13 for details.

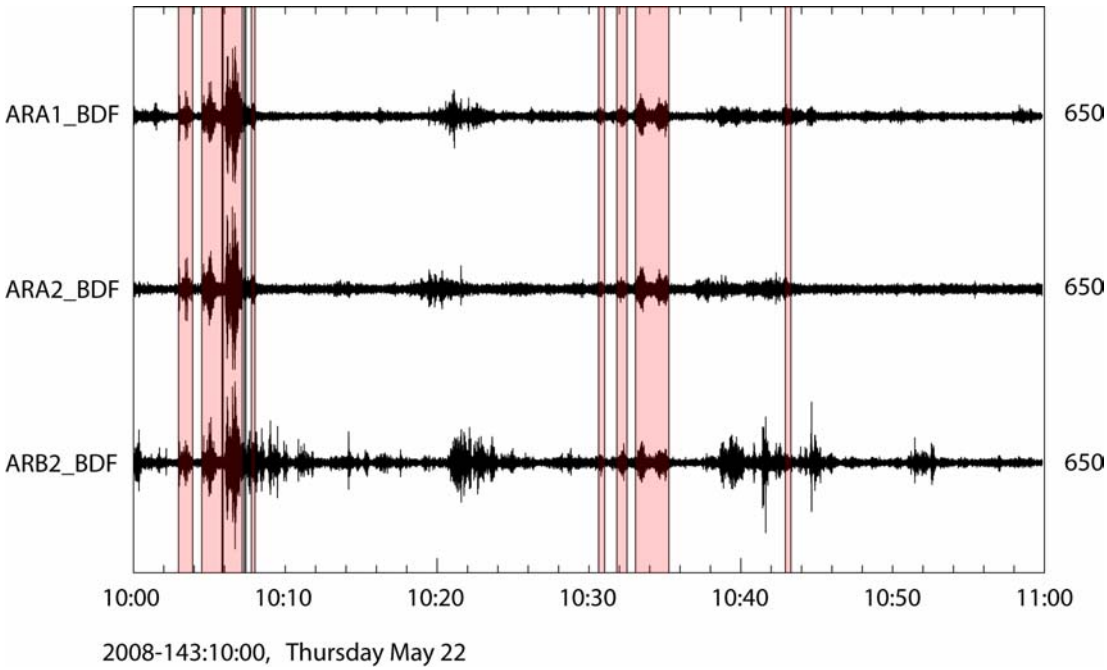

Figure 6.3.16. ARCES microbarograph data for the time interval 10:00 -11:00 on 22 May 2008, bandpass filtered between 2.0 and 5.0 Hz. Time intervals with infrasound signal detections (see Table 6.3.2) are shown red.

Figure 6.3.17 shows the infrasound processing results for the ARCES seismic sensors for the time interval 16:00 - 17:00 on 22 May 2008. During this time interval there is only one detection at 16:43:50, corresponding to the infrasound signals from the Russian explosion site previously described in this paper. The corresponding processing results and waveform plot for the three ARCES microbarographs are shown in Figures 18 and 19.

As a final example, we show in Figures 20 and 21 infrasound processing results and waveform plot at the ARCES microbarographs for the time interval 05:00 - 06:00 on 22 May 2008. Seven infrasound detections are found during this time interval, having durations ranging from 8 to 104 seconds. All detections show similar back-azimuths (170 - 173 degrees) and typical sound velocities (0.34 km/s), indicating a common source for these signals. No infrasound detections at the seismic sensors are found during this time interval.

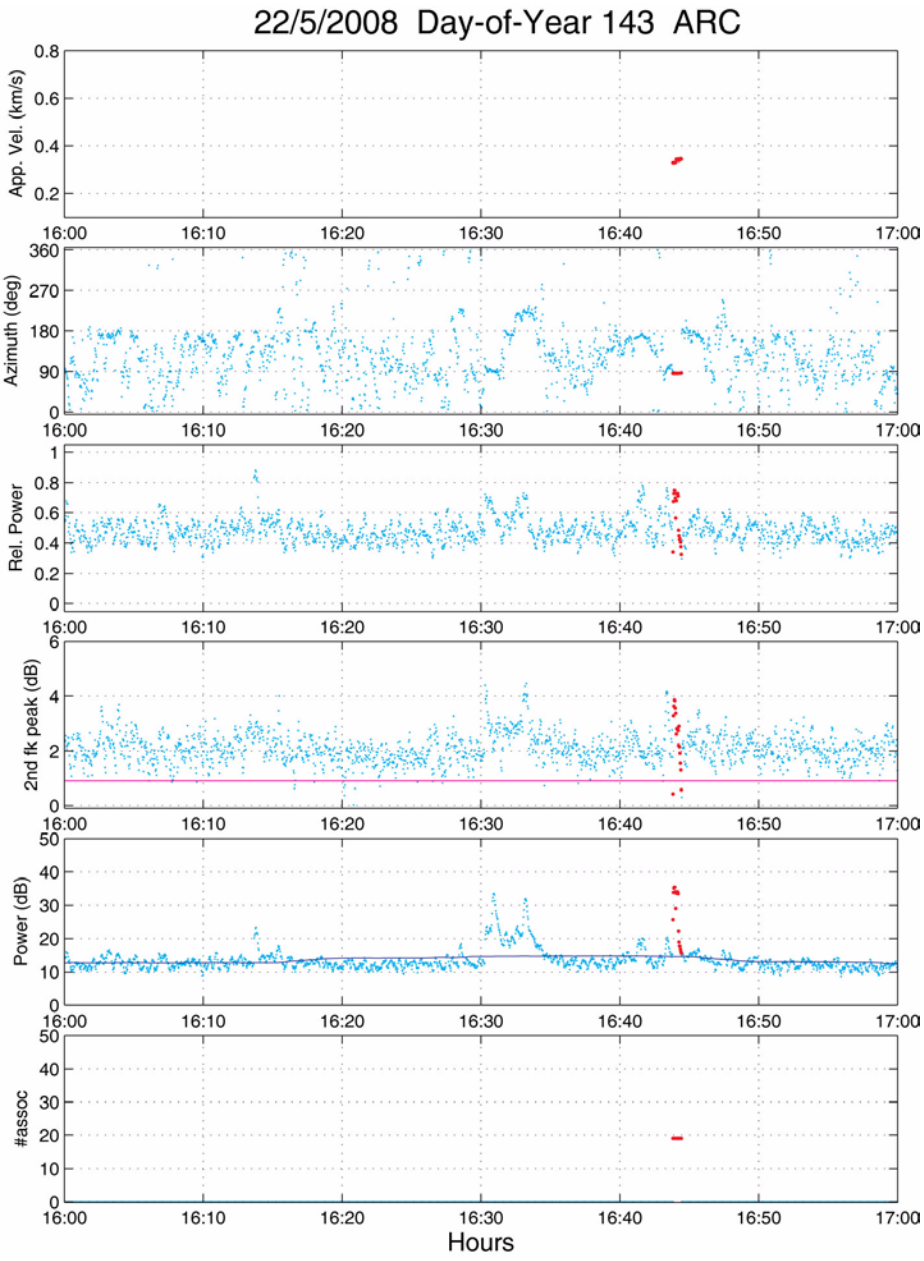

Figure 6.3.17. Processing results from continuous slowness analysis of the ARCES A- and B-ring seismic sensors for 16:00 - 17:00 GMT on 22 May 2008. The red points represent slowness estimates from candidate infrasound signals. See caption of Figure 6.3.12 for details.

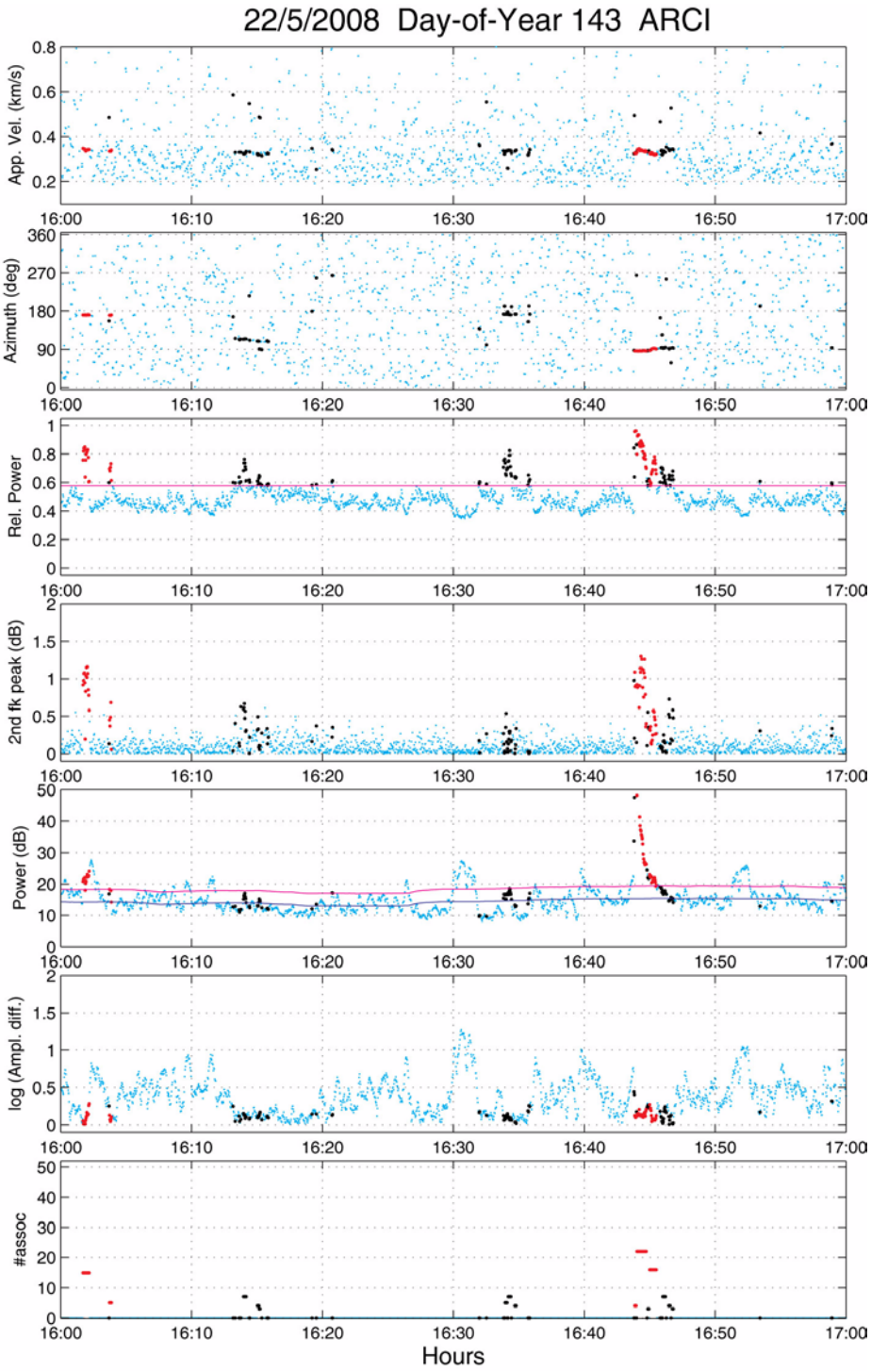

Figure 6.3.18. Processing results from continuous slowness analysis of the three ARCES microbarograph sensors for 16:00 -17:00 on 22 May 2008. The red points represent slowness estimates from candidate infrasound signals. See caption of Figure 6.3.13 for details.

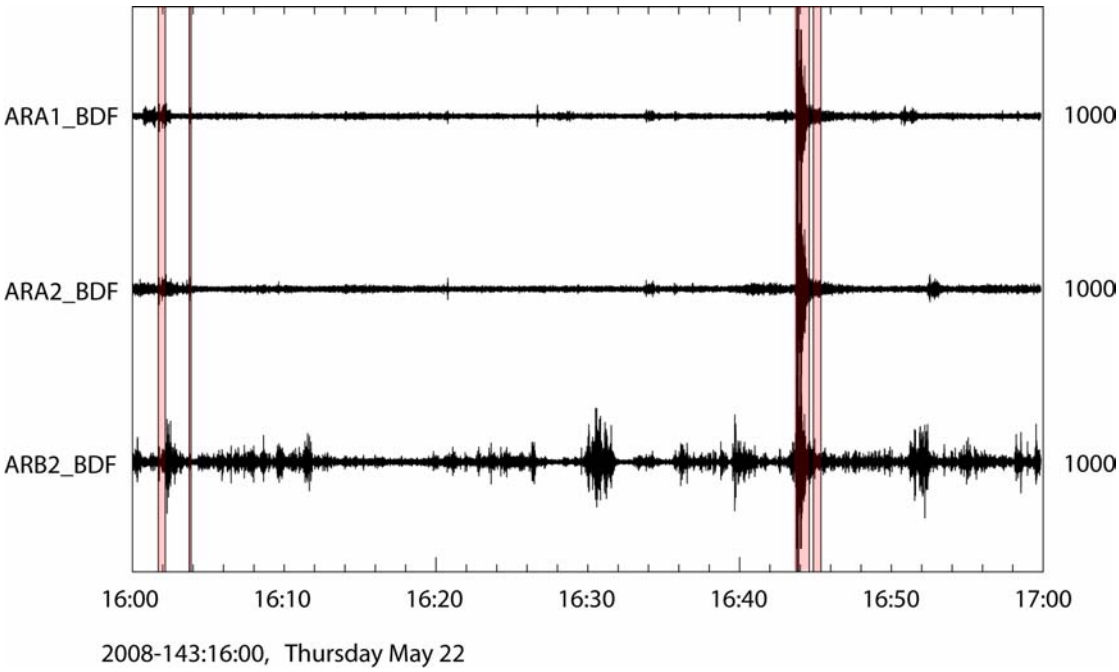

Figure 6.3.19. ARCES microbarograph data for the time interval 16:00 -17:00 on 22 May 2008, bandpass filtered between 2.0 and 5.0 Hz. Time intervals with infrasound signal detections (see Table 6.3.2) are shown red.

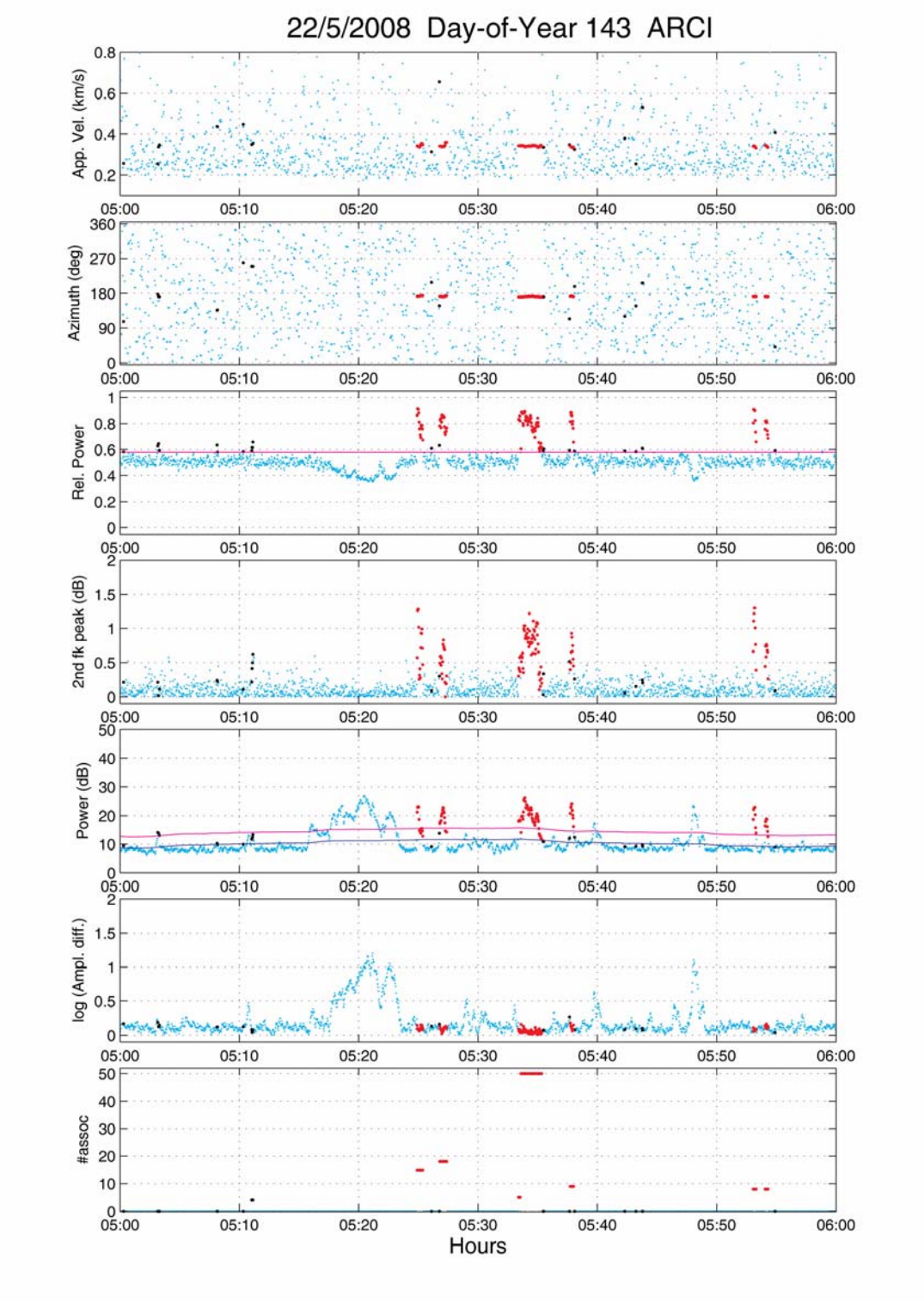

Figure 6.3.20. Processing results from continuous slowness analysis of the three ARCES microbarograph sensors for 05:00 -06:00 on 22 May 2008. The red points represent slowness estimates from candidate infrasound signals. See caption of Figure 6.3.13 for details.

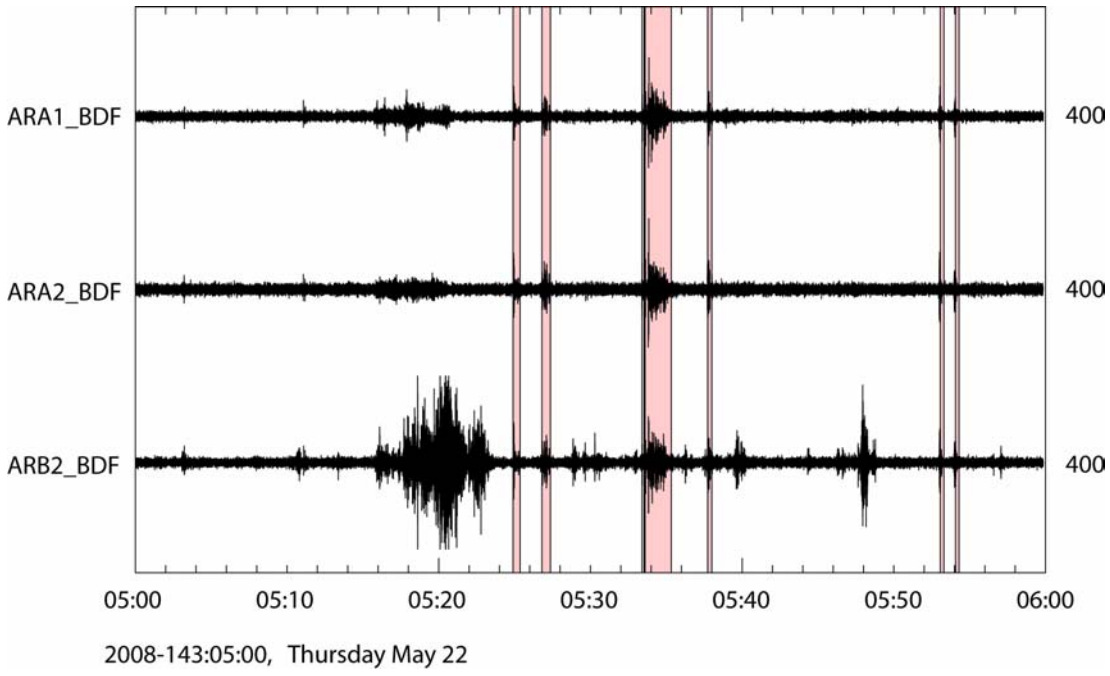

Figure 6.3.21. ARCES microbarograph data for the time interval 05:00 -06:00 on 22 May 2008, bandpass filtered between 2.0 and 5.0 Hz. Time intervals with infrasound signal detections (see Table 6.3.2) are shown red.

We have demonstrated that an infrasound signal detector based on continuous slowness analysis is applicable both to the seismometer and microbarograph data at the ARCES array. To avoid spurious detections at the microbarographs, additional constraints had to put on the SNR of the signals. Data quality checks were introduced to discard instances where sensors show anomalous amplitudes. A much larger number of detections are found on the microbarograph data, clearly illustrating the improved sensitivity to infrasound signals as compared to recordings at the seismic sensors.

In parallel with this study, we have processed the same data set using cross-correlation techniques (Gibbons et al., 2007) combined with the detection statistic of Brown et al. (2002). These results are comparable to those presented in this study, but a detailed comparison will require further work concerning setting of window and filter parameters, threshold setting and data quality control.

For the time interval April - June 2008 we have also processed the infrasound data from Apatity, as well as from the stations of the Swedish Infrasound Network using the method described above. A natural next step is to combine the signal detections from this dense network of six infrasound stations in Northern Europe to obtain information about the infrasound sources.

6.3.7 References

Baryshnikov (2004). Research of infrasound background characteristics for estimation of threshold sensitivity of infrasound method for test monitoring. Final Technical Report ISTC 1341-01 (part 1 of total 2), International Science and Technology Center (ISTC), Moscow, 255pp.

Brown, D. J., C. N. Katz, R. Le Bras, M. P. Flanagan, J. Wang and A. K. Gault (2002). Infrasonic signal detection and source location at the prototype international data centre, *Pure Appl. Geophys*, **159**, 1081-1125.

Frankel, A., S. Hough, P. Friberg and R. Busby (1991): Observations of Loma Prieta aftershocks from a dense array in Sunnyvale, California, Bull. Seism. Soc. Am. 81, 1900-1922

Gibbons, S. G., F. Ringdal and T. Kværna (2007). Joint seismic-infrasonic processing of recordings from a repeating source of atmospheric explosions, *J. Acoust. Soc. Am.*, **122**, EL158-EL164.

Kværna, T. and D. J. Doornbos (1986). An integrated approach to slowness analysis with arrays and three-component stations, *Semiann. Tech. Summary,* 1October 1985 - 31 March 1986, NORSAR Sci. Rep. No. 2-85/86, Kjeller, Norway.

Liszka, L. (2007): Infrasound - A summary of 35 years of infrasound research, Manuscript submitted for printing, 150 pp

Ringdal, F., and J. Schweitzer (2005). Seismic/Infrasonic Processing: Case study of explosions in NW Russia, Semiannual Technical Summary, NORSAR Scientific Report No. 2 - 2005. NORSAR, Kjeller, Norway. pp. 54-68.

Frode Ringdal
Tormod Kværna
Steven Gibbons

6.4 Continued overview of NORSAR system responses: the NORES and ARCES arrays

6.4.1 Introduction

At the early to mid 1980s, NORSAR began experimenting with the concept of a small-aperture seismic array configuration that would allow detection and location of seismic events at regional distances. This work initiated as a series of test deployments around NORSAR array site NC602 (for details, see Mykkeltveit et al., 1983) and developed into the Norwegian Regional Experimental Seismic System, what is known as the NORES (NORESS) array, whose operation commenced officially on 3rd June 1985 and terminated in July 2002. The array consists of 25 elements, distributed on 4 concentric rings, with one element in the center, and spreads over a diameter of 3 km. During summer and fall of 1987, a second regional array, almost identical to NORES in terms of geometry, instrumentation and data output, was installed in the vicinity of the town of Karasjok, in Finnmark, northern Norway. This is the ARCES (ARCESS) array (ARCtic Experimental Seismic System), which is part of the International Monitoring System for the CTBT (certified in November 2001 under the primary station code PS28). The geometry of ARCES is shown in Fig. 6.4.1.

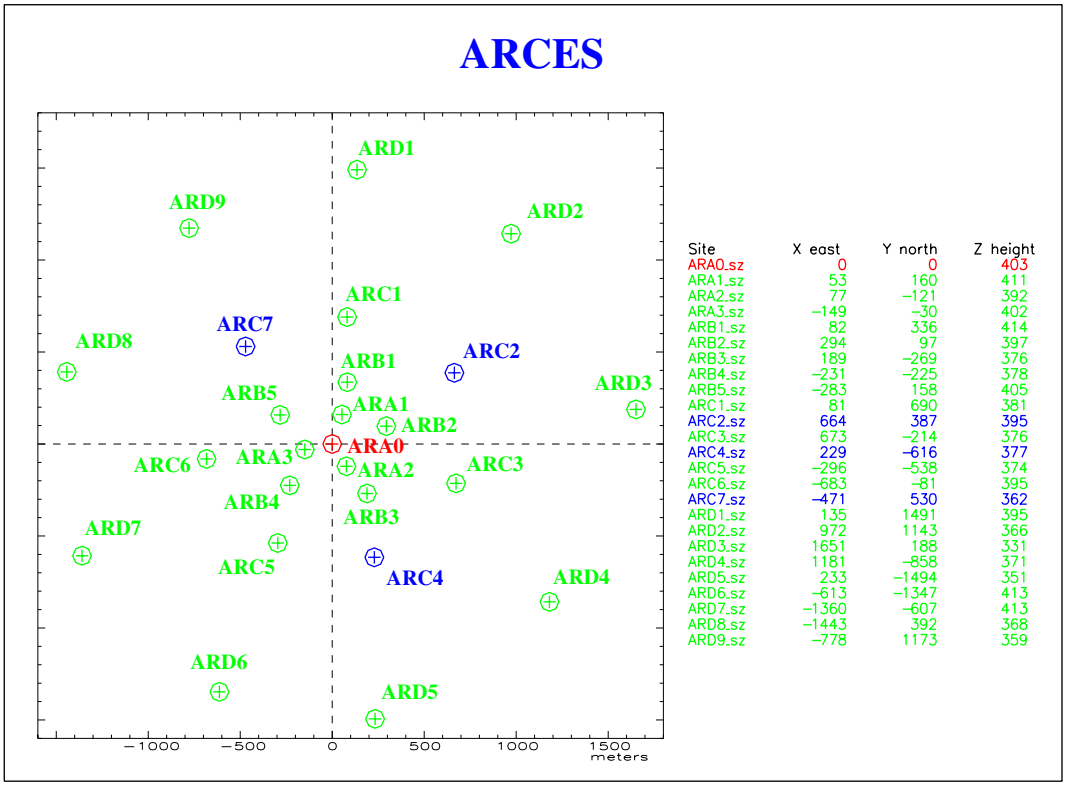

Site	X east	Y north	Z height
ARA0.sz	0	0	403
ARA1.sz	53	160	411
ARA2.sz	77	−121	392
ARA3.sz	−149	−30	402
ARB1.sz	82	336	414
ARB2.sz	294	97	397
ARB3.sz	189	−269	376
ARB4.sz	−231	−225	378
ARB5.sz	−283	158	405
ARC1.sz	81	690	381
ARC2.sz	664	387	395
ARC3.sz	673	−214	376
ARC4.sz	229	−616	377
ARC5.sz	−296	−538	374
ARC6.sz	−683	−81	395
ARC7.sz	−471	530	362
ARD1.sz	135	1491	395
ARD2.sz	972	1143	366
ARD3.sz	1651	188	331
ARD4.sz	1181	−858	371
ARD5.sz	233	−1494	351
ARD6.sz	−613	−1347	413
ARD7.sz	−1360	−607	413
ARD8.sz	−1443	392	368
ARD9.sz	−778	1173	359

Fig. 6.4.1. Geometry of the ARCES arrays. The NORES array has an identical geometry.

The instrument responses of these two systems will be presented in the following sections, covering their entire operation interval, from installation to present day status. Presentation and methodology follow the scheme initiated in Pirli and Schweitzer (2008) and is part of the ongoing effort to recalculate, organize and document all NORSAR system responses.

6.4.2 NORES array configurations

Although official opening of the NORES array did not take place before summer 1985, the array was equipped with standard instrumentation since late 1984, after the extended test period during which it operated as part of the NORSAR array. NORES seismic data cover a variety of frequency bands, the result of maintaining in operation short-, long- and intermediate-period channels, as well as high-frequency channels. No data are available any longer from the latter configuration and therefore the high-frequency response will not be discussed.

Standard NORES instrumentation is based on GS-13 short-period and KS36000 broadband sensors and Sandia 'Blue Box' digitizers. The central element and three sites on the C-ring (NRA0, NRC2, NRC4, NRC7) are equipped with 3C seismometers. A variation of the short-period channel that existed during a short time interval (September 1985 – September 1986) employed a 3-component S-3 short-period sensor, installed in a 60 m borehole. The site coincided with site NRA0 and was assigned the name NRF0. No further modifications were made to the instrumentation of the array. The installation was struck by lightning in 2002 and has been out of operation since then.

Table 6.4.1. The different instrument configurations of the NORES array.

Time	Installation Name	Components	Calib [nm/count]	Calper [s]
1984-2002	Standard_SP (NORESSP1, NORESSP2, NORESSP3)	GS-13 Couplings Box Seismometer pre-amplifier Short-period filter Distributed filter Sandia 'Blue Box' digitizer	0.0068649	1.00
1985-1986	S-3_SP_variation (NORESSP4, NORESSP5, NORESSP6)	S-3 Couplings Box Seismometer pre-amplifier Short-period filter Distributed filter Sandia 'Blue Box' digitizer	0.0068649	1.00
1984-2002	Standard_IP (NORESIP1, NORESIP2, NORESIP3)	KS36000 Couplings Box Intermediate period bandpass filter Distributed filter Interm. period spectral shaping filter Sandia 'Blue Box' digitizer	0.077364	1.00
1984-2002	Standard_LP (NORESLP1, NORESLP2, NORESLP3)	KS36000 Couplings Box Long period high pass filter Long period bandpass filter Distributed filter Long period spectral shaping filter Sandia 'Blue Box' digitizer	0.13936	25.00

The above mentioned instrumentations for which different instrument responses needed to be calculated are presented in Table 6.4.1. Each case is mentioned together with information about the time interval it could be met, the GSE response file Respid (in parenthesis), which is

an identifier for each different calculated response, and the corresponding channel sensitivity (Calib in nm/count) and calibration period (Calper in s).

As shown above, the two different NORES short-period configurations involve a short-period seismometer (Geotech GS-13 or S-3), a Sandia digitizer referred here as 'Blue Box' and an interface of pre-amplifier and filters between them. The response of the GS-13 seismometer is described by 2 poles and 2 zeros that can be obtained by the standard seimometer formula (Geotech Instruments, 1999):

$$p_{1,2} = \lambda_0\omega_0 \pm j\omega_0\sqrt{1-\lambda_0^2} \ ,$$

where $\lambda_0 = 0.75$ and $\omega_0 = 6.283$ rad/s, both of them being nominal values. The gain of the seismometer, normalized at 100 Hz will be equal to 2200 V/m/s. However, all the individual amplifier and filter stages between the seismometer and the digitizer contribute to the overall response of the GS-13, which is expressed by the formula (Durham, 1984b):

$$H_{spv}(s) = H_S(s) \cdot H_{IF}(s) \cdot H_{PA}(s) \cdot H_{SP}(s) \cdot H_{DF}(s) \ ,$$

expressed in V/m/s, where $H_S(s)$ the response of the seismometer, $H_{IF}(s)$ the response of the seismometer-amplifier interface, $H_{PA}(s)$ the response of the pre-amplifier, $H_{SP}(s)$ the response of the short period filter and $H_{DF}(s)$ the response of the distributed filter. The equations providing each individual response stage and their details can be found in Durham (1984b) and Breding (1986), as well as in the relevant to the NORES system response NORSAR documentation. The response of the S-3 short-period seismometer is identical to that of the GS-13 instrument, including the pre-amplifier and filter stages (Durham, 1984b), and is therefore described by the same transfer function(s), poles and zeros.

The 'Blue Box' digitizer, manufactured by Sandia, is a 16 bit gain ranged digitizer with a sensitivity of 100000 count/V.

NORES site E0, which is collocated with site A0, the central array element, hosts a Kinemetrics KS36000-04A broadband borehole seismometer. Two different 3-component channels, a long-period channel (lz, ln, le) and an intermediate-period channel (iz, in, ie), are outputed at this site. For each one of these channels, the system consists of the components (Durham, 1984a) listed in Table 6.4.1 under the names Standard_LP and Standard_IP respectively. The concept of interfacing the seismometer to the digitizer is the same as in the case of the short-period channels, with series of filters that contribute to the overall seismometer response. Individual stage transfer functions can be found in Durham (1984a) and the NORSAR responses documentation.

The displacement response for the different NORES channels is depicted in Fig. 6.4.2. Displacement amplitude is expressed in count/nm and phase in degrees. The short-period (SP) channel response (NORESSP) is denoted with a blue line, the intermediate-period (IP) response (NORESIP) with a green line and the long-period (LP) response (NORESLP) with a red line. Moreover, shading is used to denote the range beyond the Nyquist frequency, which is

equal to 20 Hz for the short-period channels, 5 Hz for the intermediate-period channels and 0.5 Hz for the long-period channels.

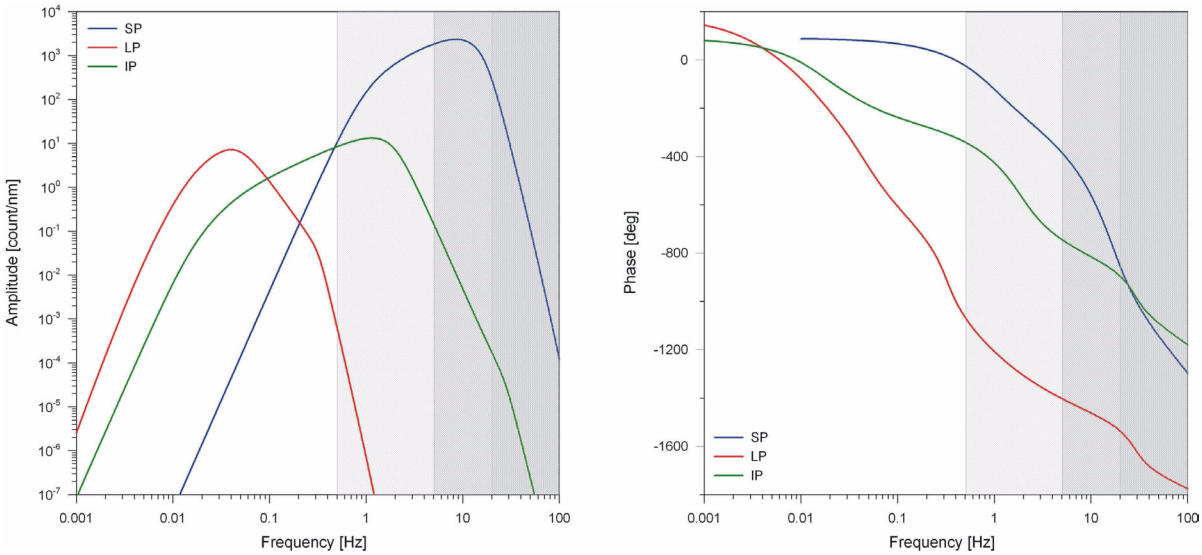

Fig. 6.4.2. Displacement amplitude and phase response for the NORES short period (NORESSP), intermediate period (NORESIP) and long period (NORESLP) configurations. The shaded areas represent the range beyond the Nyquist frequency (20 Hz for the short-period, 5 Hz for the intermediate period and 0.5 Hz for the long period channels).

6.4.3 ARCES array configurations

As already mentioned above, the ARCES array was designed as a duplicate of NORES, both in terms of geometry and instrumentation. So, the status of ARCES responses for the time interval 1987 – 1999 is the same as that described for NORES in the previous section. An extensive refurbishment of the array took place in September 1999, resulting in the replacement of all Sandia digitizers with Nanometrics HRD24 digitizers and the removal of the KS36000 seismometer and their replacement with a Güralp CMG-3T broadband instrument. From October 2003 to July 2004, a high-frequency 3-component channel operated at site ARE0, with a REFTEK 130-01 digitizer connected to the CMG-3T seismometer. Finally, since March 2008, an additional broadband 3-component channel is operating at site ARE0 with a Güralp DM24 digitizer connected to the CMG-3T sensor.

The different ARCES configurations for which separate instrument responses need to be calculated are listed in Table 6.4.2, with information about the time interval they could be met, the GSE response file Respid (in parenthesis), and the corresponding channel sensitivity (Calib in nm/count) and calibration period (Calper in s).

For the initial (Standard_SP/IP/LP) ARCES channels, system response characteristics are identical to those of standard NORES and have been described in the previous section (6.4.2).

Table 6.4.2. The different instrument configurations of the ARCES array.

Time	Installation Name	Components	Calib [nm/ count]	Calper [s]
1987-1999	Standard_SP (ARCESSP1, ARCESSP2, ARCESSP3)	GS-13 Couplings Box Seismometer pre-amplifier Short-period filter Distributed filter Sandia 'Blue Box' digitizer	0.006838	1.00
1987-1999	Standard_IP (ARCESIP1, ARCESIP2, ARCESIP3)	KS36000 Couplings Box Intermediate period bandpass filter Distributed filter Interm. period spectral shaping filter Sandia 'Blue Box' digitizer	0.077313	1.00
1987-1999	Standard_LP (ARCESLP1, ARCESLP2, ARCESLP3)	KS36000 Couplings Box Long period high pass filter Long period bandpass filter Distributed filter Long period spectral shaping filter Sandia 'Blue Box' digitizer	0.139260	25.00
1999-…	Current_SP (ARCESSP4, ARCESSP5, ARCESSP6)	GS-13 HRD24 digitizer	0.037776	1.00
1999-…	Current_BB (ARCESBB1, ARCESBB2, ARCESBB3)	CMG-3T HRD24 digitizer	0.005065	1.00
2003-2004	REFTEK_HH (ARCESHH1, ARCESHH2, ARCESHH3)	CMG-3T DAS 130-01 digitizer	0.000508	1.00
2008-…	Guralp_EH (ARCESEH1, ARCESEH2, ARCESEH3)	CMG-3 DM24 digitizer	4.019100	1.00

The current short-period configuration consists of a GS-13 seismometer and a Nanometrics HRD24 digitizer. The response of the sensor is the same as described in section 6.4.2, but no special interface is required in this case for its connection to the digitizer. The response of the digitizer consists of the following components (Nanometrics communication):

- An analogue lowpass filter with 3 poles and no zeros

- A FIR filter with 34 coeffiecients, decimating by a factor of 5 from an initial input sample rate of 30 kHz
- A FIR filter with 30 coefficients, decimating by a factor of 3
- A FIR filter with 118 coeffiecients, decimating by a factor of 2
- A FIR filter with 36 coefficients, decimating by a factor of 5
- A FIR filter with 256 coefficients, decimating by a factor of 5, down to the desired sample rate of 40 sps, and
- An IIR filter with one pole and one zero

The HRD24 is a 24-bit digitizer with a sensitivity of 6303183.11 count/V.

The same digitizer is connected, in the case of the broadband channels, to a Güralp CMG-3T sensor. The response of the seismometer can be calculated from its poles and zeros, sensitivity and normalization factor provided by the manufacturer in instrument specific calibration sheets.

As mentioned earlier (see also Table 6.4.2), there are two variations of the CMG-3T configuration, one with a REFTEK DAS 130-01 digitizer and one with a Güralp DM24 digitizer.

The REFTEK DAS 130-01 is a 24-bit output word digitizer that employs the Crystal Semiconductor CS5372/5322 chipset. This is the combination of an analog modulator and a series of digital filters that decimate from the frequency of the A/D input clock down to a desired sample rate. However, for some recording sample rates, a combination of CS5322 FIR filters and additional CPU firmware filtering has to take place. The particular ARCES data are recorded with a sample rate of 100 sps, which is achieved by the following combination of filters (REFTEK, 2008):

- CS5322 FIR filter A with 34 coefficients, decimating by a factor of 8 from an input rate of 1024 kHz
- CS5322 FIR filter B with 14 coefficients, decimating by a factor of 2
- CS5322 FIR filter B with 14 coefficients, decimating by a factor of 2
- CS5322 FIR filter B with 14 coefficients, decimating by a factor of 2
- CS5322 FIR filter B with 14 coefficients, decimating by a factor of 2
- CS5322 FIR filter B with 14 coefficients, decimating by a factor of 2
- CS5322 FIR filter C with 102 coefficients, decimating by a factor of 2, down to 200 Hz, and
- CPU firmware filter #3, decimating by a factor of 2, to the desired sample rate of 100 Hz

The sensitivity of the instrument is 62914560 count/V.

Finally, the Güralp DM24 is a 24-bit digitizer, which employs a combination of the Crystal Semiconductor CS5376 chip and internal digital filters to produce the desired data recording sample rate (see Güralp Systems website for product documentation). The filter sequence employed in the case of ARCES to obtain 100 Hz data is the following:

- CS5376 FIR filter Stage 1, Sinc 1, with 36 coefficients, decimating by a factor of 8 from an input rate of 512 kHz
- CS5376 FIR filter Stage 3, Sinc 2, with 6 coefficients, decimating by a factor of 2

- CS5376 FIR filter Stage 4, Sinc 2, with 8 coefficients, decimating by a factor of 2
- CS5376 FIR filter Stage 5, FIR 1, with 48 coefficients, decimating by a factor of 4
- CS5376 FIR filter Stage 5, FIR 2, with 126 coefficients, decimating by a factor of 2
- DM24 FIR Stage 1, SWA-D24-3D08, with 502 coefficients, decimating by a factor of 5, and
- DM24 FIR Stage 2, SWA-D24-3D07, with 502 coefficients, decimating by a factor of 4 to the desired rate of 100 sps

The sensitivity of the digitizer is 312207.306 count/V.

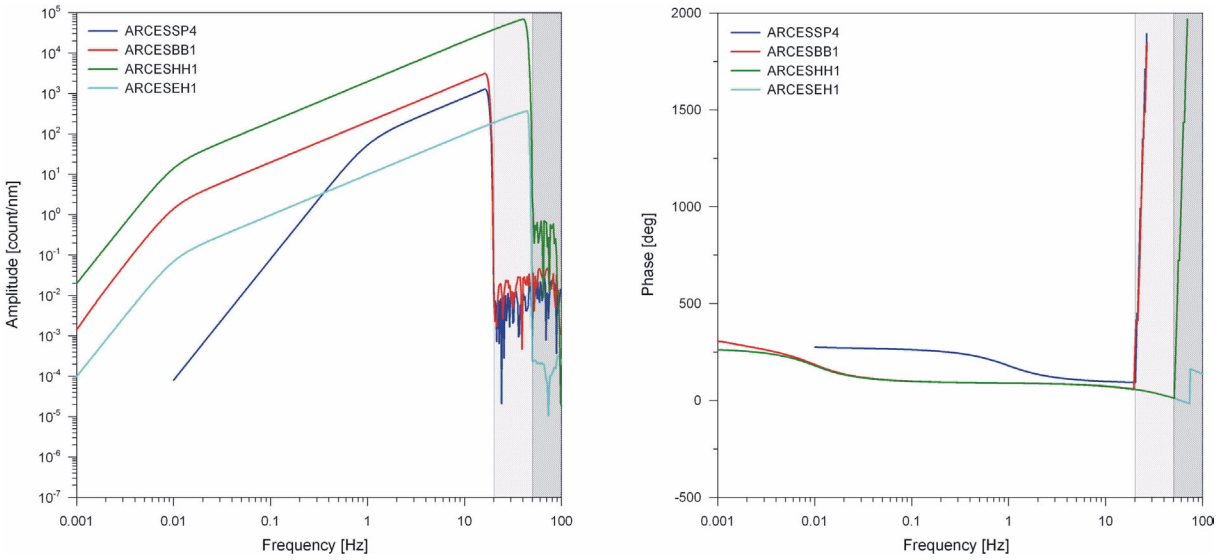

Fig. 6.4.3. Displacement amplitude and phase response of the ARCES short period and broadband installations. The current short period (ARCESSP4), the current broadband (ARCESBB1), the REFTEK high-frequency variation (ARCESHH1) and the Güralp high-frequency variation (ARCESEH1) configurations are depicted. The shaded areas represent the range beyond the Nyquist frequency (20 Hz for short period and broadband and 50 Hz for the high-frequency configurations).

The displacement response for the different ARCES channels is depicted in Fig. 6.4.3. Displacement amplitude is expressed in count/nm and phase in degrees. The initial ARCES configuration response curves are not included in the plot, since they are the same as NORES and are depicted in Fig. 6.4.2. The current short-period (SP) channel response (ARCESSP4) is denoted with a blue line, the current broadband response (ARCESBB1) with a red line, the broadband (high-frequency) REFTEK variation response (ARCESHH1) with a green line and the broadband (high-frequency) Güralp variation (ARCESEH1) with a cyan line. Moreover, shading is used to denote the range beyond the Nyquist frequency, which is equal to 20 Hz for the short-period and broadband channels and 50 Hz for the two high-frequency channels.

Myrto Pirli
Johannes Schweitzer

References

Breding, D. (1986): NSEIS subroutine.

Durham, H.B. (1984a): NRSA broad band channel response functions. Sandia National Laboratories, Albuquerque, New Mexico, 4 p.

Durham, H.B. (1984b): NRSA short period response functions. Sandia National Laboratories, Albuquerque, New Mexico, 6 p.

Geotech Instruments (1999): Operation and maintenance manual portable short-period seismometer, model GS-13. 55400D0A.WFW, Geotech Instruments, Dallas, Texas, 50 p.

Mykkeltveit, S., K. Åstebøl, D.J. Doornbos & E.S. Husebye (1983): Seismic array configuration optimization. Bull. Seism. Soc. Amer. **73**, 173-186.

Pirli, M. & J. Schweitzer (2008): Overview of NORSAR system response. NORSAR Scientific Report **1–2008**, 64-77.

REFTEK (2008): 130 Theory of Operations. Doc-130-Theory-J, Refraction Technology, Inc., Plano, Texas, 106 p.